Aus dem

Department für Diagnostische Labormedizin

der Universität Tübingen

Institut für Medizinische Mikrobiologie und Hygiene

Characterization of the YgfB-mediated molecular mechanisms contributing to multidrug resistance of *Pseudomonas aeruginosa*

Inaugural-Dissertation

zur Erlangung des Doktorgrades

der Medizin

der Medizinischen Fakultät
der Eberhard Karls Universität
zu Tübingen

vorgelegt von
Wackler, Noelle

2022

Dekan:	Professor Dr. B. Pichler
1. Berichterstatter:	Privatdozentin Dr. M. Schütz
2. Berichterstatter:	Professor Dr. D. Sauter

Tag der Disputation: 04.07.2023

Inhaltsverzeichnis

List of Figures

List of Tables

Abbreviations

AUC	Area Under the Curve
ATM	Aztreonam
Bp	Base pairs
BSI	Blood stream infection
CAP	Community-acquired pneumonia
CAZ	Ceftazidime
CF	Cystic Fibrosis
COPD	Chronic obstructive pulmonary disease
dNTP	Desoxyribonucleosidetriphosphate
Ec	*Escherichia coli*
ECDC	European Centre for Disease Prevention and Control
ESBL	Extended-spectrum-beta-lactamase
EUCAST	European Committee on Antimicrobial Susceptibility Testing
FEP	Cefepime
GlcNAc	N-acetyl-glucosamine
GOI	Gene of interest
HAP	Hospital-acquired pneumonia
HGT	Horizontal gene transfer
IMI	Imipenem
LB	Lysogeny Broth
LMM-PBP	Low molecular mass penicillin-binding protein

LPS	Lipopolysaccharides
LT	Lytic transglycosylases
MDR	Multidrug-resistant
MEM	Meropenem
MEP	Murein endopeptidase
MIC	Minimal inhibitory concentration
MurNAc	N-acetyl-muramic acid
OD	Optical density
ORF	Open reading frame
Pa	Pseudomonas aeruginosa
PBP	Penicillin-binding protein
PBS	Phosphate Buffered Saline
PCR	Polymerase chain reaction
PGN	Peptidoglycan
PIP	Piperacillin
QS	Quorum Sensing
RND	Resistance-nodulation-division
Rpm	Revolutions per minute
SD	Standard deviation
SDS-PAGE	Sodium dodecyl sulfate polyacrylamide gel electrophoresis
SOC	Super optimal broth with catabolite repression
T2SS	Type II secretion system

T3SS	Type III secretion system
T6SS	Type VI secretion system
TBE buffer	5x TRIS-Borate-EDTA buffer
TJ	Tight junction
TLR	Toll-like receptor
TRIS	Tris(hydroxymethyl)aminomethane
TZP	Piperacillin/Tazobactam
VAP	Ventilation-associated pneumonia
WT	Wildtype

1 Introduction

1.1 Pseudomonas aeruginosa

1.1.1 Pseudomonas aeruginosa

Pseudomonas aeruginosa (*Pa*) is a Gram-negative bacterium of a length of 2-4 µm. It grows aerobically but can also grow anaerobically in the presence of terminal electron acceptors, such as nitrate (NO_3^-), nitrite (NO_2^-), and nitrous oxide (N_2O), as well as when L-arginine is a substrate for growth (Zannoni, 1989).

One or more polar flagella confer motility to the bacterium which was isolated as a pure culture for the first time in 1882 by Gessard. He named it “bacterium pyocyaneum” as it was known to cause wound infections with yellowish and greenish pus secretions. A modest nutrient supply suffices for *Pa* cells to grow. This enables its wide dissemination and persistance in the environment. It can be found especially in moist habitats and inhabits the soil, waters and oceans, plants and sometimes animal and human intestines (Kayser et al., 2010, Hof and Schlüter, 2019).

Pa is an important cause of nosocomial infections (Sadikot et al., 2005). Emori and Gaynes (1993) indicate that *Pa* is responsible for about one out of ten nosocomial infections. Showers, sinks, toilets, cosmetics, inadequately concentrated disinfectants, eye drops, humidifiers, inhalators and ventilation devices, dialyzers and anaesthesia devices are regarded as sources of infection. The prevention of infection thus strongly depends on exposition prophylaxis and hospital hygiene measures. Outside hospital environments, a preferential reproduction in aerated waters such as whirlpools, leading to cases of diffuse folliculitis in immune-competent pool guests, has been described (Kayser et al., 2010, Hof and Schlüter, 2019).

The total genome size of 6,3 Mb, the amount of 5570 open reading frames (ORFs) and the high number of 521 regulatory genes distinguish the genomic characteristics of *Pa* from most other bacterial species (Botelho et al., 2019, Silby et al., 2011).

A number of 150 encoded outer membrane proteins and 300 transporters and enzymes (for nutrient uptake mostly) further illustrate this distinction (Botelho et al., 2019).

Pa disposes of vast possibilities of performing metabolic reactions, of substance uptake and export, iron acquisition and biosynthesis of amino acids, nucleic acids and cofactors (Stover et al., 2000).

Numerous gene families and a high gene family density besides the genomic size, complexity and regulation possibilities define the genomic versatility of *Pa* and its enormous capability for evolutionary adaption to different environments (Botelho et al., 2019, Silby et al., 2011, Stover et al., 2000). Interestingly, very low genetic differences between strains from different geographical origins have been observed (Klockgether et al., 2011). This reflects again the high adaptability of this old bacterial organism which can conquer new living spaces simply by employing its enormous gene and regulatory repertoire to adapt to changes in the environment (Klockgether et al., 2011).

The capability of developing antibiotic resistance also derives from this special genomic background: due to the extensive environmental distribution, intrinsic resistance mechanisms to combat naturally occurring antimicrobials have been developed, such as efflux of substances. The comprehensive regulatory genome enables adaptive resistance. Furthermore, highly developed metabolic pathways allow enzymatic drug modification, modulation of drug targets and transport of substances (Stover et al., 2000).

The European Centre for Disease Prevention and Control (ECDC) reported that the prevalence of single resistances in *Pa* was 13,2 %, and resistance to 3 different antibiotic groups was found in 3,9 % of clinical isolates responsible for invasive infections into the bloodstream or the cerebrospinal fluid system in European countries in 2019. This reflects the enormous prevalence of antibiotic resistance in *Pa* (European Centre for Disease Prevention and Control (ECDC), 2019). *Pa* resistance rates in 2003 were compared to the mean resistance rates in the period of the 5 preceding years (1998-2002) for different antibiotics. Alarmingly, within few years the resistance to imipenem increased by 15 %,

quinolone resistance raised by 9 %, and *Pa* resistance to 3rd generation cephalosporins increased by 20 % (National Nosocomial Infections Surveillance (NNIS) System, 2004).

1.1.2 Infections and pathomechanisms

1.1.2.1 Infections

Pa infections affect different organ systems. Concerning respiratory infections, *Pa*-induced community-acquired pneumonia (CAP) affects predominantly elderly patients with comorbidities (Williams et al., 2010, Liam et al., 2001). The prevalence of *Pa* in CAP ranges from 1,5 % (Sadikot et al., 2005, Sopena et al., 1999) to 4,2 % (Restrepo et al., 2018). Risk factors are recent discharge from hospital, residence in a nursing home, smoking, frequent antibiotic use (Sadikot et al., 2005, Monso et al., 2003), pre-existing lung conditions such as very severe chronic obstructive pulmonary disease (COPD) or bronchiectasis, inverse ratio ventilation, prior tracheostomy or prior infection or colonization with *Pa* (Restrepo et al., 2018). Being isolated from 18,1 % of nosocomial pneumonias, *Pa* is the second most common pathogen leading to hospital-acquired pneumonia (HAP) (Lister et al., 2009, Gaynes et al., 2005). Hospital stays modify the oropharyngeal microbial flora, and microaspirations can cause HAP in elderly patients with comorbidities (Williams et al., 2010, Kollef et al., 2005). Ventilation stretch injury (Williams et al., 2010, Pugin et al., 2008), intubation epithelial injury and the possibility of biofilm formation (Williams et al., 2010, Safdar et al., 2005, Adair et al., 1999) lead to ventilation-associated pneumonias (VAP) with a mortality rate of up to 34-48 %, prolonged ICU stays, long hospitalizations and complications such as multiorgan dysfunction and septic shock (Sadikot et al., 2005, Heyland et al., 1999, Rello et al., 1997).

Burn wound infections with *Pa* are characterized by high mortality rates of up to 33 %, long duration of hospitalization and ventilation, high numbers of implemented surgeries and necessary blood products, and high antibiotic costs in comparison to infections caused by other pathogens (Armour et al., 2007).

Considering blood stream infections (BSI), 2-6 % are caused by *Pa* which is generally considered the second most common pathogen in this context (Lister

et al., 2009). Diekema et al. (1999) found *Pa* to cause 10,6 % of BSI in Northern and Southern America and Canada. These are associated with high mortality (37 %) and morbidity, especially with cardiovascular and respiratory organ systems affected, high severity of the underlying condition, high age, neutropenia and long hospital stay prior and due to nosocomial bacteraemia (Scheetz et al., 2009).

Besides, *Pa* can cause otitis externa after water exposure of the external auditory canal with a lifetime prevalence of 10 % (Schaefer and Baugh, 2012).

1.1.2.2 Host factors

Since *Pa* is a widespread pathogen, healthy human immune systems deal with it successfully (Williams et al., 2010). However, patients with compromised mechanical mucosal barriers or immune systems as well as patients after broad-spectrum antibiotic therapy are at risk to acquire *Pa* infections more easily (Sadikot et al., 2005, Gellatly and Hancock, 2013, Lister et al., 2009, Blanc et al., 1998).

Age, cancer, neutropenia, immunosuppression, HIV and a post-transplantation condition negatively affect the efficiency of the immune system and are therefore identified as the conditions which favour *Pa* infections (Sadikot et al., 2005, Gellatly and Hancock, 2013). *Pa* pneumonia in HIV patients entails prolonged hospitalizations as well as higher rates of bacteremia and death (Sadikot et al., 2005, Vidal et al., 1999, Afessa and Green, 2000). In immunosuppressed patients, *Pa* pneumonia imposes a mortality rate of 40 % (Sadikot et al., 2005). The specific composition of the airway surface liquid and consequent respiratory epithelium mucociliary clearance of particles and pathogens are highly relevant for maintaining the host mechanical mucosal barrier (Gellatly and Hancock, 2013).

The mechanical barrier can be disrupted in case of a pre-existing cystic fibrosis (CF), COPD or different tissue injuries. These can occur due to ventilation, tracheostomy, catheter, surgical procedures or burn wounds (Lister et al., 2009). Gil-Perotin et al. (2012) observed a colonization rate of 87 % and biofilm formation on 95 % of endotracheal tubes in ventilated patients. 19 % subsequently developed VAP which often resulted in antibiotic treatment failure

and relapse of VAP. For instance, after antibiotic treatment of VAP caused by *Pa*, *Pa* cells could still be found in biofilms to an extent of 70 %.

4-15 % of COPD patients are colonized with *Pa* and display very variable symptoms for varying amounts of time (Gellatly and Hancock, 2013, Patel et al., 2002).

In CF patients` lungs, *Pa* is the prevailing pathogen especially in patients over 24 years old (Moradali et al., 2017). A mutation in the chloride channel CFTR provokes a dehydrated and thick airway secretion and strongly impeded mucociliary clearance. When mucus is retained, pathogens and particles cannot be cleared from the lung. Consequently, neutrophil motility is decreased which may lead to neutrophil necrosis, degranulation and tissue injury (Gellatly and Hancock, 2013). Finally, the retained cytokines and growth factors together with bacteria cause chronic inflammation and consequent lung damage and fibrosis (Venkatakrishnan et al., 2000, Sadikot et al., 2005). Altered mucosal barriers and cytokine and chemokine environment (Gellatly and Hancock, 2013), and its ability to anaerobic growth and biofilm formation (Davies and Bilton, 2009) facilitate *Pa* colonization.

Until the age of 3 years, 72,5 % of CF patients have been culture-positive at least once and 97,5 % show signs of infection in culture and serology. These early infections occur intermittently. Phenotypically, the causative agent *Pa* can be characterized as pigmented, non-mucoid and susceptible to antibiotics. A variety of genotypes can be found (Burns et al., 2001). The phenotypes of *Pa* infections later in life differ from the early ones to a high degree (Burns et al., 2001) and their genotypes are rather clonal (Mulcahy et al., 2010). Generally speaking, while establishing a chronic infection, cells experience stress such as inflammation, antibiotic therapy or oxidative stress and new genotypes and phenotypes emerge and spread clonally (Moradali et al., 2017).The shift from an acute, early infection to a chronic one involves mutations in Lipid A and O antigen, the loss of virulence factors such as pili and flagella, the overexpression of the exopolysaccharide alginate implying a mucoid phenotype, persistence and biofilm formation, antibiotic resistance and hypermutability (Gellatly and Hancock, 2013, Hogardt

and Heesemann, 2010, Mena et al., 2008, Moradali et al., 2017, Mulcahy et al., 2010, Sadikot et al., 2005, Smith et al., 2006, Wolfgang et al., 2004). Furthermore, it has been shown that *Pa* colonization modulates CF progression (Jacques et al., 1998).

1.1.2.3 Pathomechanisms

There are numerous virulence factors which contribute to successful *Pa* colonization.

To begin with, *Pa* employs numerous enzymes such as phospholipases, proteases, and elastases which remove immune molecules such as antibodies, complement factors or surfactant and breach through tight junctions (TJs) and epithelial barriers (Gellatly and Hancock, 2013, Azghani, 1996). Furthermore, secretion of ExoA, an inhibitor of elongation factor 2 for protein biosynthesis (Gellatly and Hancock, 2013), renders repairing of destroyed TJs impossible (Azghani, 1996). Moreover, *Pa* ExoA secretion causes cell death and a decreased immune response (Gellatly and Hancock, 2013, Schultz et al., 2000). Jaffar-Bandjee et al. (1995) found high ExoA levels in CF patients especially during exacerbations. This may explain how high anti-ExoA antibody titers are protective in *Pa*-caused human sepsis and how they can decrease mortality (Sadikot et al., 2005). Additionally, *Pa* disposes of a so-called type 3 secretion system (T3SS) which mediates the secretion of the exotoxins ExoS, T, U and Y (Gellatly and Hancock, 2013). Acute infections in the presence of these secreted exotoxins display worse clinical outcomes (Hauser et al., 2002). The main effectors are ExoS and ExoU. ExoS causes cytoskeleton alterations, cell division arrest, loss of cell-to-cell contacts and is expressed by 70-80 % of clinical isolates (Williams et al., 2010). ExoU disintegrates the host cell membrane and is responsible for early mortality above all (Gellatly and Hancock, 2013, Horcajada et al., 2019). In consequence, TJs can be destroyed and the basolateral surface of an epithelium can be invaded (Sadikot et al., 2005). Berube et al. (2016) introduce a model according to which *Pa* invasion into the bloodstream begins with T3SS-mediated destruction of immune cells and pulmonary epithelium type

I pneumocytes and continues with T2SS-mediated degradation of extracellular matrix and VE-Cadherin.

Pili for adherence, flagella for motility and fimbriae for attachment contribute to swarming, microcolony formation (Gellatly and Hancock, 2013), and stable (Moradali et al., 2017) and rapid biofilm formation (Donlan, 2002). However, their expression is very immunogenic as pili can be recognized by host toll-like receptor 2 (TLR 2) and flagella bind to TLR 5 (Gellatly and Hancock, 2013, Sadikot et al., 2005).

Pa expresses phenazines as well as the siderophores pyoverdine and pyochelin. The pigment pyocyanin provokes oxidative stress for host cells, impairing catalase activity and mitochondrial electron transport. It causes apoptosis of neutrophils, disrupts ciliary beating and antibody-mediated phagocytosis by macrophages, and modulates IL8 expression (Sadikot et al., 2005, Williams et al., 2010, Gellatly and Hancock, 2013).

Quorum sensing (QS) coordinates the response of a *Pa* population to different environments via collective auto-inducer molecule expression. 10 % of genes and 20 % of the expressed proteome are modulated by this manner (Gellatly and Hancock, 2013). QS has an impact on survival, colonization, virulence factors, phenotypical changes in switching from an acute to a chronic infection. Similarly, QS interplay reflects different stages of lung disease in CF exacerbations (Moradali et al., 2017).

Stochastically and epigenetically regulated (Fasani and Savageau, 2015), a small fraction of a genotypically identical *Pa* population can enter a phenotypically different stage of persistence under stress conditions. Persistence goes along with the initiation of metabolic changes as the arrest of cell growth and division, DNA replication, transcription and translation, protein and cell wall biosynthesis and the expression of virulence factors for the individual cell (Fasani and Savageau, 2015, Maisonneuve and Gerdes, 2014). Stress and antibiotic exposure can be survived and thus, persisters pave the way for recurrent and chronic infections (Moradali et al., 2017). *Pa* populations in CF lungs and in

biofilms exhibit an extraordinarily high persister fraction (Breidenstein et al., 2011).

Another highly relevant factor for the chronicity of *Pa* infections is its capacity to form biofilms. Biofilms consist of microbe microcolonies enveloped in the biofilm matrix of polysaccharides such as Pel, Psl and alginate, proteins and lipids. This matrix accounts for 90 % of the biofilm (Donlan, 2002), and confers mechanical stability and protection, a channel infrastructure, a nutrient and energy storage, an electrical attachment possibility, the capacity to bind water and the possibility of cell-cell-communication and horizontal gene transfer (HGT) to the bacterial population (Donlan, 2002, Gellatly and Hancock, 2013, Moradali et al., 2017). Indeed, transformation rates are 10-600-fold higher within a biofilm (Donlan, 2002). Furthermore, cells likely develop hypermutability (Williams et al., 2010). QS can support the development of stable biofilms and regulate the binding and releasing process of bacteria (Gellatly and Hancock, 2013, Moradali et al., 2017, Donlan, 2002). Within a biofilm, a union of individually possibly sensitive bacteria are commonly very resistant to the host immune system, disinfectants, and also antibiotics (Donlan, 2002, Gellatly and Hancock, 2013, Stewart and Costerton, 2001). There are several reasons for this phenomenon: firstly, because penetration of these substances is hindered by surface charge-mediated repulsion, e.g. for aminoglycosides, or by inactivation on the surface. Secondly, environmental changes such as anaerobic conditions impair aerobically effective aminoglycoside activity. Metabolically rather inactive and slowly growing bacteria prevent penicillin effectiveness. Acidic, osmotic and oxidative stress may change porin expression and permeability of bacterial cell walls which finally prevents antibiotic penetration. Furthermore, a small persister fraction might establish within the biofilm (Stewart and Costerton, 2001).

1.1.3 Antibiotic resistance and resistance mechanisms

1.1.3.1 Genetic properties of antibiotic resistance mechanisms

Antibiotic resistance can be subclassified into intrinsic, adaptive and acquired resistance. This relates to the availability of antibiotic-converting enzymes, substrate properties (such as charge and the possibility to penetrate the cell

membrane), modulation of antibiotic concentrations (which is influenced by membrane permeability, porins and efflux pumps), and the substrate specificity of the enzymes (Breidenstein et al., 2011, Jacoby, 2009).

Contributing to the intrinsic resistance of *Pa*, the *Pa* outer membrane has a low permeability of 12-100 times less than the *E. coli* outer membrane (Yoshimura and Nikaido, 1982, Breidenstein et al., 2011).

Bacteria can acquire resistance through HGT via conjugation, transformation and transduction or through genetic mutations (Breidenstein et al., 2011). Several enzymes can be passed horizontally. Among these enzymes are extended-spectrum-beta-lactamases (ESBLs) which cleave monobactams, penicillins and 1st, 2nd and 3rd generation cephalosporins. Carbapenems and β-lactamase inhibitors cannot be processed. In the presence of ESBL, mortality rates and hospitalization durations increase (Paterson and Bonomo, 2005, Bush, 2010). Carbapenemases can cleave all β-lactams and carbapenems (Bush, 2010). Selection pressure seems to be relevant for their distribution, as carbapenem treatment leads to carbapenemase exchange in CF patients (Lambert, 2002, Sacha et al., 2008). Additionally, acetyl-, adenylyl- and especially phosphotransferases modify aminoglycosides in the bacterial cytoplasm and can be passed horizontally (Breidenstein et al., 2011, Lambert, 2002, Vakulenko and Mobashery, 2003).

Conditions which favour the occurrence of mutations are (i) bacterial biofilm formation, which display an up to 105-fold increased mutability in ciprofloxacin and rifampicin resistant populations due to downregulation of enzymes preventing oxidative DNA damage (Driffield et al., 2008), (ii) previous mutations in mutator genes as *mutS* or *mutL* (Wiegand et al., 2008), and (iii) initial CF. The percentage of strains considered as hypermutable is 6 % in the environment, 13 % epidemically, 10 % in early CF isolates, 37 % in chronic CF isolates (Kenna et al., 2007) and 36 % generally in strains colonizing CF patients (Oliver et al., 2000).

Mutations are able to cause increased efflux pump expression (Lister et al., 2009). Moreover, the target structures of antibiotics can be mutationally altered,

e.g. in PBP3-encoding genes which then has great impact on the efficacy of β-lactams (Cabot et al., 2018). Furthermore, mutations in the gyrase-encoding genes *gyrA* and *gyrB* and the topoisomerase-encoding genes *parC* and *parE* have been shown to influence fluoroquinolone susceptibility (Breidenstein et al., 2011, Akasaka et al., 2001, Dunham et al., 2010). In 22 multiresistent, clonally different strains, 91 % presented a *gyrA* modification (Henrichfreise et al., 2007). Whereas *parC* mutations alone did not change MIC values in ciprofloxacin resistant PA14 strains to a relevant extent, *gyrA* or *gyrB* mutations caused an 8- to 16-fold increase, and *gyrA* and *parC* mutations entailed a 256-fold increase, bestowing resistance to every respective strain. Again, combinations with mutated efflux pump regulators were shown to exacerbate the effect (Bruchmann et al., 2013).

1.1.3.2 Role of efflux pumps in antibiotic resistance

The cell envelope of *Pa* harbours various efflux pump families (Lister et al., 2009). The efflux pump MexAB-OprM plays a significant role in intrinsic and adaptive resistance (Masuda et al., 2000) due to its high prevalence, constitutive expression and its wide spectrum of substrates (Moradali et al., 2017), especially for β-lactams (Lister et al., 2009, Putman et al., 2000). Secondly, MexXY-OprM is a less constitutively expressed efflux pump in wildtype (WT) strains, but it is still important especially for acquired and adaptive resistance, as its expression can be induced in the presence of subinhibitory concentrations of its substrates (Moradali et al., 2017, Masuda et al., 2000). Clinically scarcely important efflux pumps (Moradali et al., 2017) are MexCD-OprJ and MexEF-OprN (Lambert, 2002). 39 % of 190 investigated BSI isolates overexpressed at least one of these efflux pumps, whereby MexY was overexpressed in 33 % of β-lactam and aminoglycoside resistant isolates and 13,2 % of all isolates, MexB in 25 % of β-lactam and aminoglycoside resistant isolates and 12,6 % of all isolates, MexF in 4,2 % and MexD in 2,2 % of all isolates (Cabot et al., 2011). Gomis-Font et al. (2020) associated imipenem/relebactam resistance to mutations in genes encoding both MexAB-OprM and OprD.

1.1.3.3 Role of porins for resistance to antibiotics

Several porins are integrated into the outer membrane of *Pa*. Porins play a central role for uptake of nutrients such as for instance glucose (OprB and OprB2) or phosphate (OprP and OprO) and some of them play also an important role in antibiotic resistance or susceptibility (Chevalier et al., 2017).

OprF is considered the principal porin of *Pa* (Nicas and Hancock, 1983, Brinkman et al., 2000, Chevalier et al., 2017) and seems to play a central role for virulence probably by stabilizing membrane integrity.

OprD, however, is linked to the uptake of carbapenem antibiotics. Imipenem (Li et al., 2012) and also meropenem are substrates of OprD, whereas aminoglycosides, quinolones, and β-lactams are not (Huang and Hancock, 1993). Pre-existing OprD polymorphisms confer bacteria the capability of developing carbapenem resistance upon carbapenem exposure and selective pressure (Shu et al., 2017). Besides, the presence of OprD was associated with elevated resistance to a low pH environment and human serum, furthermore bacterial dissemination and increased toxicity against mouse macrophages in a PA14 mouse model (Skurnik et al., 2013). OprD loss is even more efficient when coinciding with increased β-lactamase expression (Livermore, 1992).

1.1.3.4 Role of β-lactamase for antibiotic resistance

AmpC is a penicillin and cephalosporin hydrolyzing β-lactamase enzyme encoded by the bla_{ampC} gene. β-lactamase inhibitors such as tazobactam, sulbactam or clavulanic acid cannot always inhibit AmpC (Jacoby, 2009, Maiti et al., 1998), however, cloxacillin, oxacillin and aztreonam impede AmpC activity (Jacoby, 2009). *ampC* overexpression is one main mechanism in acquired and adaptive β-lactam resistance (Breidenstein et al., 2011, Ziha-Zarifi et al., 1999). One study estimated that patients infected with an *ampC* overexpressing strain are 67,5 times as likely to be treated with inappropriate antibiotics and 12,2 times as likely to develop persistent bacteraemia (Tam et al., 2009).

ampC displays a relatively low basal expression in *Enterobacteriaceae* but can be induced in a complex metabolic pathway closely linked to cell wall recycling which will be explained in the following chapter. Interestingly, as *Acinetobacter*

baumannii and *E. coli* lack *ampR*, they are considered as *ampC*-uninducible (Jacoby, 2009). The stimulus for *ampC* induction is antibiotic exposure. Some antibiotics such as cefepime, cefpirome and 4th generation cephalosporins do not induce *ampC* expression (Breidenstein et al., 2011). The hydrolysable antibiotics cefotaxime, ceftriaxone, ceftazidime, cefepime, cefuroxime, piperacillin and aztreonam are classified as weak inducers. Benzylpenicilllin, amoxicillin, ampicillin, cefazolin, imipenem and cefoxitin are considered as strong inducers. Imipenem and cefoxitin cannot be hydrolyzed by AmpC (Jacoby, 2009).

Numerous mutations in the cell wall recycling effectors explained in the following chapter can cause *ampC* overexpression which is widely spread. Among 22 multiresistent, clonally different strains, 73 % showed AmpC overproduction (Henrichfreise et al., 2007). Moya et el. (2012) investigated six pan-β-lactam resistant strains and demonstrated that all of them showed *ampC* overexpression. This finding was common among 24,2 % of 190 investigated bloodstream isolates (Cabot et al., 2011). 96 % of these *ampC* overexpressing strains were resistant to piperacillin-tazobactam, 86 % were ceftazidime and cefepime resistant, 62,5 % were imipenem and meropenem resistant. All of the β-lactam and aminoglycoside resistant isolates were characterized by *ampC* overexpression. Higher AmpC production may influence imipenem, but not necessarily meropenem susceptibility (Lister et al., 2009). Out of 76 bloodstream isolates, Tam et al. (2007) found 15 to be ceftazidime resistant and 14 (18,4 %) to overexpress *ampC*. Gene expression was over 5-fold increased and basal enzyme activity increased over 20-fold, suggesting that both transcriptional and translational changes may occur in the process.

1.2 The cell wall recycling pathway

The bacterial cell wall surrounding the cytoplasmic membrane of Gram-negative bacteria is made of peptidoglycan (PGN). Figure 1 visualizes the structure of PGN. It is composed of few layers (compared to the PGN of Gram-positive bacteria) of glycan strands, N-acetyl-glucosamine and N-acetyl-muramid acid in alteration, which are cross-linked by small peptide strands whose amino acids

again can be cross-linked among each other (Vollmer et al., 2008, Irazoki et al., 2019).

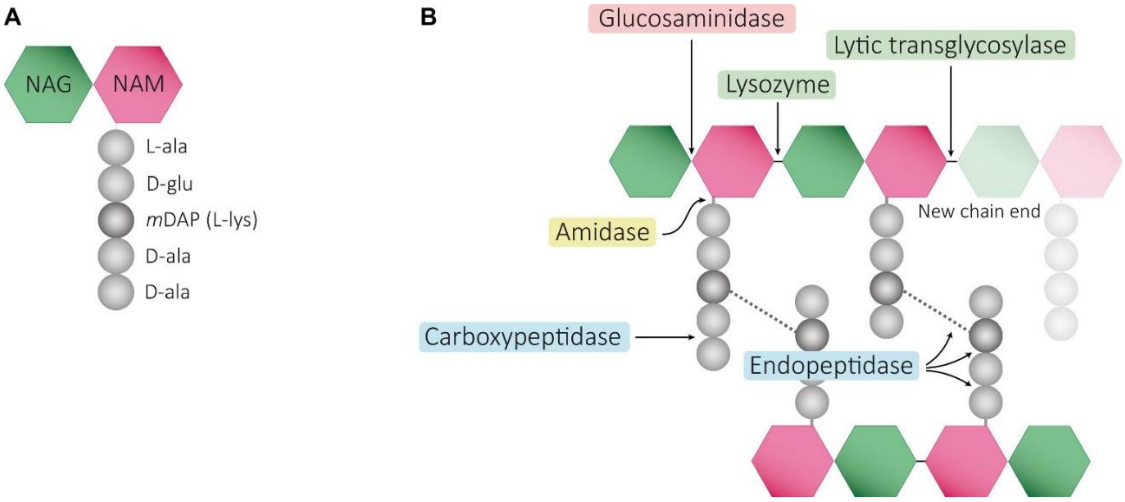

Figure 1: PGN structure

(A) PGN consists of the alternating glycan strands N-acteyl-glucosamine and N-acetyl-muramic acid. Peptide strands are connected to the glycan strands and in turn linked to one another. In this way, PGN layers are tied together by their peptide strands.

(B) Besides, different enzymes involved in the degradation of the PGN layer are designated.

This figure was kindly provided by Irazoki et al. (2019).

As illustrated in Figure 2, bacterial PGN is recycled. PGN recycling involves the degradation of old PGN elements as well as the polymerization and cross-linking of new PGN fragments which are both carried out by specialized enzymes (Park and Uehara, 2008, Reith and Mayer, 2011, Fisher and Mobashery, 2014). Old fragments released from the PGN layer, called muropeptides, are transported into the cytoplasm via the permeases AmpG (Jacobs et al., 1994, Dietz et al., 1997) and AmpP. AmpP plays only a minor role as it is expressed AmpR-and β-lactam-dependently whereas AmpG is the main and independently expressed permease (Perley-Robertson et al., 2016, Kong et al., 2010). Muropeptides are further processed by various enzymes. LdcA cleaves the terminal amino acid D-alanine (Templin et al., 1999). NagZ converts Glc-1,6-anhydro-MurNAc-peptides into 1,6-anhydro-MurNAc-peptides (Stubbs et al., 2008). The resulting 1,6-anhydro-MurNAc-peptides such as 1,6-anhydro-MurNAc-tri/penta-peptides,

derepress AmpR, the transcriptional regulator of *ampC*. Upon β-lactam exposure, PGN cross-linking is impeded. This entails increased PGN turnover and consequently the accumulation of these metabolites in the cytoplasm, finally resulting in *ampC* overexpression (Jacobs et al., 1997, Fisher and Mobashery, 2014, Dietz et al., 1997, Torrens et al., 2019).

The amidase AmpD removes the remaining amino acids (Zhang et al., 2013, Jacobs et al., 1995, Jacobs et al., 1994, Holtje et al., 1994) which leads to the generation of 1,6-anhydro-MurNAc and free peptides. 1,6-anhydro-MurNAc-peptides can then be modified by the enzymes AnmK, MupP, AmgK and MurU which finally results in UDP-MurNAc (Borisova et al., 2014, Borisova et al., 2017, Gisin et al., 2013, Fumeaux and Bernhardt, 2017, Barreteau et al., 2008). Similarly, Fructose-6-phosphate can be processed by the enzymes GlmS, GlmM and GlmU to generate UDP-GlcNAc which can be converted into UDP-MurNAc by the enzymes MurA and MurB (Barreteau et al., 2008). A peptide chain is added to the resulting UDP-MurNAc by Mur ligases MurC, MurD, MurE and MurF, forming UDP-MurNAc-pentapeptides (Barreteau et al., 2008, Kouidmi et al., 2014). UDP-MurNAc-pentapeptides, in turn, are essential for the occupation of the active site of AmpR and AmpR-dependent repression of *ampC* transcription, and therefore ensure the normally established repression of *ampC* expression (Jacobs et al., 1997).

As UDP-MurNAc-pentapeptides are designed and dedicated to form part of the bacterial cell wall, in further steps they have to be transferred across the inner bacterial membrane, through the periplasm and integrated into the bacterial cell wall. Therefore, they are ligated to the lipid carrier Und-P by the cytosolic translocase MraY. The resulting complex is called Lipid I (Bouhss et al., 2004, Ikeda et al., 1991). The addition of an UDP-GlcNAc molecule by MurG results in the formation of the Lipid II complex (Brown et al., 2013, Sonnabend et al., 2020). Lipid II is flipped across the inner membrane and into the periplasmic space by MurJ, where the arriving new PGN fragments are polymerized and crosslinked in order to build up the PGN layer (Sham et al., 2014).

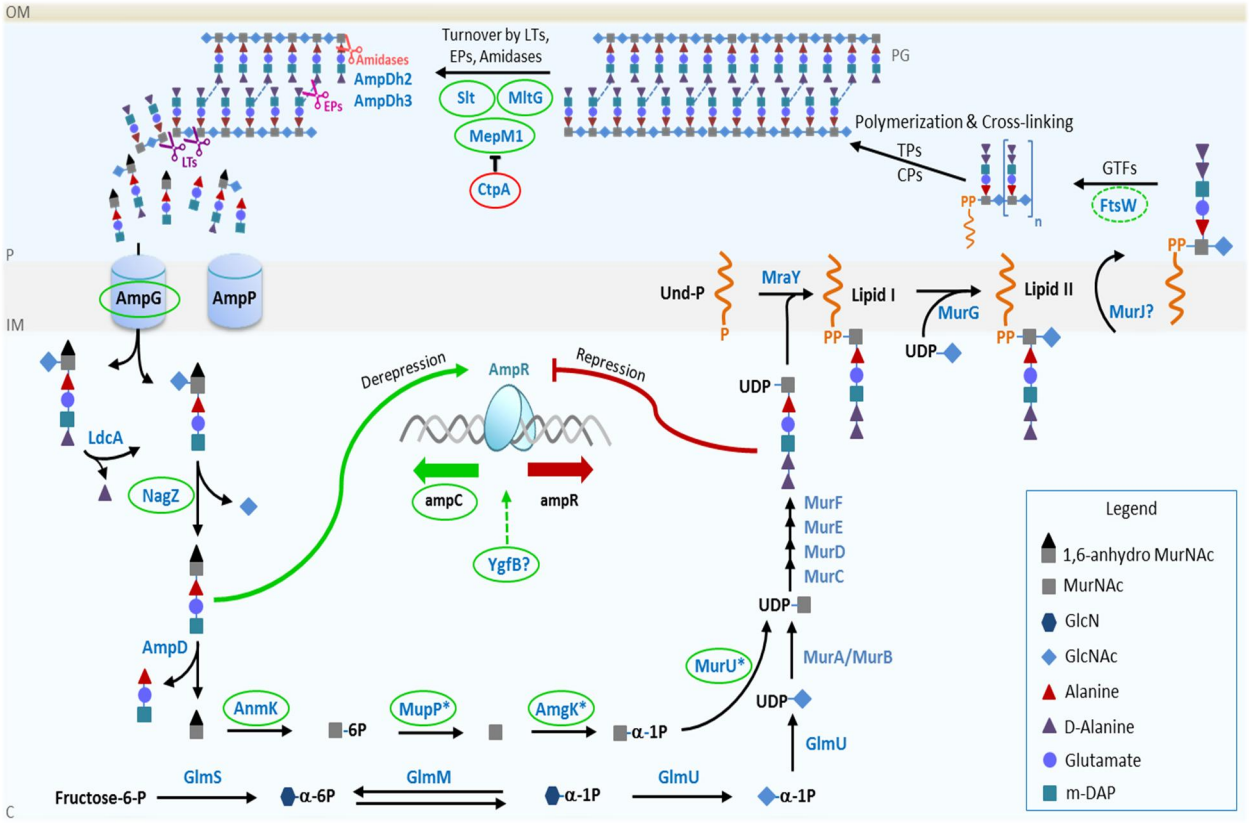

Figure 2: The PGN recycling pathway

Proteins with green and red framing were validated by Sonnabend et al.(2020) to increase or decrease, respectively, β-lactam resistance. This figure was kindly provided by Sonnabend et al. (2020) and ASM Journals.

1.3 The association between *ampC* expression and PGN recycling

1.3.1 ampR

AmpR is a global transcriptional regulator belonging to the LysR family (Bartowsky and Normark, 1993, Jacobs et al., 1997, Lindquist et al., 1989, Henikoff et al., 1988). It can bind to the *ampC* promoter region (Lodge et al., 1993). Its gene is located upstream of *ampC* (Lodge et al., 1990). AmpR contributes to the regulation of β-lactamase expression and acts in an activating way (Lindberg et al., 1985, Lindberg et al., 1988, Kong et al., 2005). The ability of AmpR to transactivate AmpR-regulated promoters is modulated by the interaction with the PGN precursors anhydro-MurNAc-tri/pentapeptides and UDP-MurNAc-pentapeptides. While predominant binding of anhydro-MurNAc-

tri/pentapeptides promotes AmpR-mediated transactivation, predominant binding of UDP-MurNAc-pentapeptides represses AmpR-mediated transactivation (Hanson and Sanders, 1999, Balcewich et al., 2010).

However, the regulatory role of AmpR is not restricted to the *ampC* promoter and affects *Pa* gene expression more globally (Balasubramanian et al., 2015, Balasubramanian et al., 2012). The set of genes regulated by AmpR comprises over 500 different genes. AmpR is involved in the upregulation of flagella synthesis, the T3SS, *ampG*, *creD, oprM* and in the downregulation of phenazines, some efflux pumps, amino acid metabolism and cell wall envelope genes, virulence factors, toxin and alginate secretion, QS and biofilm formation, adaption, protection and stress response (Balasubramanian et al., 2012, Balasubramanian et al., 2015). It is essentially involved in the shift from acute to chronic infections and is also capable of regulating genes which have been acquired horizontally. In an Δ*ampR* mutant, *creD* was upregulated and *creB* downregulated at the same time, suggesting that AmpR could contribute to CreD regulation independently of CreB (Balasubramanian et al., 2012). *creB* and *creD* are introduced in chapter 1.3.3.

Interestingly, *ampR* polymorphisms exist in *Pa* WT strains and there are *ampR* mutations which favour *ampC* overexpression. For instance, Schmidtke and Hanson (2008) isolated an *ampD* and *ampR* mutated strain which presented a 5000-fold elevated basal *ampC* RNA expression level.

Several studies demonstrated that modulation of genes involved in PGN recycling can strongly impact *ampC* expression probably by changing the amount and ratio of catabolites such as anhydro-MurNAc-peptides and UDP-MurNAc-pentapeptides finally affecting AmpR-mediated *ampC* expression. Most of these studies, however, were performed using the lab strain *Pa* PAO1 which is quite sensitive to treatment with β-lactam antibiotics (Cabot et al., 2014, Dietz et al., 1997, Fisher and Mobashery, 2014, Juan et al., 2006, Normark, 1995, Torrens et al., 2019, Zamorano et al., 2010b, Zamorano et al., 2011).

1.3.2 dacB

In the clinical context the mutation of *dacB* gene plays an important role regarding multi-drug resistant strains.

The *dacB* gene encodes the low molecular mass penicillin-binding protein (LMM-PBP) PBP4, a bifunctional acyl-serine-transferase with D,D-endopeptidase and, to a lower degree, D,D-carboxypeptidase activity. Its inhibition by antibiotics or mutational inactivation entail an increase in anhydro-MurNAc-pentapeptide levels and therefore *ampC* induction (Aguilera Rossi et al., 2016, Lee et al., 2015).

Deletion of *dacB* results in increased *ampC* expression, for PAO1 more than for PA14, increased MIC values for tested penicillins and cephalosporins and elevated CreD levels which could be due to activation of CreBC (Zamorano et al., 2010a). In PAO1 Δ*dacB* strains, *ampC* expression is basically 50 times as high as in WT strains and inducible by 2,3-fold. The loss of PBP4 in PAO1 strongly increases resistance to piperacillin, cefotaxime and ceftazidime (Cavallari et al., 2013). Moreover, 5 out of 6 pan-β-lactam resistant isolates investigated by Moya et al. (2012) disposed of a modification in PBPs in general, 4 showed an inactive PBP4 by *dacB* deletion and subsequent AmpC overproduction. Torrens et al. (2019) found 1000-fold *ampC* expression in a PAO1 Δ*dacB* Δ*ampD* mutant, 100-fold elevated anhydro-MurNAc-tripeptide and 160-fold elevated anhydro-MurNAc-pentapeptide counts. Moya et al. (2009) detected a *dacB* mutation in 30 out of 36 ceftazidime resistant strains which conferred a high AmpR- and AmpC-dependent β-lactam resistance to them. Antibiotic resistance due to mutations in *dacB* surpasses the resistance level caused by *ampD* single mutations and rather equals the resistance level of PAO1 Δ*ampD* Δ*ampDh2* Δ*ampDh3* triple mutants. AmpD and its paralogues AmpDh2 and AmpDh3 are introduced below.

1.3.3 creBC

(Moya et al., 2009) provided a model in which they claim that the reasons for hyperresistance of *Pa* after *dacB* inactivation are changes in the composition of muropeptides and the activation of CreBC leading to AmpC hyperproduction.

CreBC is a two-component system which regulates the expression of 9 different genes in *E. coli*, the *cre* regulon. Among these genes, CreD is located

downstream and encodes for an inner membrane protein whose function is still unknown. *creBC* could be considered as global regulatory genes, which especially regulate intermediary metabolism (Avison et al., 2001, Avison et al., 2004). Cariss et al. (2008) show how the CreBC two-component system (with CreB responsible for DNA interaction and transcriptional regulation) is involved in metabolic regulation processes in *E. coli*. The CreBC two-component system is also present in *Aeromonas, Pa* and *Stenotrophomonas maltophila*. The inner membrane protein CreD has been associated with the stability of the cell wall in *Stenotrophomonas maltophila* (Huang et al., 2015). *blrAB*, an *Aeromonas* species regulatory gene very similar to *creBC* in *E. coli*, modulates the expression of the β-lactamases CepH, AmpH and ImiH in *Aeromonas* species. When these *Aeromonas* β-lactamases were cloned into *E. coli DH5α*, they were regulated in a CreBC-dependent manner (Avison et al., 2001, Avison et al., 2004). 53 genes could be observed to be differently regulated in a PAO1 Δ*creBC* mutant in comparison to PAO1 WT, suggesting that *creBC* is also important for bacterial physiology and biofilm formation. It was described that BlrAB can regulate β-lactamase expression directly without AmpR in *Aeromonas* (the triggers for *BlrAB* activation being PGN changes or specific mutations), whereas *creBC* activation leads to rather general metabolic changes which influence biofilm formation, bacterial physiology and virulence, work against cell wall defects and improve effective AmpC function (Juan et al., 2017). Juan et al. (2017) also hypothesize that PGN composition changes of course induce an AmpR-dependent pathway of *ampC* (de)repression but might also be perceived by the inner membrane protein CreC, leading to CreBC activation. Similarly, a study by Tayler et al. (2010) concluded that muropentapeptides are responsible for the activation of *blrAB* in *Aeromonas* and subsequent β-lactamase expression. This is interesting as it represents the same activating metabolites as in the AmpR-dependent pathway of β-lactamase induction in other bacteria. Importantly, *creBC* deletion can indeed decrease β-lactam MICs, however, a direct impact on *ampC* expression rates and inducibility could not be observed (Juan et al., 2017).

dacB inactivation is connected to an *ampC* induction as well as to a rise in CreD expression, with a weak manifestation for weak *ampC* inducing β-lactams as

ceftazidime and a strong manifestation for strong inducers such as imipenem (Zamorano et al., 2014). Besides the fact that *dacB* inactivation leads to CreD overproduction, it has also been investigated that high MIC values correlate with CreBC activation (Zamorano et al., 2010a). (Moya et al., 2009) observed *dacB* inactivation in 30 out of 36 ceftazidime resistant mutants. All of them overproduced CreD. *creD* expression was investigated to be inducible by β-lactamase inducers. In Δ*ampD* mutants, CreD inducibility is low again whereas Zamorano et al. (2014) (summarizing previous studies) mention an increase of CreD inducibility upon deletion of *ampG, nagZ, ampR* and *ampC*. They also indicate that a deletion of *creBC* alone has no effect on β-lactam MIC values. However, an additional deletion of *creBC* in Δ*dacB* mutants can lower the previously very elevated MIC values and impair the development of ceftazidime resistant Δ*dacB* mutants.

1.3.4 ampG

Catabolic muropeptides such as Glc-anhydro-MurNAc-peptides are transported into the cytoplasm by the inner membrane permease AmpG. Mutational *ampG* inactivation prevents this transport and causes a decrease of muropeptides in the cytoplasm. Consequently, this leads to reduced *ampC* expression (Torrens et al., 2019). Moreover, additional deletion of *ampG* abrogates the resistant phenotype of PAO1 Δ*ampD* or Δ*dacB* single mutants as well as of double mutants (Zamorano et al., 2011).

1.3.5 nagZ

After transport of Glc-anhydro-MurNAc-peptides into the cytoplasm, NagZ converts this muropeptide into AmpR-activating anhydro-MurNAc-peptides. Deletion of *nagZ* prevents this conversion resulting in reduced *ampC* expression and also abrogates hyperresistance of Δ*ampD* and Δ*dacB* single or double mutants (Zamorano et al., 2011).

The importance of AmpG and NagZ leads to the idea that the inactivation of AmpG or NagZ by small molecules could be a potential therapeutic strategy.

1.3.6 ampD

Anhydro-MurNAc-peptides can be cleaved by the cytoplasmic amidase AmpD into anhydro-MurNAc and peptides which diminishes the pool of AmpR-activating anhydro-MurNAc-peptides.

Consequently, deletion of *ampD* in *Pa* entails an accumulation of anhydro-MurNAc-tri/pentapeptides and in consequence elevated β-lactamase levels (Dietz et al., 1997, Normark, 1995). In an investigation by Moya et al. (2008), 6 of 10 *ampC* overproducing strains presented an *ampD* inactivation. The degree of β-lactamase overproduction in *ampD* deletion mutants is higher for PAO1 than for PA14, without influencing CreD levels (Zamorano et al., 2010a). Juan et al. (2006) showed that mutational *ampD* inactivation leads to a 60-fold increase in AmpC production. Thus, *ampD* mutations represent - beside *dacB* mutations - an evolutionary strategy of *Pa* to establish β-lactam resistance. In addition to *ampD*, *Pa* cells possess the paralogues *ampDh2* and *ampDh3*.

To distinguish clearly between the three paralogues, Zhang et al. (2013) state AmpD to be the main amidase in the cytoplasm for processing 1,6-anhydro-MurNAc-derivates. The larger PGN fragment released from the cell wall are not processed by AmpD, but by AmpDh2 and AmpDh3. The processing of larger PGN fragments takes place in the periplasm thus suggesting a periplasmic location of AmpDh2 and AmpDh3. A signal sequence for transport into the periplasm has additionally been identified for AmpDh2 but not for AmpDh3. AmpDh2 and AmpDh3 are also able to participate in the processing of 1,6-anhydromuramyl-derivates, however, this accounts for only 6% or 12% of the overall enzyme activity, respectively. Since AmpDh2 and AmpDh3 show a higher affinity for muramyl-derivtes than for 1,6-anhydro-muramyl-derivates, it was assumed that not only AmpDh2 (which has a signal sequence for periplasmatic transport) but also AmpDh3 is located in the periplasm. However, the localization of AmpDh3 is questionable.

Pa disposes three type VI secretion systems (T6SS). Two of them serve to transfer substances after contact with other Gram-negative bacteria into the periplasmic space of these bacteria with the objective to compromise their

integrity and induce lysis (Chen et al., 2015, Wood et al., 2019, Han et al., 2019). In an environment with high bacterial density, it enables *Pa* to compete with other bacterial species in its vicinity. This is especially important in environments that are inhabited by different bacterial species, e.g. the lungs of CF Patients (Han et al., 2019, Wang et al., 2020). Thus, for instance, T6SSs have been shown to be upregulated in biofilms which consist of different species (Chen et al., 2015).

Wang et al. (2020) discovered that AmpDh3 (in contrast to AmpD and AmpDh2) is secreted via the H2-T6SS of *Pa* cells. This secretion process requires close contact to the prey cell and thus only occurred in experiments where bacteria were grown on solid but not in liquid media. It is assumed that AmpDh3 can be transferred to the periplasm of the neighboring cells (which can be other *Pa* cells, but also other species, such as *E. coli* and *Yersinia pseudotuberculosis*) where its amidase activity destroys the PGN envelope of the prey cells and exerts a toxic function.

AmpDh3 is encoded on a bicistronic operon together with PA0808 (in PAO1) or TUEID40_01954 (in ID40), respectively. PA0808 carries a signal sequence for the export into the periplasm and can mainly be found in the periplasm. Physical interaction between PA0808 and AmpDh3 has been proven and PA0808 neutralizes after binding the amidase activity of AmpDh3 and therefore protects *Pa* from AmpDh3-mediated lysis (Wang et al., 2020).

The localization of AmpDh3 itself is still debated. Whereas Zhang et al. (2013) refer to its enzymatic activity on the PGN layer as an argument for its periplasmatic localization, the absence of a periplasmatic export sequence, its impact on *ampC* expression and its secretion by T6SS could, however, lead to the assumption of a cytoplasmatic localization (Wang et al., 2020).

ampC derepression can be regulated more precisely to different degrees by the existence of AmpD paralogues: with all AmpD and both paralogues intact, *ampC* expression remained at a basal rate and was inducible. Upon the deletion of *ampD* and one additional paralogue, *ampC* expression rised to moderate or high levels and became hyperinducibe. In this case, *ampC* derepression was partial. If *ampD* and both paralogues were deleted, *ampC* expression reached a 1000-

fold higher level compared to PAO1 WT and was considered completely derepressed (Juan et al., 2006). Torrens et al. (2019) confirmed these results as they noticed an unchanged *ampC* expression in PAO1 for Δ*ampDh2* and Δ*ampDh3* single mutants, a 2-fold increase for Δ*ampDh2* Δ*ampDh3* double mutants and a 1000-fold increase for Δ*ampD* Δ*ampDh2* Δ*ampDh3* triple mutants which were characterized by producing 600 times the amount of anhydro-MurNAc-tripeptides and 150 times the amount of anhydro-MurNAc-pentapeptides. In a study by Schmidtke and Hanson (2008), nine clinical isolated were analyzed. The four CF isolates all showed partially derepressed *ampC* expression. All derepressed strains presented an *ampD* deletion, *ampDh2* WT and 67 % showed an *ampDh3* deletion.

From these data, it could be imagined that the enzymatic processing of 1,6-anhydro-MurNAc-derivates is initiated in the periplasm and is completed in the cytoplasm. Assuming this consecutive processing in the different compartments, the stepwise increased derepression of *ampC,* as soon as one or two or all AmpD paralogues are lacking, could be explained.

Thus, upon the deletion of *ampD*, AmpDh3 and, to a lower extent (Schmidtke and Hanson, 2008), AmpDh2 can complement for the amidase activity. In this manner, *Pa* is capable of developing resistance without an excessive disruption of the cell wall recycling process (Juan et al., 2006). Fitness, growth and competitiveness are unaffected in a Δ*ampD* single mutant, moderately affected in a Δ*ampD* Δ*ampDh2 or* Δ*ampD* Δ*ampDh*3 double mutant and considerably decreased in a Δ*ampD* Δ*ampDh2* Δ*ampDh3* triple mutant due to high AmpC levels. *ampDh3* seems to be a gene essentially important for virulence, too, as shown in a mouse infection model (Moya et al., 2008).

1.3.7 Identification of genes involved in PGN recycling modulating β-lactam resistance in a Multi-drug (MDR) resistant strain - ygfB

In a recent study, the MDR strain ID40 was used to identify genes involved in resistance to cefepime and meropenem (Sonnabend et al., 2020). ID40 is a clinical bloodstream isolate which carries an inactive *dacB* gene (Sonnabend et al., 2020, Willmann et al., 2018). These studies identified many already known

genes contributing to β-lactam resistance such as *ampG*, *nagZ* or the lytic transglycosylase *mltG* (Figure 2), but also some genes which were so far unknown to be associated with antibiotic resistance. Examples are the gene encoding for the murein endopeptidase MepM1 and the so far uncharacterized gene *ygfB*.

The uncharacterized gene *TUEID40_03245* (termed *PA5225* in PAO1) was named *ygfB*, as there do exist homologues in other bacterial species such as *Acinetobacter baumannii, Legionella pneumophila, E. coli* (here, 33 % of amino acids are identical) or *Haemophilus influenzae*. The *ygfB* gene is located in an operon, followed by the genes *pepP*, *ubiH*, *TUEID40_03242* (termed *PA5222* in PAO1) and *ubiI.* This operon architecture is commonly found in many other *Enterobacteriaceae* but usually lacks orthologues for *PA5222*.

PepP is a proline aminopeptidase. It is known to be involved in virulence and pyocyanin production. It is one of the critical virulence-associated genes identified using a *Pa-C. elegans* infection model (Feinbaum et al., 2012). It could contribute to protein and nutrient processing. Ubi H (2-octaprenyl-6-methoxyphenol hydroxylase) and Ubi I (2-octaprenylphenol hydroxylase) are involved in ubiquinone biosynthesis (Pelosi et al., 2016). Ubiquinone, also called coenzyme Q, functions in the respiratory electron transport chain and plays a pivotal role in energy generating processes (Aussel et al., 2014). The organization of these genes in a cluster, potentially an operon, might also suggest a connection of their functions.

It could be observed that in an ID40 Δ*ygfB* deletion mutant, resistance to many β-lactam antibiotics was decreased compared to ID40 WT and even fell below resistance breakpoints for cefepime and aztreonam (Sonnabend et al., 2020). Moreover, it could be demonstrated that the reduced β-lactam resistance is associated with decreased *ampC* mRNA expression and β-lactamase activity. These findings led to the question of how YgfB suppresses *ampC* mRNA expression. Unpublished data preceding the here presented study is illustrated in Figure 3 (Eggers et al., 2023). Transcriptomic analysis of ID40 strains shows that deletion of *ygfB* leads to increased mRNA expression of genes of the *alp* cluster

and both *ampDh3* and *TUEID40_01954* in ID40. As must be expected, *ampC* mRNA expression was significantly reduced in ID40 Δ*ygfB* compared to ID40. Amidase AmpDh3 is an enzyme involved in periplasmic processing of PGN elements recently released from the cell wall (Zhang et al., 2013). It was recently described that AmpDh3 is translocated into other bacteria by a T6SS and these bacteria are killed by the action of the amidase. TUEID40_01954 acts as an immunity protein for AmpDh3 (Wang et al., 2020). The *alp* gene cluster was proposed to be involved in the regulation of a programmed cell death pathway and in transcriptional activation of *ampDh3* (Pena et al., 2021).

Gene ID (ID40)	PAO1 orthologue	Product	Function	Δ*ygfB* vs WT	
				Log2-fold change	Adjusted p value
TUEID40_03245	PA5225	*ygfB*	unknown	-3.876	0
TUEID40_04486	PA4110	*ampC*	β-lactamase	-2.303	1.23E-7
TUEID40_01840	PA0908	*alpB*	Self-lysis pathway	2.053	0.000771
TUEID40_01839	PA0909	*alpC*	Self-lysis pathway	2.504	0.0000128
TUEID40_01838	PA0910	*alpD*	Self-lysis pathway	1.527	0.0179
TUEID40_01837	PA0911	*alpE*	Self-lysis pathway	1.367	0.0374
TUEID40_01945	PA0817	-	Glyoxalase-like domain protein	1.9	0.0000337
TUEID40_01955	PA0807	*ampDh3*	Amidase	5.395	3.446E-11
TUEID40_01954	PA0808	-	Immunity protein	2.504	1.87E-62

Figure 3: Transcriptomic analysis of ID40 and ID40 Δ*ygfB*

To address the question how YgfB might contribute to antibiotic resistance, mRNA was isolated from ID40 and ID40 Δ*ygfB* and a transcriptome analysis was performed using next generation sequencing. This figure depicts the mRNA expression of significantly altered genes in an ID40 Δ*ygfB* deletion mutant in comparison to ID40 WT. It was kindly provided by Eggers et al. (2023).

In an experiment of the working group shown in Figure 4 (A), an ID40 Δ*ygfB* deletion mutant which was complemented with a rhamnose inducible *ygfB* gene was used to investigate the relationship between YgfB, AmpDh3 and AmpC. After induction of *ygfB* expression with rhamnose, *ampDh3* mRNA expression decreased and, with a delay of approximately 90 minutes, *ampC* mRNA expression increased.

These data suggested that YgfB acts as a suppressor of *ampDh3* mRNA expression and that the AmpDh3 levels have to be kept low if high β-lactam resistance has to be achieved in ID40. Figure 4 (B) visualizes that the additional deletion of *ampDh3* restores *ampC* mRNA expression, demonstrating that indeed the modulation of *ampDh3* expression by YgfB is required to achieve the high *ampC* expression in ID40.

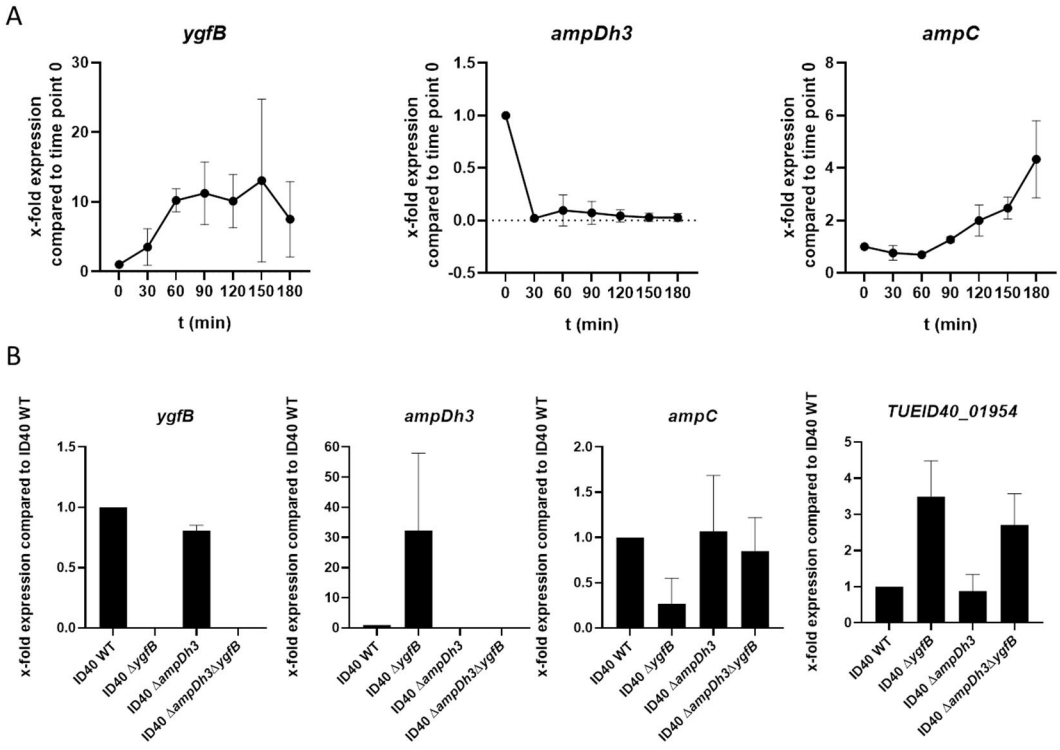

Figure 4: Relationship between *ygfB*, *ampDh3* and *ampC* mRNAexpression

(A) Expression of *ygfB* in *Pa* ID40 Δ*ygfB*::rha-*ygfB* strain was induced by the addition of 0.1 % rhamnose to the growth medium at time point zero. Samples were withdrawn in 30 minutes intervals and RNA was isolated to perform qRT-PCRs.

(B) *Pa* strains as indicated were grown for 3h in LB. RNA was isolated and used for a qRT-PCR. Data depict mean and standard deviation (SD) of three independent experiments.

This figure was kindly provided by Elias Walter, unpublished.

Further preliminary experiments of the working group indicated that YgfB represses *ampDh3* mRNA expression at a transcriptional level. Therefore, a construct was generated which linked the transcriptional activity of the *ampDh3* promoter to luciferase activity. As depicted in Figure 5, upon addition of rhamnose and induction of *ygfB* in ID40 Δ*ygfB*::rha-*ygfB*, luciferase activity and thus transcriptional activity from the *ampDh3* promoter decreased.

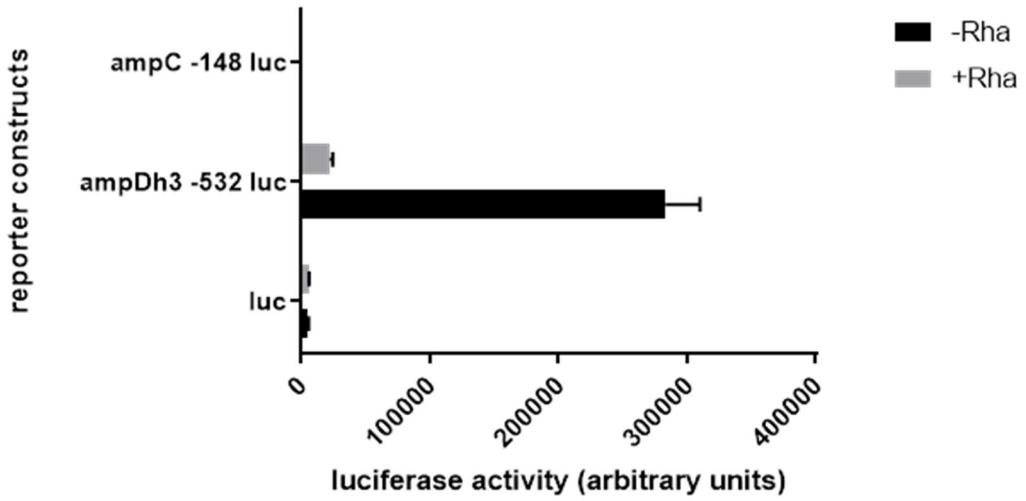

Figure 5: Transcriptional activity of the *ampDh3* promoter

The *ampDh3* (-532 to -1) promoter fused to a *nanoluc luciferase* reporter gene was cloned into pBBR1 resulting in pBBR-ampDh3-532-luc. To assess background activity, Nanoluc was cloned into pBBR1 without a promoter (pBBR-luc). Luciferase activity was quantified using ID40 Δ *ygfB*::rha-*ygfB* grown in the absence or presence of 0.1 % rhamnose. This figure was kindly provided by Elias Walter, unpublished.

In addition, Figure 6 illustrates how the deletion of *ygfB* not only led to increased *ampDh3* mRNA expression but also to reduced levels of anhydro-MurNAc-peptides. The amount of UDP-MurNAc-peptide remained constant. Additional deletion of *ampDh3* restored anhydro-MurNAc-peptide levels (Eggers et al., 2023). Anhydro-MurNAc-peptides are required to derepress AmpR-mediated transactivation of the *ampC* promoter (Torrens et al., 2019, Jacobs et al., 1997).

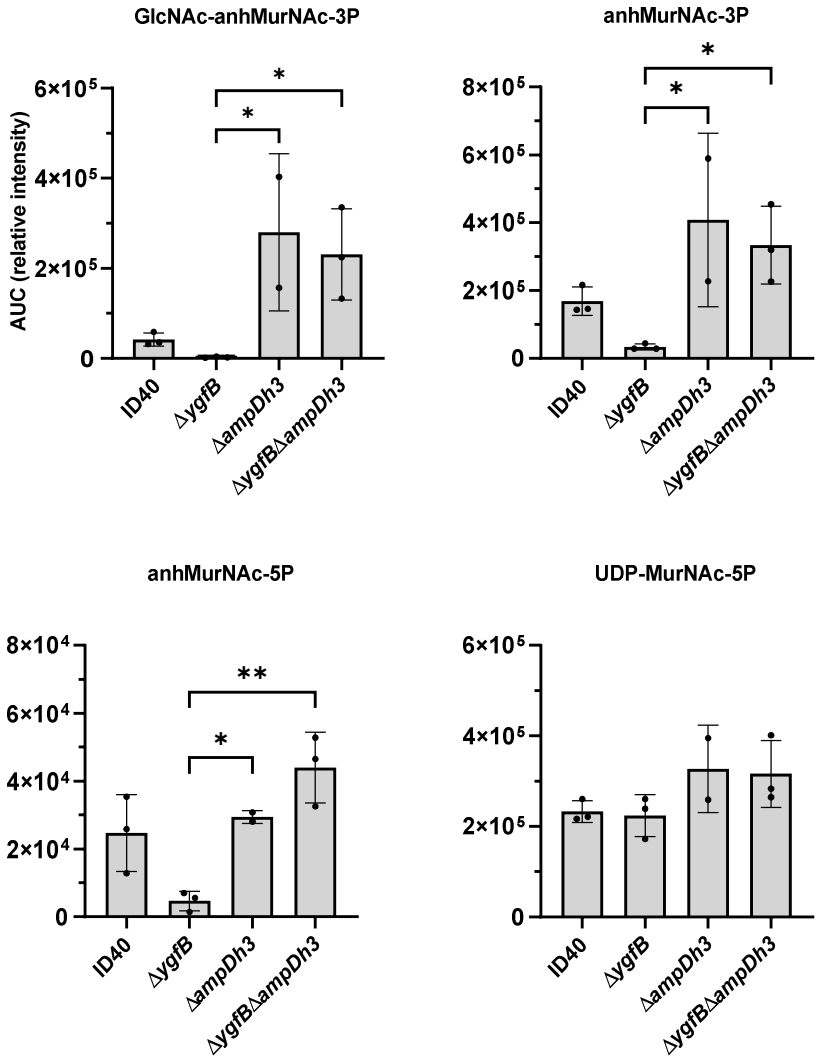

Figure 6: Impact of YgfB and AmpDh3 on the composition of PGN precursors

(G-anhM-3P: GlcNAc-anhydro-MurNAc-tripeptide, anhM-3P: anhydro-MurNAc-tripeptide, anhMurNAc-5P: anhydro-MurNAc-pentapeptide, UDP-MurNAc-5P: UDP-MurNAc-pentapeptide)

Pa strains were grown for 6 h in LB medium, cytosolic extracts were prepared and analyzed by HPLC-mass spectrometry. The graphs depict the area under curve (AUC) for the peaks obtained for various catabolites. This figure was kindly provided by Eggers et al. (2023).

Interestingly, the lab strain PA14 which carries a functional *dacB* gene and is sensitive to β-lactam antibiotics expresses *ampDh3* mRNA at a higher level compared to ID40 (Eggers et al., 2023).

All of these findings lead us to the following working model:

YgfB suppresses in ID40 at a transcriptional level *ampDh3* mRNA expression. The low levels of AmpDh3 contribute to the maintenance of higher levels of anhydro-MurNAc-peptides which leads to increased AmpR-mediated *ampC* mRNA expression and consequently high β-lactam resistance.

1.4 Aim of this study

The preceded work raised various questions and the aim of this study was to start to answer these questions.

1. Since the β-lactam resistant strain *Pa* ID40 which carries an inactive *dacB* gene shows a much lower *ampDh3* mRNA expression than the β-lactam sensitive PA14 strain which carries a functional *dacB* gene, we wondered whether the mutation of *dacB* in ID40 is associated with *ygfB*-mediated suppression of *ampDh3* mRNA expression. We hypothesize that the *dacB* inactivity in ID40 might cause in a YgfB-dependent manner the suppression of *ampDh3* mRNA expression, e.g. by activation of the two-component system CreBC. To address this hypothesis, we intended to generate various ID40 and PA14 mutants to understand the general role of *dacB* and *creBC* for β-lactam resistance but also whether these genes directly influence YgfB-mediated suppression of *ampDh3* mRNA expression.
2. Preceding studies of the working group (unpublished) suggested that the *ampDh3* mRNA expression levels of ID40 and PA14 are different and that deletion of *ygfB* increases *ampDh3* mRNA expression. This raises the question whether these findings hold true on AmpDh3 protein level and whether then higher levels of AmpDh3 in PA14 compared to ID40 would be associated with lower levels of YgfB in PA14. To address this question, it was planned to generate mutants in which it would be possible to detect AmpDh3 protein levels by immunoblot analysis.
3. Wang et al. (2020). demonstrated that *Pa* strains secrete AmpDh3 via a T6SS. This raises the question whether deletion of *ygfB* leads to increased T6SS secretion. To be able to perform such studies later, we intended to

generate strains which could be used to measure AmpDh3 secretion, and also in control strains lacking a T6SS.

4. So far, the localization of AmpDh3 either in the periplasm or cytoplasm is not finally clarified. The suggested secretion of AmpDh3 by a T6SS argues for a cytoplasmic localization. If otherwise AmpDh3 would be also present in the periplasm, the immune gene *TUEID40_01954* should be able to neutralize toxic effects of AmpDh3 in the periplasm and lack of TUEID40_01954 should lead to a growth defect. Therefore, it was planned to investigate whether deletion of *TUEID40_01954* affects growth of *Pa.*

2 Materials and Methods

2.1 Materials

2.1.1 Software

Table 1: Software

Software	Manufacturer
Adobe Photoshop CS6	Adobe Inc., San José (USA)
EndNote	Thomson Reuters, New York City (USA)
Graph Pad Prism 8.4.0	Graph Pad Software, San Diego (USA)
i-control 1.11 (for Tecan infinite reader)	Tecan Trading AG, Männedorf (CH)
LightCycler® 480 Software 1.5	Roche, Basel (CH)
Microsoft Office 2010	Microsoft Corporation, Redmond (USA)
Snap Gene 4.1.9	GSL Biotech LLC, Chicago (USA)

2.1.2 Instruments

Table 2: Instruments

Instrument	Manufacturer
Balance OHAUS Scout pro 400gr	OHAUS Europe GmBH, Nänikon (CH)
Bench Thermo HeraSafe HS18	Heraeus INSTRUMENTS, Hanau
Bio-Rad power Pac 200 and 300	Bio-Rad Laboratories Inc., Hercules (USA)
Branson sonifier 250	Branson Ultrasonics, Danbury (USA)
Centrifuge 5415 R and 5417 R	Eppendorf, Hamburg
Dymo Label writer 450	Newell Brands, Sandy Springs (USA)
Freezer -20°C Liebherr Premium	Liebherr, Bulle (CH)
Fridge 4°C	Kirsch Medical, Willstätt-Sand
Gene pulser® II	Bio-Rad Laboratories Inc., Hercules (USA)

Gel documentation system FAS-V	Nippon Genetics, Düren
Microwave Severin 900	Severin, Sundern
Mini-PROTEAN® Tetra System	Bio-Rad, München
Mini-Sub-Cell GT and Sub-Cell GT chambers for gel electrophoresis	Bio-Rad, München
Multichannel pipette (Finnpipette™ 5-50 µl and 50-300 µl)	Thermo Fisher Scientific Inc., Waltham (USA)
Multifuge® 3 S-R	Heraeus, Hanau
Nanodrop One spectrometer	Thermo Fisher Scientific, Schwerte
Photometer, BioPhotometer	Eppendorf, Hamburg
Pipettes Eppendorf reference and research (10 µl, 20 µl, 100 µl, 200 µl, 1000 µl)	Eppendorf, Hamburg
Power supply PowerPac 300	Bio-Rad, München
Premium NoFrost freezer	Liebherr, Biberach a. d. Riβ
Tecan reader infinite 200® PRO	Tecan, Männedorf (CH)
Thermo-Cycler C1000 Touch	Bio-Rad Laboratories Inc., Hercules (USA)
Thermomixer Comfort	Eppendorf, Hamburg
Vortex Genie 2	VWR International LLC, Radnor (USA)
Water bath	Memmert GmBH & Co.KG, Schwabach
Westernblot detection system Fusion Solo 3S.WL	Vilber, Marne-la-Vallée (FR)
Wide mini sub cell GT chambers for gel electrophoresis	Bio-Rad Laboratories Inc., Hercules (USA)
Mc Farland densitometer Densi check plus	bioMérieux, Marcy-l`Étoile (FR)

2.1.3 Chemicals

Table 3: Chemicals

Name	Manufacturer
4 x Laemmli sample buffer	Bio-Rad, Hercules (USA)
Agar agar	Carl Roth, Karlsruhe
Clarity™ Western ECL Substrate	Bio-Rad, Hercules (USA)
Distilled water	Ampuwa Fresenius Kabi, Bad Homburg
Gene ruler 1 kb plus DNA ladder	Thermo Fisher Scientific Inc., Waltham (USA)
L-Rhamnose monohydrate	Sigma Life Science, Merck, Darmstadt
Nuclease-free water	Thermo Fisher Scientific Inc., Waltham (USA)
Orange G	Sigma-Aldrich, Taufkirchen
PageRuler™ Prestained Protein Ladder	Thermo Fisher Scientific, Schwerte
SeaKem® LE Agarose	Lonza Group, Basel (CH)
Sucrose for microbiology	Merck, Darmstadt
SYBR safe DNA gel stain (0,01%)	Thermo Fisher Scientific Inc., Waltham (USA)
β-Mercaptoethanol	AppliChem, Darmstadt

2.1.4 Consumables

Table 4: Consumables

Name	Manufacturer
96-well-microplate f-bottom chimney well white lumitrac	Greiner bio-one, Kremsmünster (AT)
96-well-microplate f-bottom clear	Greiner bio-one, Kremsmünster (AT)
Cellulose membrane, ZelluTrans (3.5 kDa)	Carl Roth, Karlsruhe
Cuvettes (polystyrol/polystyrene), 1,5 ml	Sarstedt, Nümbrecht

Falcon cellstar tubes (15 ml)	Greiner bio-one, Kremsmünster (AT)
Inoculation loops	Greiner bio-one, Kremsmünster (AT)
Kryo-tubes, 1,5ml	Thermo Fisher Scientific Inc., Waltham (USA)
Low residual volume reagent reservoir 25 ml	Integra Biosciences, Zizers (CH)
Micronaut-S Pseudomonas MIC plates	Merlin, Bruker comPany, Billarica (USA)
Parafilm Bemis PM-996	Amcor, Zurich (CH)
PCR reaction tubes single cap 8er soft strips 0,2ml	Biozym Scientific GmBH, Hessisch Oldendorf
Pipette filter tips (100 µl, 200 µl, 1000 µl)	Nerbe plus, Winsen/Luhe
Pipette tips 10 µl	Brand, Wertheim
Pipette tips 200 µl	Sarstedt, Nümbrecht
Pipette tips 1000 µl	Ratiolab, Dreieich
Pipettes Stripette (10 ml, 25 ml, 50 ml)	Corning Inc., Corning (USA)
Polystyrene round-bottom tubes (5 ml, 14 ml)	Corning Inc., Corning (USA)
Polypropylene conical tubes (50 ml)	Corning Inc., Corning (USA)
Reaction tubes safe-lock tubes (1,5 ml, 2 ml, 1,5 ml amber)	Eppendorf, Hamburg
SDS gel, Mini-protean TGX™ Precast Gels (4-20%)	Bio-Rad, München
Sensititre™ EUX2NF MIC plates	Thermo Fisher Scientific Inc., Waltham (USA)
Sensititre™ GN2F MIC plates	Thermo Fisher Scientific Inc., Waltham (USA)
Steritop™ Millipore express milliporefilter	Merck, Darmstadt

2.1.5 Enzymes

Table 5: Enzymes

Name	Manufacturer
Desoxyribonucleosidetriphosphate (dNTPs) (10mM)	Roche Diagnostics, Rotkreuz (CH)
DpnI restriction enzyme	Thermo Fisher Scientific, Schwerte
Gibson Mix	Kindly provided by Andrea Eipper (Tübingen); contains • T5 Exonuclease (10 U/µl); Epicentre, Madison (USA) • Phusion DNA Polymerase; New England Biolabs, Ipswich (UK) • Taq DNA Ligase (40 U/µl); New England Biolabs, Ipswich (UK) • 5X isothermal (ISO) reaction buffer (25% PEG-8000, 500 mM Tris-HCl pH 7.5, 50 mM MgCl2, 50 mM DTT, 1 mM each of the 4 dNTPs, and 5 mM NAD)
MangoMix PCR reaction mix	Bioline, London (UK)

2.1.6 Culture media

Table 6: Culture media

Name	Constituents
Lysogeny broth (LB) agar	15 g bactoagar LB-medium ad 1L
LB medium pH = 7,5	10 g Trypton 5 g yeast extract 10 g NaCl

	pH 7,5 was adjusted using NaOH purified water ad 1L
Müller Hinton II Broth Micronaut	BioTrading Benelux B.V.
SOC (Super Optimal broth with catabolite repression)	20 g Trypton 5 g yeast extract 10 ml 1M MgSO4 10 ml 1M MgCl2 10 ml 1M KCl 2 ml 5M NaCl 20 ml 1M Glucose Purified water ad 1000 ml

2.1.7 Buffers

Table 7: Buffers

Name	**Manufacturer/Components**
1 x transfer buffer	100 ml 10x Transfer buffer 200 ml Methanol (20%) H_2O ad 1 L
10 x TBS buffer	60.6 g TRIS-base 87.6 g NaCl H_2O ad 1 L pH was adjusted to 7,6
10 x Transfer buffer	30 g TRIS-base 144.4 g glycine H_2O ad 1 L
4x Laemmli loading dye	900 µl 4x Laemmli sample buffer 100 µl β-Mercaptoethanol
5 x SDS running buffer	60.55 g TRIS-base 288.15 g glycine 10 g sodium dodecyl sulfate (SDS) H_2O ad 2 L

TBS-T buffer (1 x TBS + 0.1% Tween-20)	100 ml 10x TBS buffer 1 ml Tween-20 H_2O ad 1 L

2.1.8 Antibiotics

Table 8: Antibiotics

Name	**Manufacturer**
Gentamicinsulfate	Appli Chem, Darmstadt
Irgasan	Sigma-Aldrich, Taufkirchen

2.1.9 Antibodies

Table 9: Antibodies

Name	**Manufacturer**
anti-RNA polymerase beta	Abcam #mAb EPR18704
Polyclonal rabbit-anti-ygfB antibody	AG Bohn/Schütz, Eurogentec
Monoclonal rabbit anti HA-Tag antibody (C29F4)	Cell Signaling mAb #3724
Goat F(ab`) anti-Rabbit IgG (H+L)-HRPO	Dianova #111-035-045 (SKU)

2.1.10 Commercial kits

Table 10: Commercial kits

Name	**Manufacturer**
β-Lactamase Activity Kit	BioVision, Milpitas (USA)
DNeasy® UltraClean® Microbial Kit	Qiagen, Venlo (NL)
KAPA HiFi PCR Kit	Roche, Basel (CH)
Monarch® Plasmid Miniprep Kit	New England BioLabs, Ipswich (USA)
QuantiFast® SYBR® Green RT-PCR Kit	Qiagen, Hilden
Wizard® SV Gel and PCR Clean-Up System	Promega, Madison (USA)
Nano-Glo® HiBiT Lytic Detection System	Promega, Madison (USA)

2.1.11 Plasmids

Table 11: Plasmids

Name	**Characteristics**	**Origin**
pEXG2	Mutator plasmid with selective *sacB*-gene, pBR origin and gentamicin resistance cassette	Hmelo et al. (2015)
pEXG2 Δ*creBC*	pEXG2 derivative for deletion of *creBC*	Provided by AG Bohn/Schütz
pEXG2 Δ*ampR*	pEXG2 derivative for deletion of *ampR*	This study
pEXG2 Δ*icmF2*	pEXG2 derivative for deletion of *icmF2*	This study
pEXG2 Δ*dacB*(PA14)	pEXG2 derivative for deletion of *dacB*(PA14)	This study
pEXG2 Δ*TUEID40_01954*	pEXG2 derivative for deletion of *TUEID40_01954*	This study
pJM220		(Choi and Schweizer, 2006)
pJM220 *dacB*(PA14)		Provided by AG Bohn/Schütz
Helper plasmid pTNS3		(Choi et al., 2008)
Helper plasmid pFLP2		(Hoang et al., 1998)
pBBR1-MCS5		(Kovach et al., 1995)
pBBR-luc		Provided by AG Bohn/Schütz
pBBR-ampDh3-532-luc		Provided by AG Bohn/Schütz

2.1.12 Oligonucleotides

2.1.12.1 Primers used for Gibson cloning

Table 12: Primers used for Gibson cloning

Name	Sequence 5`- 3`
CreBC_up_F	AGCTAATTCCACACATTATACGAGCCGGAAGATCAGGATCAGCGTGTTGAG
CreBC_up_R	TCAGCCGCGCGGCAGCCAGAGCAGCGCCTCTTCATCTTCGACGATCAGGATATGC
CreBC_dn_F	ATGCCGCATATCCTGATCGTCGAAGATGAAGAGGCGCTGCTCTGGCTG
CreBC_dn_R	TCGAGCCCGGGGATCCTCTAGAGTCGACCTCAGTCGGCCTTCAGGATGACC
ampR_up_F	AGCTAATTCCACACATTATACGAGCCGGAACACGTCGAGGTGGGTCTG
ampR_up_R	TTATCTCCCCCGCGCCTCAACGGCAGCCATGGCGTTCAGCGGCAAATG
ampR_dn_F	TTGGTTCGACCCCATTTGCCGCTGAACGCCATGGCTGCCGTTGAGGC
ampR_dn_R	TCGAGCCCGGGGATCCTCTAGAGTCGACCTCAGGTGTTCCGCGCCTTC
icmF2_up_F	AGCTAATTCCACACATTATACGAGCCGGAAAGCGGTTCGTTCATTGGC
icmF2_up_R	ATGAAAAACTTCTTCAAGAAAGTCGGCGCCTTCGATCTCGCGGTCCTGC
icmF2_dn_F	GCGGAAGCTGCGCAGGACCGCGAGATCGAAGGCGCCGACTTTCTTGAAG
icmF2_dn_R	TCGAGCCCGGGGATCCTCTAGAGTCGACCTGACCGTCCTCCTCGATCAC
TUEID40_01954_up_F	AGCTAATTCCACACATTATACGAGCCGGAAGAGGTGCTCCAAGGGTTCTTG

TUEID40_01954_up_R	ATGACTGCCGTCGCACAGGTCGTCGCCAAGG AGCATGGCATCGCCTTG
TUEID40_01954_dn_F	GGCCACCAGGTTCAAGGCGATGCCATGCTCCT TGGCGACGACCTGTGC
TUEID40_01954_dn_R	TCGAGCCCGGGGATCCTCTAGAGTCGACCTAC CATGCTGACCATCGACTAC
dacBPA14_up_F	AGCTAATTCCACACATTATACGAGCCGGAACA AGTCGATCGATCCGGCAA
dacBPA14_up_R	ATGTTCAAGTCGCTGCGTACTCTTGCCTTCGTA CTGCTGAGCCTGCACG
dacBPA14_dn_F	TTATTTCCGCGCGTGCAGGCTCAGCAGTACGA AGGCAAGAGTACGCAGCG
dacBPA14_dn_R	CAGAGCGAGTTGAATAGTTCGTCAGGGGCTTC AGAGTAATGCTATCCGCATGTAC
CreBfürtag_F	AGCTAATTCCACACATTATACGAGCCGGAAGC CGTGCTAGTCCTATGTG
CreBfürtag_R	TCGAGCCCGGGGATCCTCTAGAGTCGACCTC GGTGTCCACCAGGGTTTC
HA-CreB_F	GATTACGCTTACCCATACGATGTTCCAGATTAC GCTCCGCATATCCTGATCGTCGAAGATGAAGC
HA-CreB_R	ATCTGGAACATCGTATGGGTAAGCGTAATCTG GAACATCGTATGGGTACATGGCGTGACGGCG GCTG
gib_uni_pEXG2_F	AGGTCGAC TCTAGAGGATCC
gib_uni_pEXG2_R	TTCCGGCTCGTATAATGTGT
pEXG2_seq_F	TACTGTGTTAGCGGTCTG
pEXG2_seq_R	GATCCGGAACATAATGGTG

2.1.12.2 Flanking primers used to verify deletions and insertions

Table 13: Flanking primers used to verify deletions and insertions

Name	**Sequence 5`- 3`**
ampR_seq1_F	GTCGTTGGCTGCATGAGAAAC

ampR_seq2_R	ATGCTCGAGAGCGAGATCG
ampR_inside3_R	CAACCGACCGTGAAGGTTC
icmF2_seq1_F	CGTACTGCCGATGATCCTGTC
icmF2_seq2_R	TATTTCCGATGCGCTCTACC
icmF2_inside3_R	CGTGACGTGATGGTGCTC
TUEID40_01954_seq1_F	TCAGCCAGGTGATCCTGT
TUEID40_01954_seq2_R	GAGAAATACCCGGCCTGAGC
TUEID40_01954_inside3_R	GCGGAAATGCTGATCCGC
dacBPA14_seq_F	AAACCCTCGATCCGGATTTC
dacBPA14_seq_R	GAAAGCGTTCACCGCATC
dacBPA14_inside_R	GCCTGGTGATGGAGAACG
CreBtagproof_F	CTGTCGGCCAAGGACATC
CreBtagproof_R	TGGAACATCGTATGGGTAAGC
CreB_inside3_R	GCTTGCAGGCCTCGAAAC
ampDh3hibitproof_R	TAATCTTCTTGAACAGCCGCCAG
ampDh3proof_1	ATTCGGCCATTCGATGAG
ampDh3proof_3	GCCTTCCAGATGCATTTCC
CreB_seq1_F	CAAGGGCTTGCGCAAATTC
CreB_seq2_R	AGGCCGTCGATCATCAAC
CreB_inside3_R	GCTTGCAGGCCTCGAAAC
05723_seq_F	CATGACCTTCACTTCGTTG
05723_seq_R	CTTGTCGAGAATCTGCAC
05723_inside_R	GGAAGTCATGGAATACCTG

2.1.12.3 Primers used in the generation of complementation mutants

Table 14: Primers used in the generation of complementation mutants

Name	Sequence 5`-3`
pJM_dacB_PA14_F	ATTCAACTAGTGCTCTGCAGGAATTCCTCGAGAAGCTTATGTTCAAGTCGCTGCGTAC
pJM_dacB_PA14_R	CTGGTTGGCCTGCAAGGCCTTCGCGAGGTATTATTTCCGCGCGTGCAG
Gib_uni_pJM220_F	TACCTCGCGAAGGCCTTGCA
Gib_uni_pJM220_R	AAGCTTCTCGAGGAATTCCTGC
pJM220_seq_F	TTTTCAAGATACAGCGTGAA
pJM220_seq_R	GCCCAAACATAACAGGAAGA
ID27_glmS2_down_F	CACAGCATAACTGGACTGATTTC
Tn7L_R	TCCATGCCGAAGCCTACCC
pJM220_Gen_F	TCTCCGAACTCACGACCGAAA
pJM220_Gen_R	TGTTCGGGCAGTTGGTGATG

2.1.13 Bacterial strains and mutants

2.1.13.1 Provided bacterial strains used in this study

Table 15: Provided bacterial strains used in this work

Bacterial strain	Characteristics	Origin
Pa ID40	Clinical isolate from bloodstream infection	(Willmann et al., 2018)
Pa PA14	Laboratory *Pa* strain	DSMZ (Nr. 19882) (Rahme et al., 1995) (Schroth et al., 2018)

		(Mathee, 2018)
Pa ID40 Δ*ygfB*	*ygfB* deletion mutant of *Pa* ID40	Provided by AG Bohn/Schütz
Pa ID40 Δ*ampDh3*	*ampDh3* deletion mutant of *Pa* ID40	Provided by AG Bohn/Schütz
Pa ID40 Δ*ygfB* Δ*ampDh3*	*ygfB* and *ampDh3* deletion mutant of *Pa* ID40	Provided by AG Bohn/Schütz
Pa PA14 Δ*ygfB*	*ygfB* deletion mutant of *Pa* PA14	Provided by AG Bohn/Schütz
Ec Top 10	Chemically competent *Ec* strain	Thermo Fisher Scientific, Schwerte
Ec SMλpir	Chemically competent *Ec* strain	(Hmelo et al., 2015)
Ec DH5α	Chemically competent *Ec* strain	Thermo Fisher Scientific, Schwerte
Ec SMλpir Δ*creBC*	*Ec* strain with mutator plasmid for *creBC* deletion mutagenesis	Provided by AG Bohn/Schütz
Ec SMλpir HA-CreB	*Ec* strain with mutator plasmid for HA-CreB insertion mutagenesis	Provided by AG Bohn/Schütz
Ec SMλpir ampDh3-strep-HiBiT	*Ec* strain with mutator plasmid for ampDh3-strep-HiBiT insertion mutagenesis	Provided by AG Bohn/Schütz
Pa ID40::pJM220 *dacB*(PA14)	*Pa* ID40 chromosomally complemented with *dacB* gene of PA14 under control of a	Provided by AG Bohn/Schütz, unpublished

	rhamnose inducible promoter	
Pa ID40 Δ*creBC*::pJM220 *dacB*(PA14)	*Pa* ID40 Δ*creBC* chromosomally complemented with *dacB* gene of PA14 under control of a rhamnose inducible promoter	Provided by AG Bohn/Schütz, unpublished

2.1.13.2 Deletion mutants of *Pa* ID40 and *Pa* PA14 generated in this study

Table 16: Deletion mutants of *Pa* ID40 and *Pa* PA14 generated in this study

Deletion mutant	**Deleted gene(s)**
Pa ID40 Δ*creBC*	*creBC*
Pa ID40 Δ*creBC* Δ*ygfB*	*creBC, ygfB*
Pa ID40 Δ*creBC* Δ*ampR*	*creBC, ampR*
Pa ID40 Δ*ampR*	*ampR*
Pa ID40 Δ*icmF2*	*icmF2*
Pa ID40 Δ*TUEID40_01954*	*TUEID40_01954*
Pa PA14 Δ*creBC*	*creBC*
Pa PA14 Δ*creBC* Δ*ygfB*	*creBC, ygfB*
Pa PA14 Δ*creBC* Δ*ygfB* Δ*ampR*	*creBC, ygfB, ampR*
Pa PA14 Δ*ampR*	*ampR*
Pa PA14 Δ*icmF2*	*icmF2*
Pa PA14 Δ*TUEID40_01954*	*TUEID40_01954*
Pa PA14 Δ*dacB*	*dacB*
Pa PA14 Δ*dacB* Δ*ygfB*	*dacB, ygfB*
Pa PA14 Δ*dacB* Δ*creBC*	*dacB, creBC*
Pa PA14 Δ*dacB* Δ*ygfB* Δ*creBC*	*dacB, ygfB, creBC*

2.1.13.3 Tag-labelled mutants of Pa ID40 and Pa PA14 generated in this study

Table 17: Tag-labelled mutants of *Pa* ID40 and *Pa* PA14 generated in this study

Insertion mutant	Description
Pa ID40 HA-CreB	Allelic exchange of *creB* gene by HA-tagged *creB* gene
Pa ID40 Δ*ygfB* HA-CreB	Allelic exchange of *creB* gene by HA-tagged *creB* gene
Pa PA14 HA-CreB	Allelic exchange of *creB* gene by HA-tagged *creB* gene
Pa PA14 Δ*ygfB* HA-CreB	Allelic exchange of *creB* gene by HA-tagged *creB* gene
Pa ID40 ampDh3-strep-HiBiT	Allelic exchange of *ampDh3* gene by *ampDh3* gene fused to strep-HIBIT tag
Pa ID40 Δ*ygfB* ampDh3-strep-HiBiT	Allelic exchange of *ampDh3* gene by *ampDh3* gene fused to strep-HIBIT tag
Pa PA14 ampDh3-strep-HiBiT	Allelic exchange of *ampDh3* gene by *ampDh3* gene fused to strep-HIBIT tag
Pa PA14 Δ*ygfB* ampDh3-strep-HiBiT	Allelic exchange of *ampDh3* gene by *ampDh3* gene fused to strep-HIBIT tag

2.2 Microbiological methods

2.2.1 Cultivation of bacteria

In order to start a bacterial culture, some bacteria were taken from a corresponding cryoculture with an inoculation loop and used to inoculate 5 ml LB medium. The culture was left at 37°C with shaking at 200 rpm overnight. To perform MIC assays, bacteria from the cryoculture were streaked onto a LB plate and left at 37°C overnight. Furthermore, a culture was sometimes initiated with bacterial material from another overnight culture and therefore streaked onto specific plates (e.g. antibiotic grid plates or 3-loop plates containing sucrose for mutagenesis).

For subcultivation, a 1:20 dilution of the bacteria in LB was performed, if not otherwise stated, for 2-3 hours at 37°C depending on the assay performed. For selection the appropriate antibiotics were added.

2.2.2 Production of glycerol-cultures

Cryocultures themselves originated from a 5 ml bacterial overnight culture which was firstly centrifugated for 5 minutes at 4.500 x g and whose pellet was then resuspended in 4 ml LB + 20% glycerol. 1 ml aliquots were subsequently transferred into four cryotubes and frozen immediately at -80°C.

2.2.3 Measurement of bacterial counts using a photometer

Photometry count was used to measure the cell density of cell suspensions such as bacterial cultures. It constitutes a monochromatic measurement technique. Light with a wavelength of 600 nm is emitted and dispersed by bacteria in the suspension as their density differs slightly from the medium density. Thus, fewer of the emitted light reaches the opposite detector. This phenomenon is called extinction, or optical density and it allows to draw conclusions on the bacterial concentration of the culture according to the Lambert Beer principle:

$$\mathrm{E} = \lg \frac{I_0}{I} = c \cdot d \cdot \mathrm{E}_\lambda$$

$\mathrm{E} = extinction, optical\ density$

$I_0 = intensity\ of\ emitted\ light$

$I = intensity\ of\ transmitted\ light$

$c = concentration$

$d = layer\ thickness\ of\ the\ object\ transversed\ by\ the\ light\ (cuvette = 1cm)$

$\mathrm{E}_\lambda = specific\ extinction\ coefficient\ for\ each\ suspension$

For *Pa* cultures, an optical density of 1 equals a concentration of $c = 10^9/ml$. The detector requires an optical density between 0,1-1 for an appropriate measurement sensitivity, otherwise the measured suspension must be diluted or concentrated further. Precisely, 1 ml of bacteria suspension was filled into a cuvette and measured by photometer count in comparison to a cuvette which served as a blank and was filled only with LB medium. The resulting values could be secondly used to adjust the bacterial content of a certain volume of solution considering the formula

$$c_1 \cdot v_1 = c_2 \cdot v_2$$

$$v_2 = \frac{c_1 \cdot v_1}{c_2}$$

$c_1 = original\ concentration$

$v_1 = original\ volume$

$c_2 = adjusted\ concentration$

$v_2 = adjusted\ volume$

The process of adjusting consists of taking v_2 of bacterial suspension and mixing it with $desired\ end\ volume\ (e.g. 1\ ml) - v_2$ of LB medium. It was performed for all luciferase assays.

2.2.4 Growth curves

Growth curves were recorded to monitor potential differences in growth between the WT strain and deletion mutants. First, LB cultures were inoculated with bacteria and grown overnight. Next day, the OD600 nm was measured, and cultures were adjusted to 1 x 10^7 cells/ml using fresh LB. In a 24 well plate, 1 ml of bacterial suspension was added per well. Plates were incubated with a lid and with shaking at 300 rpm at 37°C for the indicated time interval of 15 hours. All growth curves were recorded in triplicates using an Infinite® PRO 200 plate reader (Tecan).

2.2.5 Testing sensitivity to antibiotics

2.2.5.1 Determining MIC by Microbroth dilution assays

MIC assays allow to determine the minimal inhibitory concentration of certain antibiotics for different bacterial strains. Above all, β-lactam antibiotics were tested in various deletion mutants due to the suspected influence of the *ygfB* gene cluster on β-lactamase activity.

Overnight cultures were grown on LB plates. Some of the material was picked with a pipette tip and resuspended in physiological 0,9 % NaCl solution. The suspensions were adjusted to a certain optical density using a McFarland standard. McFarland standard values were adjusted to 0,45-0,55. Consequently, 62,5 µl of suspensions were added to 15 ml of Müller Hinton bouillon medium (MHII broth, bioTrading). Following the plate manufacturer`s protocol, 50 µl of the suspension were filled into each well using a multichannel pipette. Different wells contained different antibiotics and concentrations and positive control wells. Herein Thermo Fisher Scientific Sensititre™ GN2F and Sensititre™ EUX2NF plates were used.

The MIC plates were sealed with foils and incubated at 37°C for 18 hours. Eventually, foils were removed and the (yet optically visible) turbidity or absorption of all wells was measured with a Tecan plate reader.

Concerning calculations, the negative control well absorption was substracted from each antibiotic well absorption value. This resulting absorption value was

then compared to a cut off value of 0,5. Higher values indicated growth of bacteria, whereas lower values indicated that bacterial growth was inhibited by the respective antibiotic at the given concentration. In a continuous range of a certain antibiotic`s concentrations the minimal inhibitory concentration then equals the lowest concentration with no bacterial growth to be observed. Lower MIC values meant increased susceptibility of the bacterial strain for the tested antibiotic, and the equivalent WT behaviour was used as a reference. Using the European Committee on Antimicrobial Susceptibility Testing (EUCAST) table of clinical breakpoints (valid from January 2020), different strains could subsequently be categorized as susceptible, intermediate and resistant.

2.2.5.2 β-lactamase-activity assay (nitrocefin assay)

The fundamental concept of this assay is that nitrocefin, a chromogenic cephalosporin, is hydrolized by β-lactamases, causing a change in the wavelength of the emitted light from yellow to red (490 nm). This emission can be measured and as it is proportional to the activity of the hydrolysing β-lactamases, it can be used for quantification of β-lactamase activity in different bacterial strains.

Overnight cultures were subcultured after a dilution of 1:20 into fresh LB medium for 3 hours. As PA14 strains were supposed to show lower β-lactamase activity than ID40 strains more bacterial biomass was required for testing. Therefore, for PA14 mutants 8 tubes à 5 ml were grown while for ID40 only 4 tubes à 5 ml were grown in LB for 3 hours at 37°C. The subcultured bacterial suspensions were centrifuged in several centrifugation steps, steadily reducing their volume and solidifying their pellet. The finally obtained compact pellet was exactly weighted. Afterwards, PA14 strains were resuspended in 10 µl assay buffer/mg pellet while the resuspension volume for ID40 strains was 20 µl/mg pellet. For lysis, these cell suspensions were sonified with a Branson Sonifier for 2 cycles with 2 minutes of sonification, followed by a pause of 1 minute, and one final cycle of sonification for 1 minute. The bacterial lysates were then kept on ice for 5 minutes and centrifuged for 20 minutes at 4°C and 16.000 x g. Consequently, as listed in Table

18, the supernatant was further diluted depending on which strain was used for analysis.

Table 18: Strain preparation for β-lactamase activity assay

Strain	Resuspension of the pellet in assay buffer	Dilution in assay buffer (1. assay) (2. and 3. assay)	Dilution during well filling	Final amount of pellet / well (1. assay) (2. and 3. assay)
Pa PA14	10 µl / mg	1:5	1:1	1 mg
Pa PA14 Δ *dacB*	10 µl / mg	1:25	1:1	0,2 mg
Pa PA14 Δ *dacB* Δ *ygfB*	10 µl / mg	1:5	1:1	1 mg
Pa ID40	20 µl / mg	1:25 1:50	1:50	0,002 mg 0,001 mg
Pa ID40 Δ *ygfB*	20 µl / mg	1:5 1:50	1:50	0,01 mg 0,001 mg
Pa ID40 Δ *creBC*	20 µl / mg	1:25 1:50	1:50	0,002 mg 0,001 mg
Pa ID40 Δ *ygfB* Δ *creBC*	20 µl / mg	1:5 1:50	1:50	0,01 mg 0,001 mg
Pa ID40 Δ *ampDh3*	20 µl / mg	1:25 1:50	1:50	 0,001 mg
Pa ID40 Δ *ygfB* Δ *ampDh3*	20 µl / mg	1:25 1:50	1:50	0,002 mg 0,001 mg
Pa ID40 Δ *ampR*	20 µl / mg	1:1	1:50	0,05 mg

The standard curve was created according to the manufacturer`s protocol with a continuous range of 0-20 nmol hydrolysed nitrocefin.

Each strain was given into wells in duplicates. Reaction mix was added and mixed with a multichannel pipette as described in the assay protocol. Bubbles that eventually formed were removed by a short centrifugation step of 30 s and 400 x g. The plate was then analysed with a Tecan plate reader.

Concerning calculations, previously a superordinate standard curve was generated from all acquired individual standard curves. Next, the enzyme rate was calculated as followed:

The measured emission curves were plotted. A linear enzyme rate was chosen for each mutant, and by means of the observed absorption difference and the standard curve equation, nitrocefin turnover was calculated. Moreover, all dilution steps were considered when calculating the final amount of pellet in each plate well. Further including the time difference of the linear enzyme rate range, the enzyme rate equals the following term.

$$enzyme\ rate = \frac{Nitrocefin\ turnover}{min \cdot (mg\ pellet\ per\ well)}\ \left[\frac{nmol}{min \cdot mg}\right]$$

2.3 Molecularbiological methods

2.3.1 Isolation of Plasmid DNA

5 ml of overnight cultured bacteria were harvested by centrifugation (4.500 x g, 5 minutes). The bacterial pellet was then used for plasmid DNA isolation using the Monarch Plasmid Miniprep Kit following exactly the manufacturer´s instruction. The DNA was finally eluted with 30-50 µl water. DNA concentrations were determined using a Nanodrop One spectrometer.

2.3.2 Isolation of gDNA

1.8 ml of overnight cultured bacteria were transferred to a 2 ml Eppendorf cap and centrifuged at 10.000 x g for 1 minute. The supernatant was decanted, and a second centrifugation was performed (1000 x g, 1 minute) to remove the remaining supernatant with a pipette. The completely dry pellet was then used for gDNA isolation following exactly the protocol of the DNA DNeasy® UltraClean® Microbial Kit (QIAGEN). Finally, the gDNA was eluted with 50 µl water.

2.3.3 Preparation of DNA for colony PCR

A bacterial colony was picked and resuspended in 50 µl water. After boiling for 5 minutes at 95°C, the suspension was centrifuged for 5 minutes at 16.000 x g and 3 µl of the supernatant were used for PCR.

2.3.4 Polymerase chain reaction

Polymerase chain reaction (PCR) is an efficient method to amplify DNA fragments. A double-stranded DNA fragment is denatured and separated into single-stranded DNA fragments. An upstream and a downstream primer with a complementary base sequence to the DNA fragments can anneal and a DNA polymerase can copy the original sequence. As a result, two double-stranded DNA fragments originate from the template in one cycle. PCR was usually performed with 30 cycles.

2.3.4.1 PCR with KAPA HiFi PCR kit

Kapa HiFi PCR was used to amplify DNA fragments which served as inserts to generate plasmid vectors for mutagenesis. *Pa* ID40 or *Pa* PA14 wildtype genomic DNA (gDNA) as well as plasmid DNA were applied as templates. Table 19 gives detail of the composition of the employed Kapa HiFi PCR reaction mix, whereas Table 20 specifies the applied PCR programme.

Table 19: Compounds and quantities for Kapa HiFi PCR

Compound	**Quantity**
Kapa HiFi GC buffer	5 µl
10 mM Kapa dNTPs	0,75 µl
Kapa polymerase	0,5 µl
H_20	16,25 µl
Primer forward (10 µM)	0,75 µl
Primer reverse (10 µM)	0,75 µl
Template (20-50 ng gDNA or 2-5 ng plasmid DNA)	1 µl
total	25 µl

Table 20: PCR programme for KAPA HiFi PCR

Initial denaturation	95°C	5 minutes	
Denaturation	95°C	0:30 minutes	30 cycles
Annealing	According to primers used	0:30 minutes	
Extension	72°C	0:30 minutes/1 kbp fragment length	
Final extension	72°C	5 minutes	
Pause	4°C	∞	

2.3.4.2 PCR with Mango Mix

Mango Mix PCR was employed for verification of the length of a specific gene fragment amplified by PCR, e.g. upon the generation of deletion mutants. The PCR reaction was composed as depicted in Table 21. As a template either plasmid DNA (2-5 ng), gDNA (20-50 ng) or for colony PCR 3 µl supernatant of a boiled bacterial suspension was used. Table 22 specifies the applied PCR programme.

Table 21: Components and quantities for Mango Mix PCR

Component	**Quantity**
Mango Mix	7,5 µl
H_2O	3,5 µl
Primer forward (10 µM)	0,5 µl
Primer reverse (10 µM)	0,5 µl
Template	3 µl
total	15 µl

Table 22: PCR programme for Mango Mix PCR

Initial denaturation	95°C	5 minutes	
Denaturation	95°C	0:30 minutes	30 cycles
Annealing	According to primers used	0:30 minutes	
Extension	72°C	0:30 minutes/1 kbp fragment length	
Final extension	72°C	5 minutes	
Pause	4°C	∞	

2.3.5 Agarose gel electrophoresis

For agarose gel electrophoresis 1 % Agarose in 0.5 x Tris-borate-EDTA (TBE) buffer was boiled in a microwave oven. Subsequently SYBR Safe DNA Gel Stain was added (5 µl to 100 ml agarose suspension) and the agar suspension poured in a gel tray with a comb inserted. DNA fragments are negatively charged and pass through the pores of the agarose gel towards the anode when applying voltage. Their velocity depends on their length and conformity. To illustrate this point, short DNA fragments with a linear conformity pass through the gel more rapidly than longer fragments. As a reference, a marker which consists of DNA molecules of known lengths was loaded in one gel pocket and passes through the gel along with the samples. For loading, the samples were mixed with a loading buffer containing Orange G and glycerol. Mango Mix already includes glycerol and a dying substance, whereas for all KAPA PCRs, 3 µl of Orange G loading buffer were added to 5 µl of a sample and subsequently loaded into a well. The electrophoresis was carried out at a voltage of 100 V for 45 minutes. DNA bands were detected by UV illumination using a camera system.

2.3.6 Creation of Pa ID40 and Pa PA14 deletion mutants

Pa mutagenesis was implemented following a protocol which was established by Hmelo et al. (2015). To generate genomic deletions, the regarding allele was

exchanged by another genomic fragment which carries the deletion and is introduced by a vector plasmid and homologous recombination.

2.3.6.1 PCR amplification and purification of gene fragments

Initially, gene fragments were generated that later served as an insert for the mutator vector pexG2. This mutational vector already contains the deletion in the gene of interest. Upstream and downstream of this genomic region of the deleted gene of interest, specific genomic sequences are located which are homologous to the respective genomic regions upstream and downstream the wildtype gene of interest in the bacterial strains (Hmelo et al., 2015). In other words, to facilitate allelic replacement the inserts consisted of an approximately 800-900 bp long upstream region followed by the first 30 bp (starting with ATG) of the gene of interest (GOI). To this part the last 30 bp of the gene of interest (ending with a stop codon) followed by an approximately 800-900 bp long downstream region of the GOI were fused (Hmelo et al., 2015). The used primers are listed in Table 12. At this point it is appropriate to explain in more detail the nomenclature of the primers used. Primers “UpF” and “UpR” bind to the genome sequence which is located upstream of the GOI. Similarly, primers “DownF” and “DownR” bind to the genome sequence which is located downstream the GOI. For the later Gibson cloning into the linearized pEXG2 vector primer “UpF” carries at the 5´ end 30 bp which overlap with pEXG2 and “UpR” carries at the 5´end 30bp which overlap with the downstream fragment. Primer “DownF” carries at the 5´ end 30 bp which overlap with the upstream fragment and “UpR” carries at the 5´ end 30 bp which overlap with the linearized pEXG2 vector. Eventually, primers “SeqF” and “SeqR” can bind at two genomic sites upstream and downstream of the GOI and enable the PCR amplification of the entire genomic region around the GOI (Hmelo et al., 2015).

Therefore, two KAPA PCRs with *Pa* ID40 or *Pa* PA14 wildtype genomic DNA as template were prepared with 8 tubes for each mix and run as gradient PCRs with 8 different annealing temperatures ranging from 52°C to 70°C. The upstream and the downstream fragment of *dacB* (PA14) was also produced by gradient PCR. Alternatively, for *ampR, icmF2* and *TUEID40_01954* fragments, an annealing

temperature of 56°C could be chosen to perform a simple PCR in one tube for the generation of the fragment.

PCR reactions were analysed using gel electrophoresis. The remaining PCR reaction material of those samples with suiting bands was collated and purified using the Wizard® SV Gel and PCR Clean-Up System following the manufacturer`s instructions.

2.3.6.2 Gibson assembly of up- and downstream fragments and the linearized vector

Gibson assembly is a method to assemble PCR fragments as previously described (Gibson et al., 2009). In our case this method was used to insert and fuse upstream and downstream fragments of GOIs into the pEXG2 vector. The linearized pEXG2 plasmid was already available. For the generation of the linearized pEXG2, the primers “gib_uni_pEXG2_F” and “gib_uni_pEXG2_R” were used.

10 µl of Gibson mix, 1 µl (100-200 ng) of each PCR fragment and 1 µl (100-200 ng) of linearized pEXG2 plasmid DNA were mixed to start a Gibson reaction. The reaction mix was incubated at 50°C for 30 minutes. Next, 1 µl of DpnI restriction enzyme was added to remove the pEXG2 template DNA used for pEXG2 linearization and incubated at 37°C for 60 minutes.

2.3.6.3 Transformation of the vector construct into *E. coli* Top 10 and colony PCR of the resulting colonies

Chemically competent *E. coli* Top10 cells were thawed on ice and mixed with 8 µl of the Gibson reaction mix. To facilitate transformation of the plasmid into *E. coli* cells, cells were kept on ice for 20 minutes, heat-shocked at 42°C for 30 seconds, again placed on ice for 2 minutes and finally suspended in 1 ml of SOC medium. The mixture was then incubated with shaking at 37°C for 60 minutes. Afterwards, the reaction mix was centrifuged at 10.000 x g for 1 minute, most of the supernatant was removed and 10 and 100 µl of the cells were streaked onto two individual LB-agar plates containing gentamicin at a concentration of 15 µg/ml. After incubation at 37°C overnight, a colony PCR was performed to identify the clones that carried the plasmid. Therefore, plasmid specific primers as

specified in Table 12 in the material section were used (Hmelo et al., 2015). After successful transformation, approximately 12-24 colonies were picked with a pipette tip, streaked in defined sectors of a LB-agar grid plate containing gentamicin at a concentration of 15 µg/ml. Using the same pipette, the remaining bacteria were resuspended in a tube filled with 50 µl of distilled H_2O. The tubes were heated to 95°C for 5 minutes for bacterial lysis and shortly centrifuged at 10.000 x g. 3 µl of the supernatants were used as template for a colony PCR with plasmid pEXG2 sequencing primers (as listed in Table 12). By gel agarose gel electrophoresis those bacterial clones carrying the correct inserts could be identified. Bacteria carrying the correct inserts were then picked from the LB agar plate, grown in 5 ml LB containing 15 µg/ml gentamicin and used for plasmid DNA preparation as described in section 2.3.1. The correct DNA inserts were then verified by Sanger sequencing. For this purpose, 15 µl (50-100 ng) plasmid DNA were mixed with 2 µl of 10 µM of gene specific sequencing primers (Table 13) as well as the primers “pEXG2_seq_F” and “pEXG2_seq_R” (Table 12) and sent to Eurofins Genomics.

2.3.6.4 Transformation of the mutator plasmid into *E. coli* SMλpir and colony PCR of resulting colonies

Verified mutator plasmids were transformed into *E. coli* SMλpir cells and uptake was verified with a colony PCR with the same plasmid specific primers for pEXG2. For the genes of interest *dacB* (PA14), *ampR, icmF2* and *TUEID40_01954,* mutagenesis was performed from the very beginning. For all the other GOIs, *E. coli* SMλpir strains carrying the mutator plasmid had already been generated previously. They were kindly provided and could conveniently be employed in this work. Mutagenesis for all the other genes of interest began with the following step, with biparental mating.

2.3.6.5 Biparental mating of *E. coli* SMλpir and *Pa* PA14 or *Pa* ID40 wildtype/mutants

The next step is called *“biparental mating*”, which describes the conjugation and plasmid transfer from an *E. coli* donor to a *Pa* recipient (Hmelo et al., 2015). A culture of the desired *Pa* ID40 or *Pa* PA14 strain was grown overnight in 5 ml LB

as well as a verified clone of mutator plasmid containing *E. coli* SMλpir in 5 ml LB containing 15 µg/ml gentamicin. The next day, 200 µl of the *E. coli* donor and 400 µl of the *Pa* recipient were mixed and centrifuged at 10.000 x g for 1 minute. The pellet was resuspended in 100 µl LB and applied to a LB-agar plate as one big drop and incubated at 37°C overnight.

2.3.6.6 Allelic exchange

The following steps use different selective media to select only *Pa* strains with the desired genomic features.

The next day, the bacterial material was scraped off the plate and resuspended in 2 ml LB. 10 and 100 µl of it were spread on two individual LB-agar plates containing 25 µg/ml irgasan and 75 µg/ml gentamicin and incubated at 37°C overnight. pEXG2 derivates are suicide vectors and cannot replicate in *Pa*. Therefore, the insertion of the vector genome by homologous recombination is necessary for vector genome persistence and survival of *Pa* in an antibiotic selection medium as the plasmid encodes for gentamicin resistance. This event is called single-cross over (Hmelo et al., 2015). The growth medium contains (in addition to LB agar and gentamicin) irgasan for the elimination of *E. coli* cells.

4 single colonies were picked and each used to inoculate 5 ml LB without selective agents. The cultures were grown with shaking at 37°C overnight to take away selection pressure again. A so-called double-crossover follows. In this process, homologous recombination takes place for the second time. The purpose of this step is the excision of the inserted vector including the gentamicin resistance and the *sacB* gene. The remaining genomic material of the plasmid can be removed (Hmelo et al., 2015).

Therefore, 100 µl of the overnight culture were used to inoculate 5 ml LB containing 20 % sucrose until the afternoon. Then, these cultures were plates onto LB + 15 % sucrose by a 3-loop streak and kept at 37°C overnight. It is important to note that the vector contains the *sacB* gene which was found originally in *Bacillus subtilis* species. It encodes for the enzyme levansucrase which hydrolyses sucrose (present in counterselection medium) to levan polysaccharides, high molecular weight fructose polymers with a toxic effect on

Pa cells. The first cross-over of *Pa* cells which undergo sucrose counter-selection is followed by a second homologous cross-over that results either in *Pa* cells that returned to wildtype, cells that have acquired the desired deletion or merodiploids which have evaded the second crossover and acquired a loss of function mutation only in the *sacB* gene (Hmelo et al., 2015).

Single colonies were picked, and streaked on a LB-agar grid plate containing 75 µg/ml gentamicin as well as on a LB-agar grid plate and incubated at 37°C overnight.

2.3.6.7 PCR verification of resulting deletion mutants

Eventually, gentamicin sensitive and sucrose resistant (double recombinant) colonies were assayed by PCR using primers flanking the allele (“seqF”, “seqR”), resulting either in a small DNA fragment (mutant) or a larger DNA fragment (wildtype) of distinct length.

Suitable clones were grown in 5 ml LB at 37°C overnight. Genomic DNA was isolated and served as a template for another conformation PCR which consisted of two different approaches. On the one hand, target gene-flanking primers (“SeqF”, “SeqR”) were used to amplify the genomic area containing the GOI or its respective deletion. We called this step proof PCR 1. On the other hand and in a second PCR approach, “SeqF” primer is combined with an “insideR” primer. This primer anneals to a region within the wildtype allele which was deleted in the mutant genome. Therefore, only wildtype strains can run through polymerase chain reaction and show bands in the consecutive gel electrophoresis. We called this step proof PCR 2. Wildtype genomic DNA was used as a control for both approaches.

2.3.7 Production of complementation mutants of Pa ID40 with a functional dacB gene

The strains ID40::*dacB*(PA14) and ID40Δ*creBC*::*dacB*(PA14) were provided by AG Bohn/Schütz. Nevertheless, the generation is described here for sake of clarity.

To generate conditional complementary strains a protocol was used based on the description by Choi and Schweizer (2006) using the expression vector pJM220 (pUC18T-miniTn7T-gm-rhaSR-PrhaBAD). In this procedure a cassette consisting of a gentamicin resistance cassette and the GOI under control of a rhamnose inducible promoter and flanked by Tn7R and Tn7L is inserted into the Tn7 attachment site adjacent to the *glmS* gene.

To complement *Pa* ID40 with a functional *dacB* gene derived from PA14, the *dacB* gene of PA14 was amplified by PCR using the primers "pJM_dacB_PA14_F" and "pJM_dacB_PA14_R". pJM220 was linearized by PCR using the primers "Gib_uni_pJM220_F" and "pJM220_R". Subsequently, the purified PCR fragments were fused by Gibson assembly (as described in section 2.3.6.2). 8 µl Gibson assembly mix were then used to transform *E. coli* Top10 cells. Subsequently, bacterial colonies carrying the appropriate plasmid were verified by colony PCR using the primers "pJM220_seq_F" and "pJM220_seq_R". Four verified bacterial clones were regrown in 5 ml LB containing 15 µg/ml gentamicin, the DNA was isolated using the Monarch plasmid kit and outsourced for sequencing. 50 ng of verified pJM220 *dacB*(PA14) plasmid DNA (with the correct sequence) was then together with 50 ng pTNS3 helper plasmid electroporated into ID40 strains according to the electroporation protocol described in section 2.3.9.1. The pTNS3 helper plasmid expresses a transposase which is required to integrate parts of pJM220 at a distinct Tn7 attachment site of the *Pa* chromosome.

The bacteria were then plated on LB agar plates containing 75 µg/ml gentamicin. Gentamicin resistant clones should have the fragment Tn7R-Genr-rhaSR-rha-dacB-Tn7L integrated into the genome. This was verified by a PCR using the primers "Tn7R_F" and "ID27_glmS2_down_F".

To get rid of the helper plasmid pTNS3, the bacteria were now grown overnight on LB agar plates. Subsequently single clones were picked and tested for loss of carbenicillin resistance by streaking them both on LB agar plates and LB agar containing 200 µg/ml carbenicillin.

Since the gentamicin cassette is flanked by *frt* sites, the gentamicin resistance cassette can be removed by introducing now the pFLP2 plasmid which encodes for a flp recombinase. This recombinase attaches to the *frt* sites and catalyzes the removal of the gentamicin cassette.

For this purpose, the bacteria were electroporated with 50 ng pFLP2 according to the electroporation protocol and then grown in 1 ml LB with shaking for 1 h at 37°C. 10 µl of the culture were then diluted with 990 µl LB and 100 µl and 10 µl of this suspension were plated on LB agar containing 200 µg/ml carbenicillin and incubated at 37°C overnight. Subsequently 16 clones were picked and streaked on both an LB agar plate with 75 µg/ml gentamicin and on one with 200 µg/ml carbenicillin and incubated overnight at 37°C.

The flp recombinase removes the gentamicin cassette and the bacterial clones should now be gentamicin sensitive but still carbenicillin resistant.

To get rid of the pFLP2 plasmid carrying the carbenicillin resistance, a gentamicin sensitive clone was streaked on and grown overnight on a LB agar plate.

Several clones were then picked and grown on NSLB-agar plates containing 15 % sucrose. Since the pFLP2 plasmid also carries a *sacB* gene, only bacteria lacking the plasmid should grow on this plate.

Clones with a carbenicillin sensitive, gentamicin sensitive, sucrose resistant phenotype were finally checked by PCR by amplifying the region of the gentamicin resistance gene and the rhamnose promoter with primers “pJM220_Gen_F” and “pJM220_Gen_R”.

Primer pairs and the expected fragment lengths for the different PCR steps in the process of generating ID40::*dacB*(PA14) and ID40Δ*creBC*::*dacB*(PA14) are listed in Table 23.

Table 23: Primer pairs used for the generation of complementation mutants and lengths of the synthesized fragments

Primer pairs	Expected fragment length
Gib_uni_pJM220_F Gib_uni_pJM220_R	6686 bp
pJM_dacB_PA14_F pJM_dacB_PA14_R	1499 bp
pJM220_seq_F pJM220_seq_R	1863 bp
ID27_glmS2_down_F Tn7L_R	491 bp
pJM220_Gen_F pJM220_Gen_R before flp recombinase	1000 bp
pJM220_Gen_F pJM220_Gen_R after flp recombinase	/

2.3.8 Production of tag-labelled mutants of Pa ID40 and Pa PA14

Knock-in mutants were labelled with a sequence encoding for a protein tag either at the 5´ end or 3` end of the coding sequence of GOIs. The protein tag can in the further course be targeted by specific antibodies and by this means, the expression of the regarding gene can be analysed in a Western Blot analysis.

Two genes were therefore marked with a tag: an HA-tag was attached to the *creB* gene whereas a Strep-tag followed by a HiBiT-tag was connected to the *ampDh3* gene in four different bacterial strains (*Pa* ID40, *Pa* PA14, *Pa* ID40 ∆*ygfB*, *Pa* PA14 ∆*ygfB*). HA-tags and Strep-tags origin in hemagglutinin and streptavidin, respectively. Strep-tags constitute a peptide sequence (Trp-Ser-His-Pro-Gln-Phe-Glu-Lys) (Schmidt and Skerra, 2007). Both tags can be detected by specific antibodies. In contrast, the HiBiT-tag can bind to LgBiT which leads to reconstitution of a functional luciferase. The functional luciferase can convert furimazine into fumiramide with additional light emission (Promega, Manufacturer`s protocol).

Knock-in mutagenesis is based on the same principle as knock-out mutagenesis (described in section 2.3.6). However, in contrast to the knock-out mutagenesis, knock-in mutagenesis allelic exchange leads to the insertion of a gene fragment. Mutagenesis started with the conjugation of the four Pa recipient strains mentioned above, each with two donor strains: *E. coli* SMλpir ampDh3-strep-HiBiT or *E. coli* SMλpir HA-CreB. The following steps were performed analogously to the mutagenesis of deletion mutants.

Only for PCR verification of the mutations different primer choices were necessary: firstly, gentamicin sensitive and sucrose resistant clones were tested by a PCR with primers which display the tag sequence (HA-CreB: “CreBtagproof_F” and “CreBtagproof_R”, ampDh3-strep-HiBiT: “ampDh3hibitproof_R” and “ampDh3proof_3”). Because “CreBtagproof_R” and “ampDh3proof_3” bind within the tag region, only mutants but not wildtype controls were supposed to show bands in the agarose gel electrophoresis after PCR. Genomic DNA was subsequently isolated from clones with inserted tag mutations and secondly, two PCR approaches were performed: as proof PCR 1, the first PCR with tag-proofing primers was repeated with genomic DNA. Additionally, a PCR was implemented with primers which bind upstream and downstream of the tag sequence as proof PCR 2 (HA-CreB: “CreBtagproof_F” and “CreB_inside3_R”, ampDh3-strep-HiBiT: “ampDh3proof_1” and “ampDh3proof_3”). In this case, wildtype controls were supposed to show a smaller band than knock-in mutants.

2.3.9 Luciferase-assay

2.3.9.1 Generation of strains carrying *nanoluc* reporter gene to measure the transcriptional activity of the *ampDh3* promoter

To measure transcriptional activity of the *ampDh3* promoter the plasmid pBBR-ampDh3-532-luc was used. This plasmid carries as a promoter element the gene fragment -532 to -1 upstream of the coding sequence of *ampDh3* fused to the *nanoluc luciferase* gene (see also Figure 25). Whenever this promoter is active,

the luciferase is produced and can convert furimazine in fumiramide, and light emission can be recorded. In strains carrying pBBR-ampDh3-532-luc, the luciferase activity indicates the degree of *ampDh3* promoter activity, AmpDh3 production and amount in the cells. To determine basal luciferase activity independent of *ampDh3* transcriptional activity a pBBR derivate was used which encoded only the Nanoluc luciferase lacking any promoter (pBBR-luc).

Therefore, overnight cultures of the respective bacterial strains were grown and centrifuged at 4.500 x g for 5 minutes. The pellet was resuspended in 6 ml of 300 mM sucrose. This washing step was repeated twice and the pellet was then resuspended in 1 ml 300 mM sucrose and transferred to an Eppendorf cap. The suspensions were further centrifuged at 10.000 x g for 1 minute and the pellets were resuspended in 200 µl of 300 mM sucrose. Electroporation cuvettes were filled with 100 µl of the bacterial suspensions and 1 µl of plasmid DNA (50-100 ng) was added so that each plasmid could be electroporated into appropriate bacterial strains. The electroporation at 2,5 kV destabilizes bacterial membranes, accordingly the plasmid can be taken up by the cells. Next, 1 ml prewarmed LB medium was added to the electroporated cells. Then, bacteria were grown at 37°C for 1 hour with shaking. Afterwards, they were centrifuged at 10.000 x g for 1 minute and the supernatant was decanted, leaving approximately 150 µl of medium on the pellet. As the plasmids also encode for gentamicin resistance, 10 µl and 100 µl were plated onto LB agar containing 75 µg/ml gentamicin and incubated at 37°C overnight. The resulting plasmid-carrying strains could then be picked from the plates and grown in LB medium containing 75 µg/ml gentamicin for cultures or cryocultures.

2.3.9.2 Luciferase-assay

To measure luciferase activity the Nano-Glo® Luciferase Assay System (Promega) was used. To this end, overnight cultures of strains carrying pBBR-ampDh3-532-luc or pBBR-luc were subcultured for 2 hours also in LB medium containing 75 µg/ml gentamicin. The OD of 1 ml bacterial culture was measured and used to calculate the volume of bacterial suspension required for an amount of $2 \cdot 10^8$ bacteria as followed:

$$c \cdot v = 2 \cdot 10^8$$

$$OD \cdot 10^9/ml \cdot v = 2 \cdot 10^8$$

$$v = \frac{2 \cdot 10^8}{OD \cdot 10^9/ml} = \frac{0{,}2}{OD}\ ml = \frac{200}{OD}\ \mu l$$

The calculated volume of bacterial suspension was transferred into an Eppendorf cap and filled with LB medium up to 1 ml. For each strain, 3 wells of a 96-well-microplate F-bottom chimney well white lumitrac plate were filled with 50 µl of the bacterial suspensions of known number of bacteria. The Nano-Glo® Luciferase Assay reaction mix was prepared from assay buffer and the substrate furimazine by mixing them in a ratio of 50:1 according to the manufacturer`s instructions. 50 µl of reaction mix were pipetted per well with a multichannel pipette in the 96-well-plate. This was done as fast as possible because the luciferase reaction starts immediately, and measurements should preferably start synchronously. Luciferase activity was quantified as chemiluminescence using a Tecan plate reader (mode: luminescence, attenuation: automatic, integration time: 500 ms).

2.3.10 Western Blot analysis

For Western Blot analysis, cell lysates were prepared. For this purpose, bacteria cultured overnight in LB medium were diluted 1:10 and then subcultured in LB medium (both at 37°C with shaking). Next, the optical density of 1 ml culture was measured photometrically. Subsequently, 1 ml of the subculture was centrifuged at 4.500 x g for 5 minutes. The pellet was then resuspended in equal volumes of H_2O and 4x Laemmli buffer (containing β-Mercaptoethanol). The volume of H_2O and buffer, respectively, was calculated as followed: x µl = OD_{600} · ml subculture · 50. These suspensions were frozen at -20°C and prior to use boiled at 95°C for 10 minutes. After cooling down on ice and a short centrifugation step, they were loaded on an SDS-polyacrylamide gel.

SDS-PAGE was performed using a 4 - 20 % Mini-PROTEAN® TGX™ Precast Protein gel. The gel was loaded with 13 µl sample and 10 µl marker (Page ruler prestained, Thermo Scientific), respectively per well. It was run in 1 x SDS running buffer at 110 V for 60 minutes.

Subsequently, the proteins were transferred onto a nitrocellulose membrane via electroblotting. Therefore, the Western Blot was assembled in a tank filled with transfer Buffer and containing a cooling unit. The protein transfer was performed at 0,35 Ampère (constant current) at 4°C for 1 hour.

The membrane blot sandwich was carefully disassembled, and the membrane was washed shortly in VE water. Afterwards, it was stained in Ponceau S solution for 10 minutes on a shaking rocker. The unbound dye was removed by washing with VE water 3 times before recording the coloured membrane. As marker bands were clearly visible at that stage, the membrane could subsequently be cut into various smaller membrane fragments, according to the analysed protein and its specific size. This allows incubation with different antibodies and detection of various proteins using only one membrane.

Consequently, the membrane parts were blocked in 5-10 ml 1 x Serva Blue Block at room temperature on a shaking rocker for 60 minutes. Then, for all membranes except for ampDh3-strep-HiBiT detection membranes, primary antibodies were added and incubated at 4°C overnight under constant shaking. The membrane parts were washed 3 times with 5-10 ml TBS-T buffer and then, secondary antibodies were added in 5-10 ml 1 x Serva Blue Block at room temperature on a shaking rocker for 60 minutes. Table 24 gives an overview of all utilized antibodies and appropriate dilutions. The membrane was washed likewise and placed into PBS for 5 minutes before adding Clarity Western ECL solution (Bio-RAD). Proteins were detected with the Western Blot detection system Fusion Solo 3S.WL.

Table 24: Antibodies and dilutions employed in Western Blot analysis

Protein	Primary antibody	Dilution	Secondary antibody	Dilution
RpoB	anti-RNA polymerase beta (Abcam)	1:2000	Goat F(ab`) anti-Rabbit IgG (H+L)-HRPO (Dianova)	1:2000
YgfB	Polyclonal rabbit-anti-YgfB *Pseudomonas aeruginosa* (self made, Bohn lab)	1:200	Goat F(ab`) anti-Rabbit IgG (H+L)-HRPO	1:2000
HA	Anti-HA (Dianova)	1:1000	Rabbit anti-mouse HRP (Thermoscientific)	1:2000

For detection of AmpDh3, membranes were washed directly after blocking with 5 ml 1 x TBS-T and 5 ml 1 x TBS for 5-10 minutes in each case. According to the manufacturer´s description, a detection buffer was mixed (containing 97 % lytic buffer, 2 % furimazine solution and 1 % LgBiT solution) and added to the membrane. Chemiluminescence could then be detected using the Western Blot detection system Fusion Solo 3S.WL.

3 Results

3.1 Generation of *Pa* ID40 and *Pa* PA14 mutants

3.1.1 Cloning of mutator plasmids

Answering the fundamental question of whether and how *ygfB, creBC, dacB* and other genes influence antibiotic resistance in *Pa* requires the generation of deletion mutants for these relevant genes. By deleting a gene, it is possible to impede its effects on the bacterial cell.

In the course of constructing the mutator plasmid, an upstream fragment was generated by PCR using the primer pair "(GOI)_up_F" and "(GOI)_up_R". Likewise, a downstream fragment originated from a PCR with primers "(GOI)_dn_F" and "(GOI)_dn_R". The upstream fragment consisted of the approximately 800 bp upstream of the target and of around 30 bp of the 5` region of the target gene itself. Similarly, the downstream fragment consisted of around 30 bp which mark the end of the target gene and of approximately 800 bp downstream the GOI. Table 25 summarizes the primer pairs used for PCR and the expected length of the resulting PCR products.

Table 25: List of fragments generated, primer pairs used for amplification and expected lengths of fragments

Fragment	Primer	Length
pexG2_*ampR*_up	ampR_up_F ampR_up_R	892 bp
pexG2_*ampR*_down	ampR_dn_F ampR_dn_R	986 bp
pexG2_*icmF2*_up	icmF2_up_F icmF2_up_R	846 bp
pexG2_*icmF2*_down	icmF2_dn_F icmF2_dn_R	940 bp
pexG2_*TUEID40_01954*_up	TUEID40_01954_up_F TUEID40_01954_up_R	900 bp
pexG2_*TUEID40_01954*_down	TUEID40_01954_dn_F	929 bp

	TUEID40_01954_dn_R	
pexG2_*dacB*(PA14)_up	dacBPA14_up_F dacBPA14_up_R	929 bp
pexG2_*dacB*(PA14)_down	dacBPA14_dn_F dacBPA14_dn_R	919 bp

The up- and downstream fragments synthesized by PCR were further verified for their correct length by agarose gel electrophoresis (Figures 7 and 8). Subsequently the PCR products were purified by a DNA purification kit (Promega).

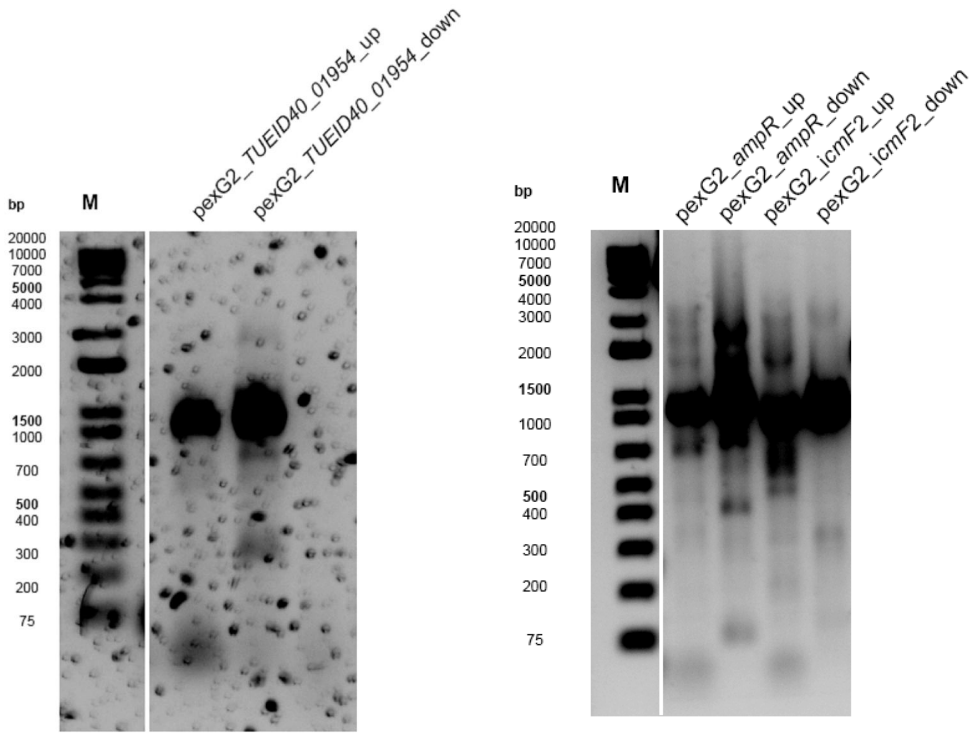

Figure 7: Validation of PCR reactions for amplification of the up- and downstream fragments of *TUEID_01954, ampR* and *icmF2*

For the generation of mutator plasmids to delete *TUEID40_01954, ampR* and *icmF2,* an upstream and a downstream fragment were synthesized by PCR. The corresponding gel electrophoresis showed bands of the expected lengths.

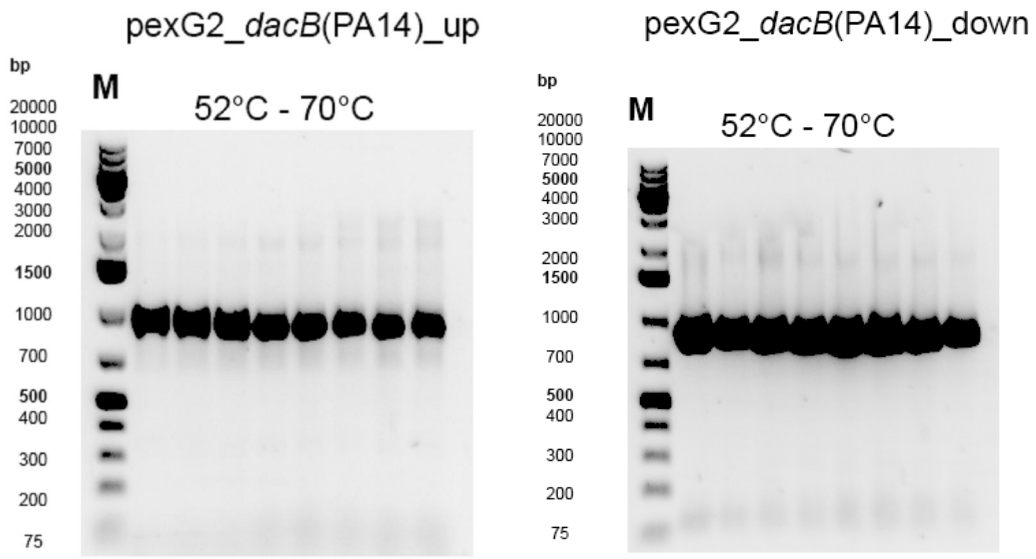

Figure 8: Validation of PCR reactions for amplification of the up- and downstream fragments of *dacB*(PA14)

For the deletion of *dacB*(PA14), an upstream and a downstream fragment were synthesized by PCR. Gradient PCRs with annealing temperatures ranging from 52°C to 70 °C were performed. The corresponding gel electrophoresis showed bands of the expected lengths.

The upstream fragment, the downstream fragment and an already available PCR product of the linearized vector pEXG2 could be assembled to form the mutator plasmid by a Gibson reaction.

Afterwards the closed plasmid resulting from the Gibson Assembly could be horizontally transferred to *E. coli* Top10 bacteria by transformation. A colony PCR followed the transformation step to verify whether the plasmid had been taken up. For this purpose, primers “pEXG2_seq_F” and “pEXG2_seq_R” were employed which amplify the region where the inserts (up- and downstream fragment) should have been integrated into pEXG2. As described in Table 26, each mutator plasmid yielded a PCR product of the desired length in the colony PCR.

Table 26: Mutator plasmids and corresponding lengths of their inserts

Plasmid	**Length**
pexG2 Δ*ampR*	2471 bp
pexG2 Δ*icmF2*	2396 bp
pexG2 Δ*TUEID40_01954*	2445 bp
pexG2 Δ*dacB*(PA14)	2552 bp

For colonies which had shown the correct band size in gel electrophoresis, the plasmid DNA was isolated and sent for sequencing using the primers “pEXG2_seq_F” and “pEXG2_seq_R” (Table 12) as well as gene specific sequencing primers (Table 13). Plasmids with the correct sequence were then transformed into *E. coli* SMλpir. As another form of horizontal gene transfer, the plasmid was consequently passed on to *Pa* strains by conjugation and biparental mating. Table 27 depicts the biparental matings which were performed.

Table 27: Donor and recipient strains used for biparental matings

***Pa* recipient strain**	***Ec* SMλpir donor strain**	**Deletion mutant**
Pa ID40	*Ec* SMλpir Δ*creBC*	*Pa* ID40 Δ*creBC*
Pa ID40 Δ*ygfB*	*Ec* SMλpir Δ*creBC*	*Pa* ID40 Δ*creBC* Δ*ygfB*
Pa ID40 Δ*creBC*	*Ec* SMλpir Δ*ampR*	*Pa* ID40 Δ*creBC* Δ*ampR*
Pa ID40	*Ec* SMλpir Δ*ampR*	*Pa* ID40 Δ*ampR*
Pa ID40	*Ec* SMλpir Δ*icmF2*	*Pa* ID40 Δ*icmF2*
Pa ID40	*Ec* SMλpir Δ*TUEID40_01954*	*Pa* ID40 Δ*TUEID40_01954*
Pa PA14	*Ec* SMλpir Δ*creBC*	*Pa* PA14 Δ*creBC*
Pa PA14 Δ*ygfB*	*Ec* SMλpir Δ*creBC*	*Pa* PA14 Δ*creBC* Δ*ygfB*
Pa PA14 Δ*creBC* Δ*ygfB*	*Ec* SMλpir Δ*ampR*	*Pa* PA14 Δ*creBC* Δ*ygfB* Δ*ampR*
Pa PA14	*Ec* SMλpir Δ*ampR*	*Pa* PA14 Δ*ampR*
Pa PA14	*Ec* SMλpir Δ*icmF2*	*Pa* PA14 Δ*icmF2*
Pa PA14	*Ec* SMλpir Δ*TUEID40_01954*	*Pa* PA14 Δ*TUEID40_01954*
Pa PA14	*Ec* SMλpir Δ*dacB*	*Pa* PA14 Δ*dacB*
Pa ID40 Δ*ygfB*	*Ec* SMλpir Δ*dacB*	*Pa* PA14 Δ*dacB* Δ*ygfB*
Pa PA14 Δ*dacB*	*Ec* SMλpir Δ*creBC*	*Pa* PA14 Δ*dacB* Δ*creBC*
Pa PA14 Δ*dacB* Δ*ygfB*	*Ec* SMλpir Δ*creBC*	*Pa* PA14 Δ*dacB* Δ*ygfB* Δ*creBC*

In the following allelic exchange steps, the plasmid genome should be integrated into the Pa genome by homologous recombination. An antibiotic selection ensured this first cross-over. Secondly, the plasmid backbone was lost in a second cross-over. This loss could be verified by sucrose counter-selection. The second cross-over can generally result in either the desired deletion mutants or in genomic WT variants. In order to distinguish WT and mutant strains, proof PCRs were performed as graphically illustrated in Figure 9.

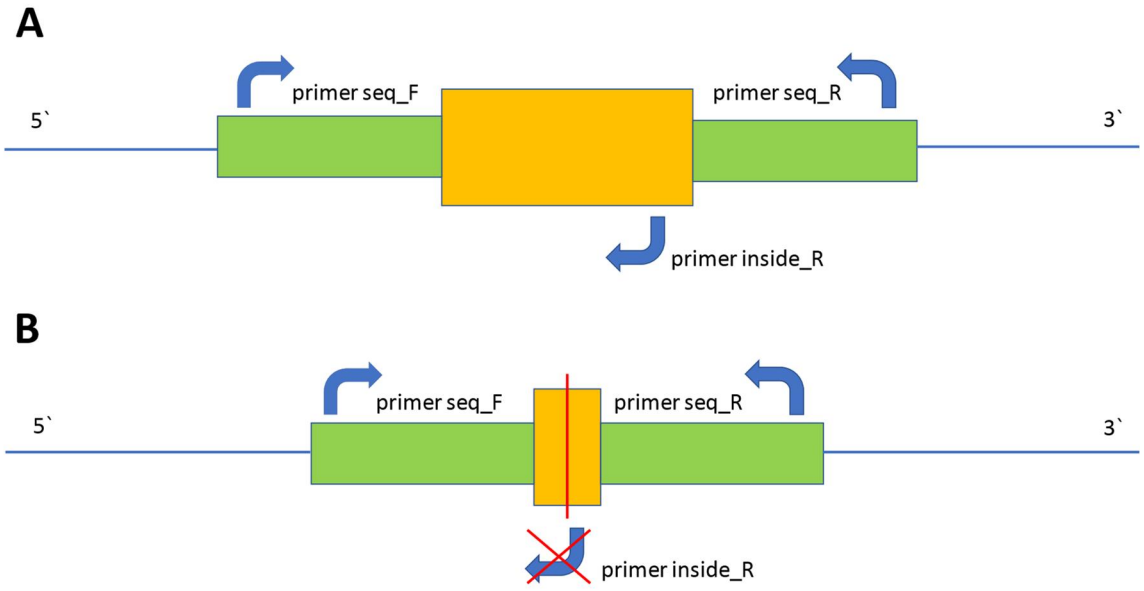

Figure 9: Binding sites for the primers employed in proof PCRs for deletion verification

(A) WT variant

(B) deletion mutant

Primers “seq_F” and “seq_R” can attach to both genomic variants as they bind to a preserved genomic area. Primer “inside_R” however attaches to a genomic area which is included in the region that was deleted. Consequently, this primer can only bind in genomic WT variants but not in deletion mutants. This PCR thus yields a product in WT strains only.

In proof PCR 1, primers (“seq1_F” and “seq2_R”) bind to the genomic sequence flanking the potential deletion site. In deletion mutants, the resulting PCR fragments are shorter than in WT strains. The bands in agarose gel electrophoresis consequently show different lengths.

Proof PCR 2 was performed with primer “seq1_F” which binds upstream of the target gene and was already employed in proof PCR 1, and primer “inside3_R”.

The latter binds to a genomic region inside the potentially deleted area. For this reason, WT strain genome can be amplified by proof PCR 2 and showed according bands whereas proof PCR 2 shows no band in deletion mutants. Table 28 summarizes the expected PCR fragment sizes of the performed proof PCRs.

Table 28: Primers and fragment lengths used for the verification of deletions by proof PCRs

Mutation	**Proof PCR type**	**Primers**	**WT length**	**Mutation length**
Δ*ampR*	Proof PCR 1	ampR_seq1_F ampR_seq2_R	1241 bp	429 bp
	Proof PCR 2	ampR_seq1_F ampR_inside3_R	454 bp	/
Δ*icmF2*	Proof PCR 1	icmF2_seq1_F icmF2_seq2_R	4109 bp	660 bp
	Proof PCR 2	icmF2_seq1_F icmF2_inside3_R	437 bp	/
Δ*TUEID40_01954*	Proof PCR 1	TUEID40_01954_seq1_F TUEID40_01954_seq2_R	1346 bp	412 bp
	Proof PCR 2	TUEID40_01954_seq1_F TUEID40_01954_inside3_R	436 bp	/
Δ*dacB*	Proof PCR 1	dacBPA14_seq_F dacBPA14_seq_R	2001 bp	630 bp

	Proof PCR 2	dacBPA14_seq_F dacBPA14_inside_R	490 bp	/
Δ*creBC*	Proof PCR 1	CreB_seq1_F CreB_seq2_R	2462 bp	408 bp
	Proof PCR 2	CreB_seq1_F CreB_inside3_R	356 bp	/
Δ*ygfB*	Proof PCR 1	05723_seq_F 05723_seq_R	1084 bp	1525 bp
	Proof PCR 2	05723_seq_F 05723_inside_R	655 bp	/

The following passage comprises the documentation of the deletions of the single target genes. Preferably, all deletions in a target gene were visualized in one agarose gel electrophoresis. The employed primers and characteristic lengths of the amplified fragments are indicated in Table 28, respectively. For each figure, the bands in agarose gel electrophoresis of proof PCR 1 can be seen on the lefthand side. The righthand side represents proof PCR 2.

Particular technical defiances or merely the high amount of deletion mutants in one target gene sometimes necessitated various pictures for the documentation of deletions.

In Figure 10 *ampR* deletion was validated. Proof PCR1 shows for all mutants a band at the expected size and proof PCR2 only for the WT strains. Unfortunately, no bands were visible for the WT strains with proof PCR1. This was possibly due to the fact that the elongation time was optimized to obtain the fragments corresponding to the length of strains that carry the desired deletion (which are reasonably shorter).

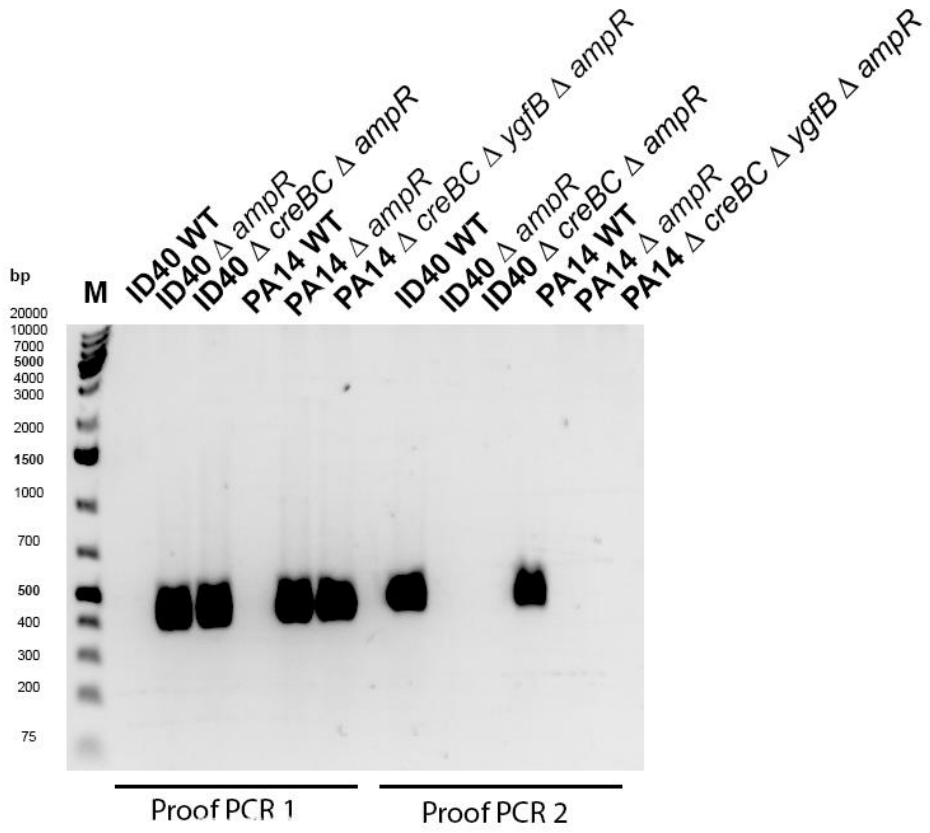

Figure 10: Agarose gel electrophoresis of proof PCRs for *ampR* deletion

Deletions in the gene of interest *ampR* were verified by two proof PCRs.

In Figure 11 and 12 *icmF2* deletion mutants and *TUEID40_01954* deletion mutants, respectively, were validated. In these cases, for PCR1 and PCR2 the expected bands could be detected. However, additional unspecific bands were detectable, which is probably due to unspecific binding of the primer in the *Pa* gDNA.

However, due to the presence of the expected bands with correct lengths in PCR1 and 2, the production of the desired deletion mutants can still be confirmed in all likelihood.

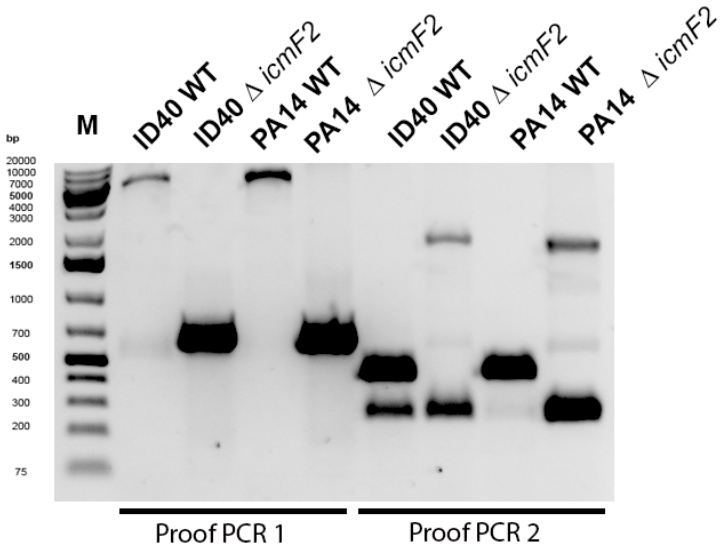

Figure 11: Agarose gel electrophoresis of proof PCRs for *icmF2* deletion

Deletions in the gene of interest *icmF2* were verified by two proof PCRs.

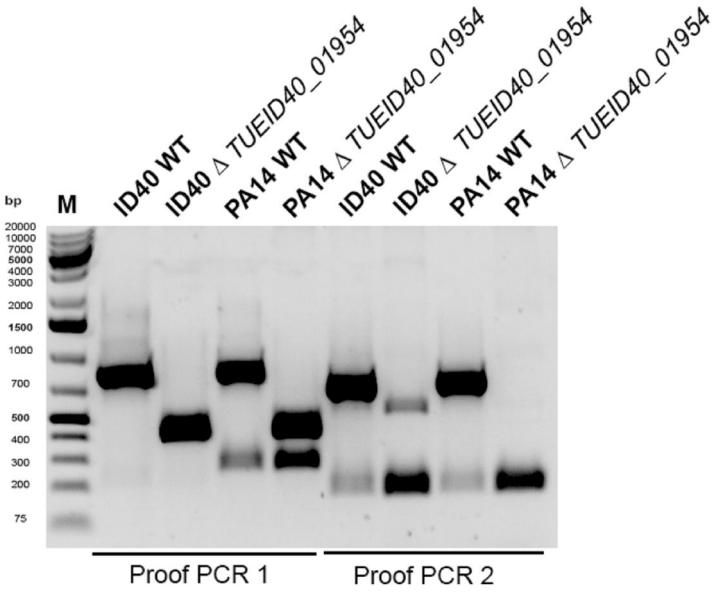

Figure 12: Agarose gel electrophoresis of proof PCRs for *TUEID40_01954* deletion

Deletions in the gene of interest *TUEID40_01954* were verified by two proof PCRs.

Figures 13 and 14 depict validation of the *creBC* and *ygfB* deletions with the correct bands for the mutants. Only weak WT bands were seen for ID40 but not PA14. This could be again due to the specific choice of elongation time. However, numerous PCR reactions confirmed the expected length of WT PCR products and the comparison between WT und mutant strains is still possible for the respective mutant bands.

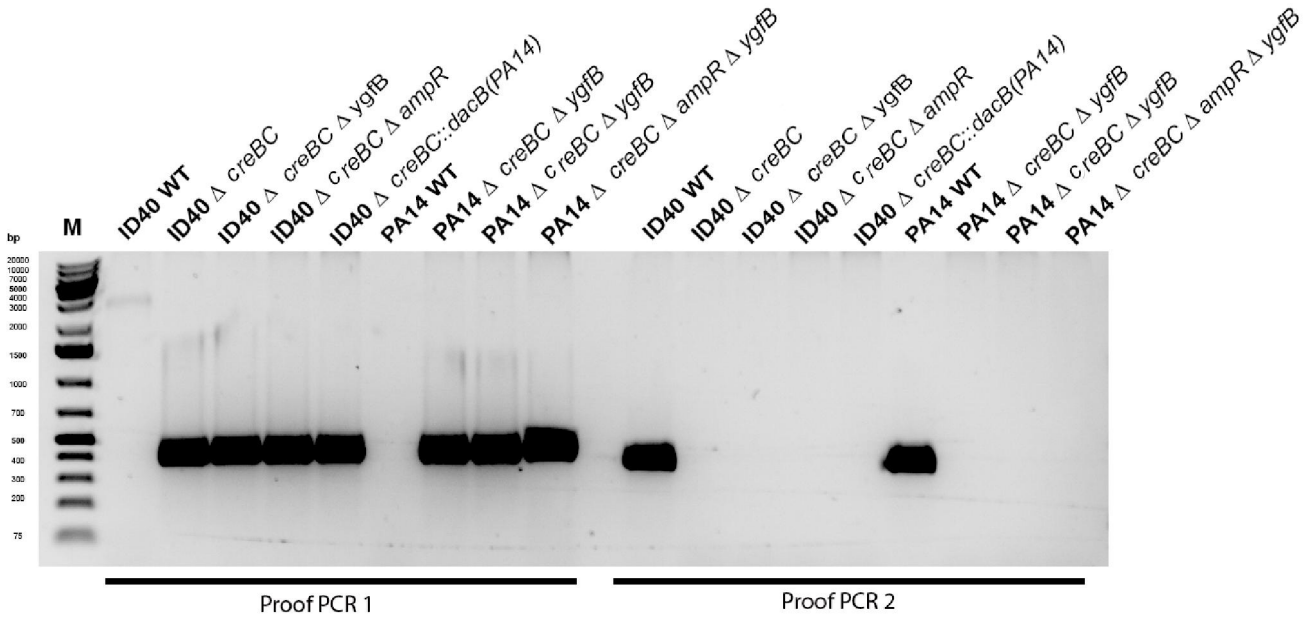

Figure 13: Agarose gel electrophoresis of proof PCRs for *creBC* deletion

Deletions in the gene of interest *creBC* were verified by two proof PCRs.

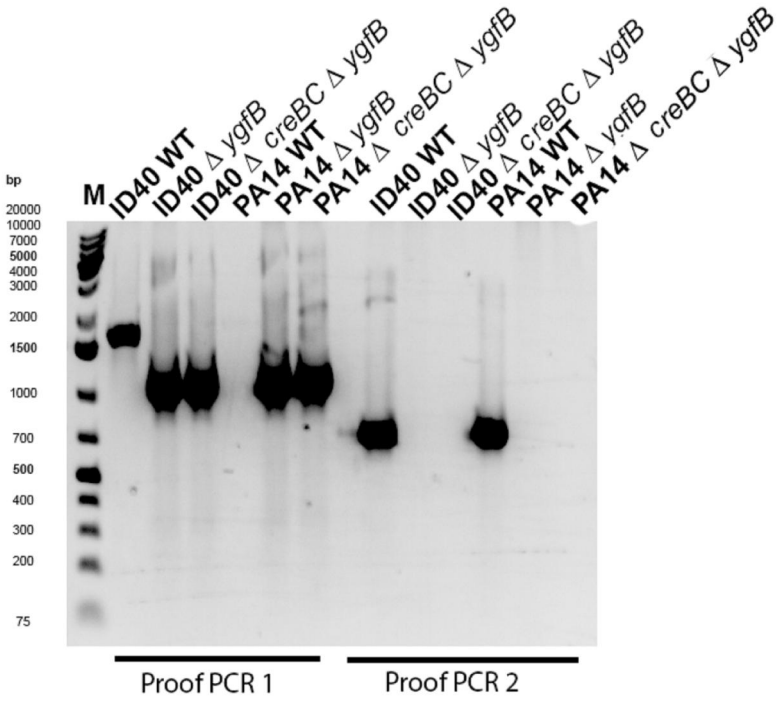

Figure 14: Agarose gel electrophoresis of proof PCRs for *ygfB* deletion

Deletions in the gene of interest *ygfB* were verified by two proof PCRs.

Figures 15 and 16 present the validation of *dacB* deletions. ID40 wildtype strain shows a similar band to PA14 wildtype strain as inactivation of *dacB* in ID40 occurs due to a point mutation (Sonnabend et al., 2020).

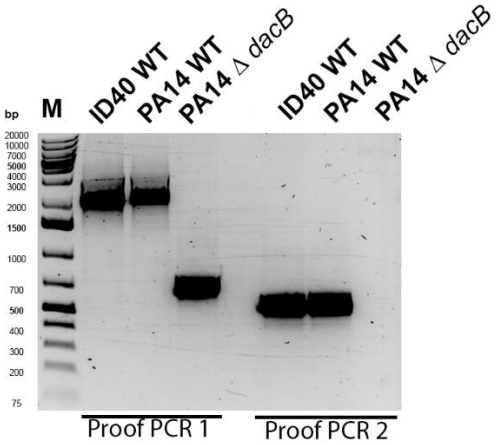

Figure 15: Agarose gel electrophoresis of proof PCRs for *dacB* deletion

Deletion of *dacB* was verified by two proof PCRs.

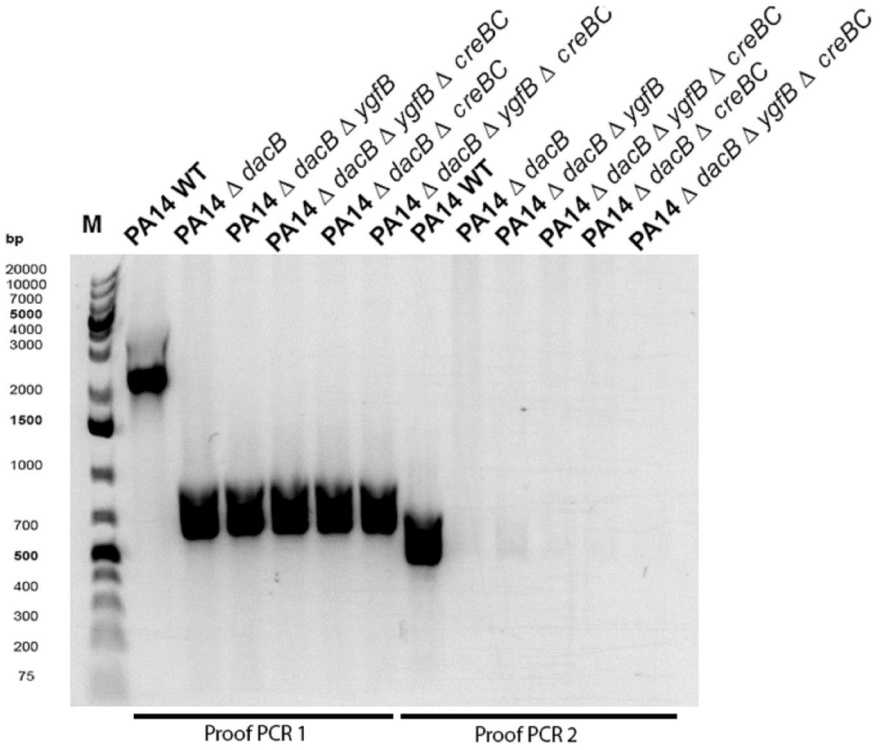

Figure 16: Agarose gel electrophoresis of proof PCRs for *dacB* deletion

Deletion of *dacB* in the indicated strains was verified by two proof PCRs.

Besides, for all the deletion mutants in the *dacB* gene, additional PCR steps were enclosed to rule out deletions in other than the genes desired to be deleted. These additional steps are shown in Figures 17-20. In Figure 17, *creBC* deletions were validated. The gel electrophoresis of proof PCR 2 shows as expected no bands for strains in which *creBC* was deleted and bands for strains in which *creBC* was still present. PCR 1 shows a clear band indicating *creBC* deletion for all *creBC* deleted strains with exception of PA14 Δ*dacB* Δ*creBC.* This strain was later checked by additional and also verified (data not shown).

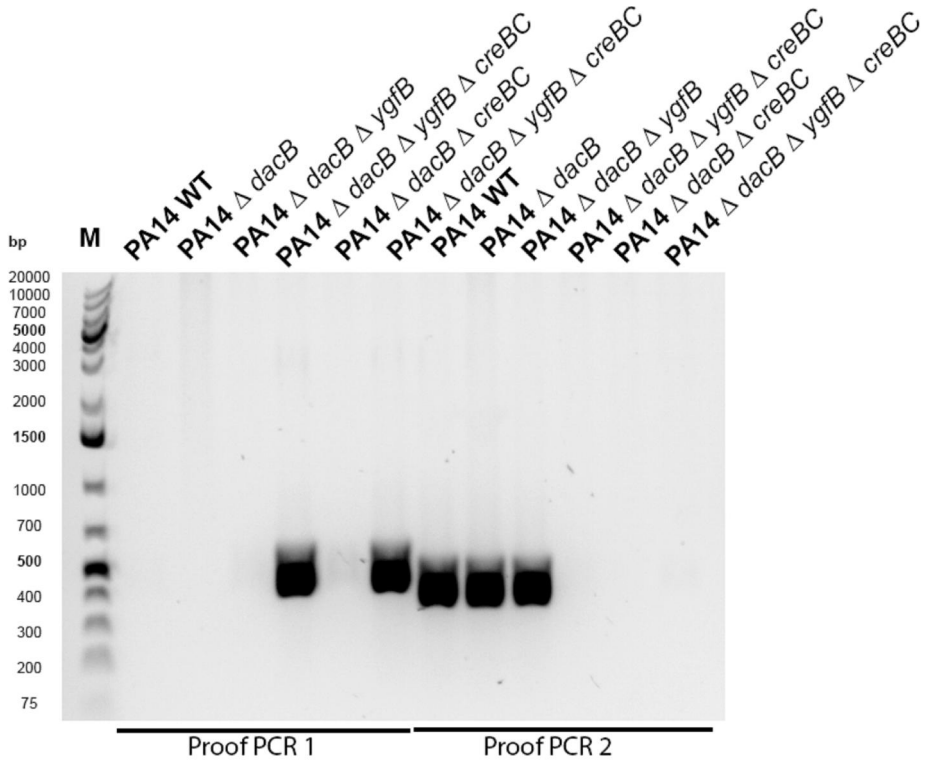

Figure 17: Agarose gel electrophoresis of proof PCRs for *creBC* deletion

Deletion of *creBC* in the indicated strains was verified by two proof PCRs. PA14 Δ*dacB* and PA14 Δ*dacB* Δ*ygfB* were included into the set of bacterial strains to demonstrate that in these strains *creBC* is still present.

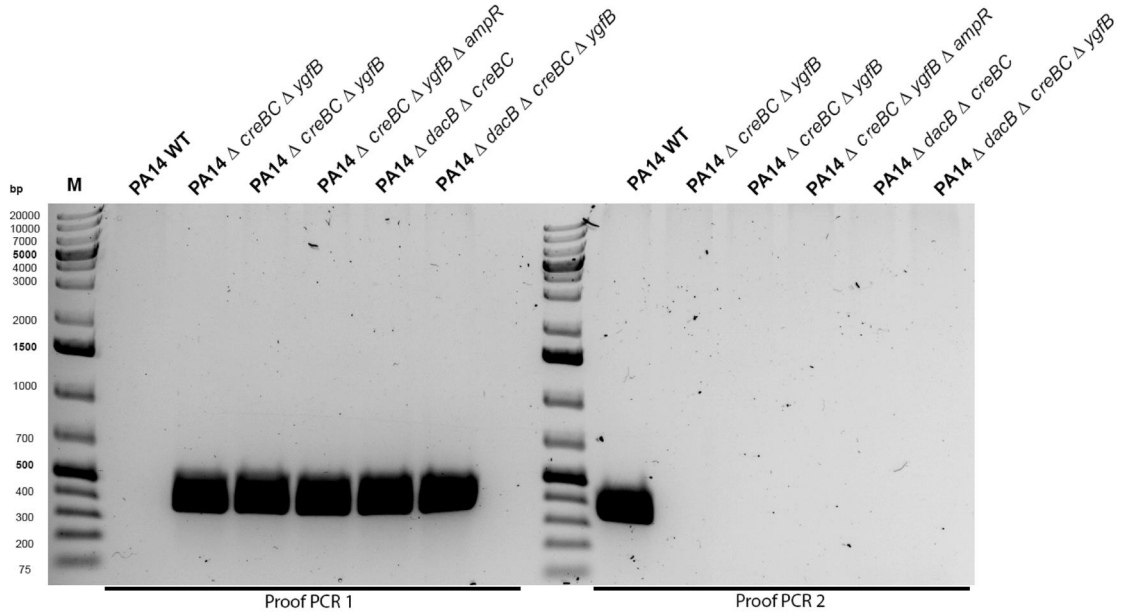

Figure 18: Agarose gel electrophoresis of proof PCRs for *creBC* deletion

Deletion of *creBC* in the indicated strains was verified by two proof PCRs.

In Figure 19, no gel electrophoresis bands can be seen for proof PCR1 of PA14 WT, PA14 Δ*dacB* and PA14 Δ*dacB* Δ*creBC*, probably as the elongation time of the corresponding PCR reaction was chosen particularly to obtain the fragments which carry the desired *ygfB* deletions and are thus considerably shorter than the fragments which carry an intact *ygfB* gene.

Similarly, Figure 20 lacks visible gel electrophoresis bands for proof PCR 1 of PA14 WT and PA14 Δ*dacB* Δ*creBC.*

However, in Figures 19 and 20, the occurrence of bands of the expected lengths for proof PCR 2 enables the confirmation of the intended *ygfB* deletions.

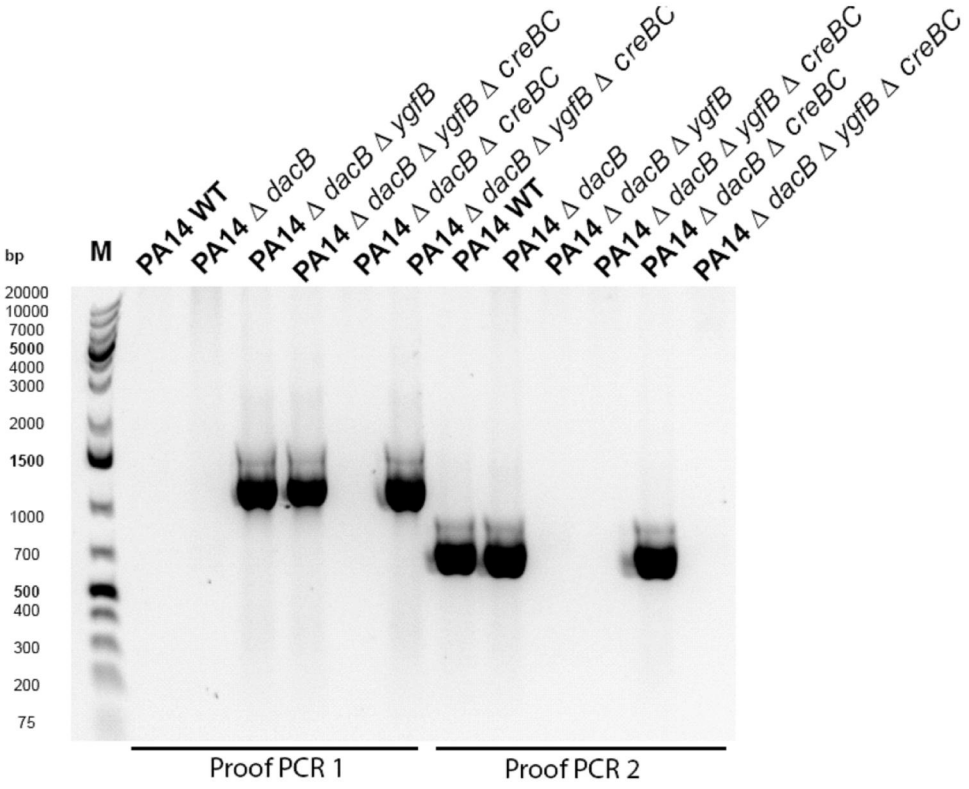

Figure 19: Agarose gel electrophoresis of proof PCRs for *ygfB* deletion

Deletion of *ygfB* in the indicated strains was verified by two proof PCRs. PA14 Δ*dacB* and PA14 Δ*dacB* Δ*creBC* were included into the set of bacterial strains to demonstrate that in these strains *ygfB* is still present.

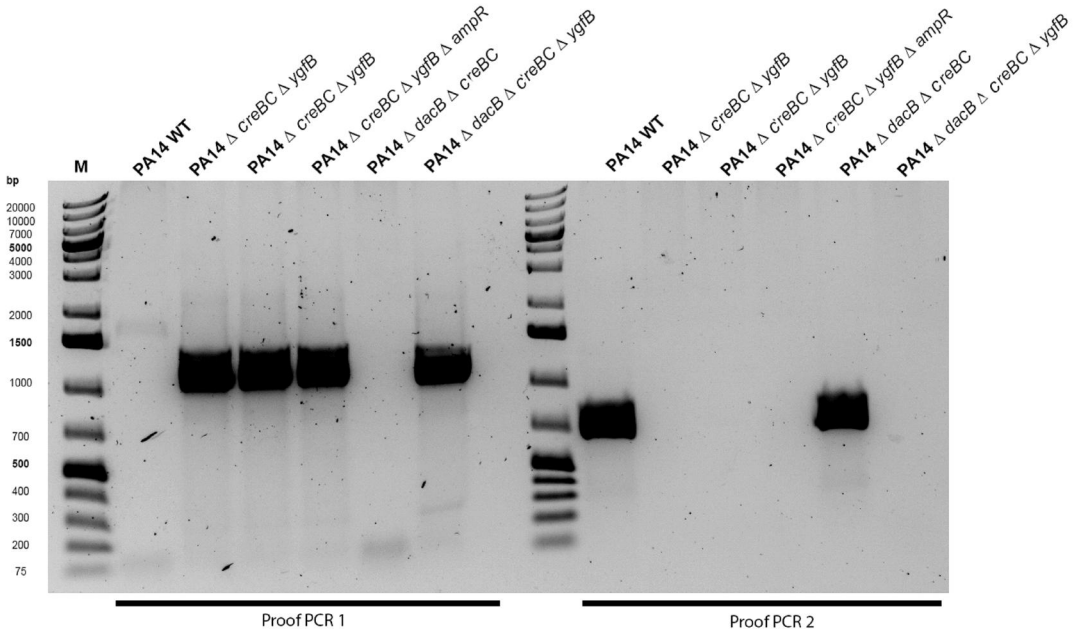

Figure 20: Agarose gel electrophoresis of proof PCRs for *ygfB* deletion

Deletion of *ygfB* in the indicated strains was verified by two proof PCRs. PA14 Δ*dacB* Δ*creBC* was included into the set of bacterial strains to demonstrate that in this strain *ygfB* is still present.

3.1.2 Production of tag-labelled mutants

For later detection of CreBC and AmpDh3 proteins, gene sequences were chromosomally introduced encoding for either a HA-tag or a HiBiT-tag. The biparental matings which were performed for knock-in mutagenesis are depicted in Table 29.

Table 29: Donor and recipient strains for biparental mating

***Pa* recipient strain**	***Ec* SMλpir donor strain**	**Tag labelled mutant**
Pa ID40	*Ec* SMλpir HA-CreB	*Pa* ID40 HA-CreB
Pa ID40 Δ*ygfB*	*Ec* SMλpir HA-CreB	*Pa* ID40 Δ*ygfB* HA-CreB
Pa PA14	*Ec* SMλpir HA-CreB	*Pa* PA14 HA-CreB
Pa PA14 Δ*ygfB*	*Ec* SMλpir HA-CreB	*Pa* PA14 Δ*ygfB* HA-CreB
Pa ID40	*Ec* SMλpir ampDh3-strep-HiBiT	*Pa* ID40 ampDh3-strep-HiBiT
Pa ID40 Δ*ygfB*	*Ec* SMλpir ampDh3-strep-HiBiT	*Pa* ID40 Δ*ygfB* ampDh3-strep-HiBiT
Pa PA14	*Ec* SMλpir ampDh3-strep-HiBiT	*Pa* PA14 ampDh3-strep-HiBiT
Pa PA14 Δ*ygfB*	*Ec* SMλpir ampDh3-strep-HiBiT	*Pa* PA14 Δ*ygfB* ampDh3-strep-HiBiT

The process of generating tag-labelled mutants resembles the deletion mutagenesis in all consequent steps of allelic exchange. Likewise, for the verification of tag inclusions, two proof PCRs were carried out. The primers for proof PCR 2 were designed to validate the correct insertion in the pEXG2 mutator plasmid and for the determination of mutants (Figures 21 and 22). Tag-labelled mutants can be identified by the inclusion of the tag, resulting in longer fragments in agarose gel electrophoresis (Table 30). Proof PCR 1 was performed using a primer pair in which one primer binds to the region encoding for the tag. Therefore, only in mutants a PCR fragment can be generated (Table 30).

Table 30: Primers and fragment lengths for the verification of deletions by proof PCRs

Tag	Proof PCR type	Primers	WT length	Mutation length
HA-CreB	Proof PCR 1	CreBtagproof_F CreBtagproof_R	/	492 bp
	Proof PCR 2	CreBtagproof_F CreB_inside3_R	640 bp	694 bp
ampDh3-strep-HiBiT	Proof PCR 1	ampDh3proof_3 ampDh3hibitproof_R	/	211 bp
	Proof PCR 2	ampDh3proof_3 ampDh3proof_1	413 bp	524 bp

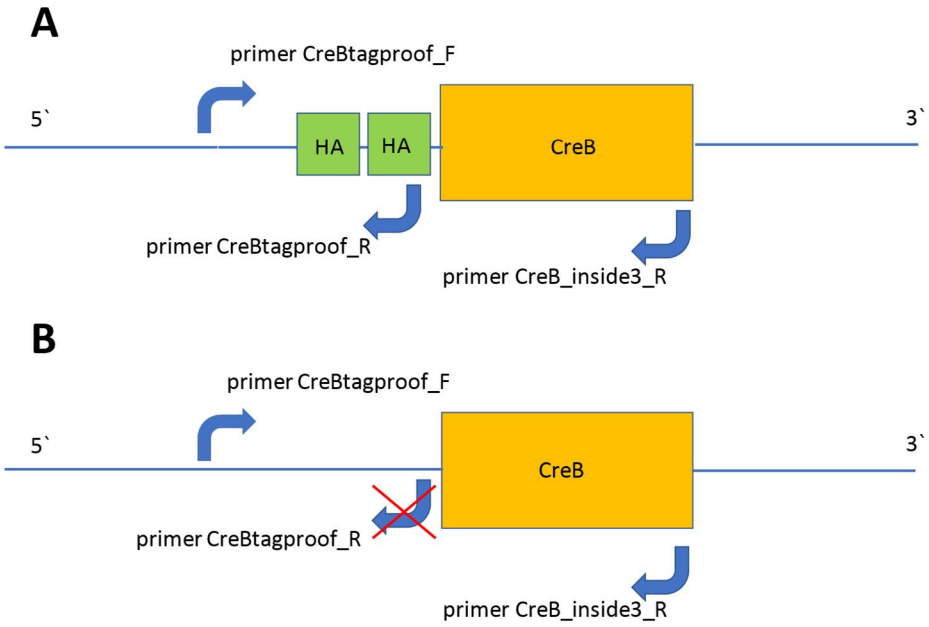

Figure 21: Binding sites for the primers employed in proof PCRs for verification of HA-CreB inclusion

(A) HA-CreB-labelled knock-in mutant

(B) wildtype variant

Primers "CreBtagproof_F" and "CreB_inside3_R" can attach to both genomic variants as they bind to an unaltered genomic area. Primer "CreBtagproof_R" however attaches to a genomic area which belongs only to the tag. Proof PCR 1 forms only in tag-labelled mutants a PCR product.

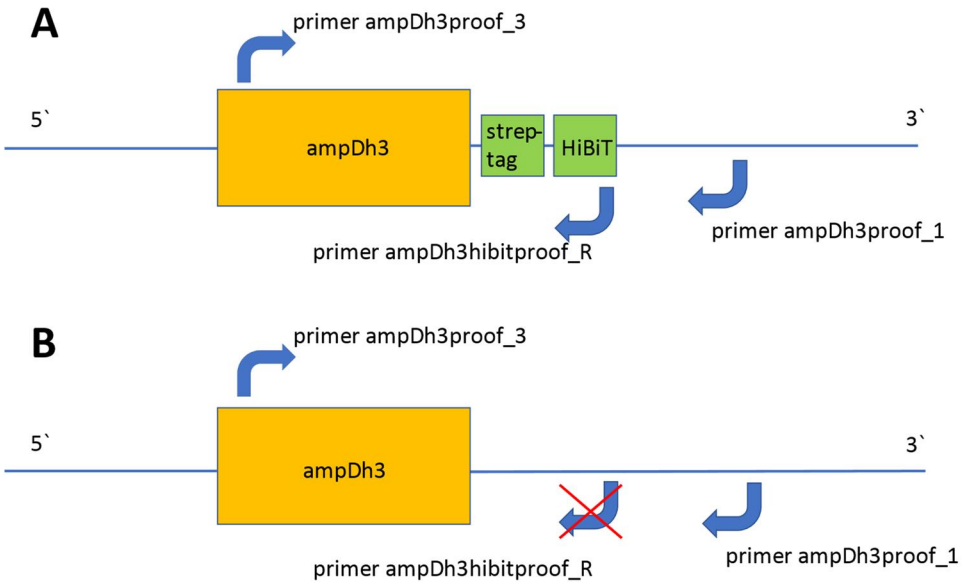

Figure 22: Binding sites for the primers employed in proof PCRs for verification of ampDh3-strep-HiBiT inclusion

(A) ampDh3-strep-HiBiT-labelled knock-in mutant

(B) wildtype variant

Primers “ampDh3proof_3” and “ampDh3hibitproof_1” can attach to both genomic variants as they bind to an unaltered genomic area. Primer “ampDh3proof_R” however attaches to a genomic area which belongs only to the tag. Proof PCR 1 forms only in tag-labelled mutants a PCR product.

As shown in Figures 23 and 24, various knock-in mutant strains could be validated by correct sizes of the bands. In proof PCR 1, no bands could be detected for ID40 and PA14 WT.

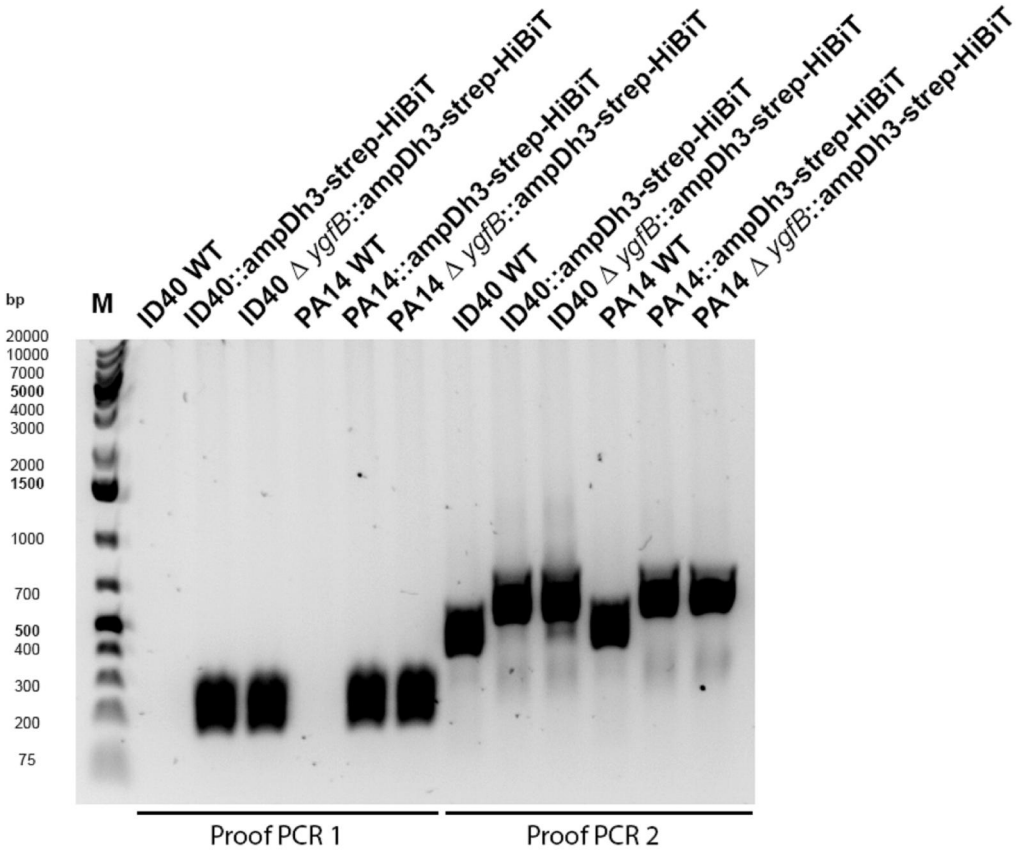

Figure 23: Agarose gel electrophoresis of proof PCRs validating the correct introduction of the strep-HiBiT gene sequence at the 3`end of the *ampDh3* gene

Proof PCR 1 is shown on the lefthand side, proof PCR 2 is shown on the righthand side for indicated strains.

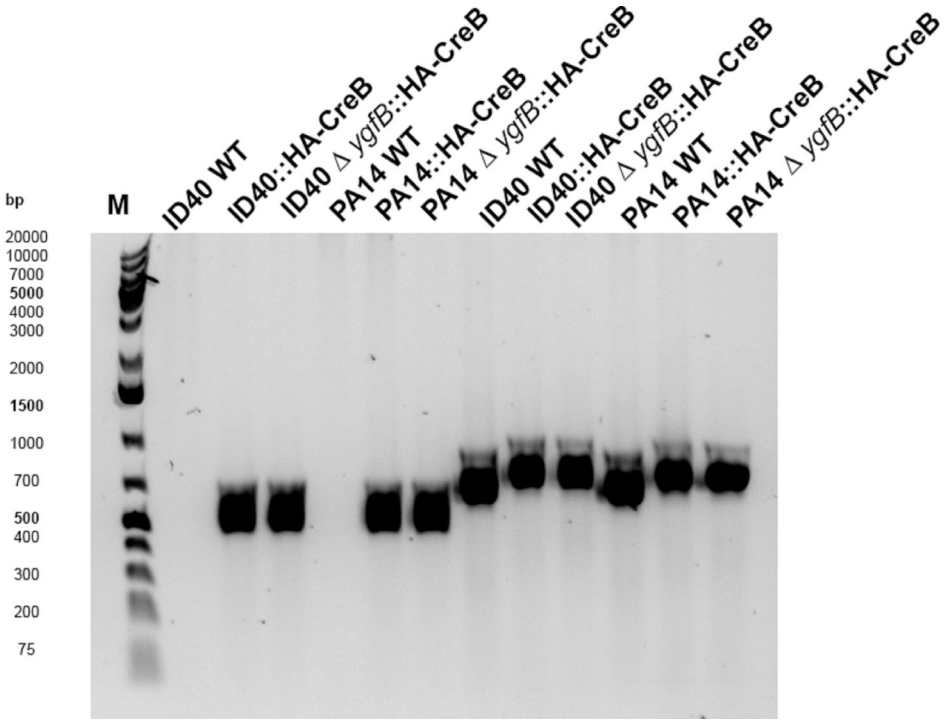

Figure 24: Agarose gel electrophoresis of proof PCRs validating the correct introduction of the HA-tag encoding sequence at the 3`end of the *creB* gene

Proof PCR 1 is shown on the lefthand side, proof PCR 2 is shown on the righthand side for indicated strains.

3.2 Impact of the presence of various genes on the transcriptional activity of the *ampDh3* promoter

As already outlined in the introduction previous work of the working group revealed that *ygfB* deletion led to increased *ampDh3* mRNA expression, and that the increased AmpDh3 production is causative for the reduced β-lactamase activity and finally β-lactam resistance (Eggers et al., 2023). Interestingly, the transcriptional changes caused by the deletion of *ygfB* in ID40 seem to be very specific and affect only the *ampDh3* operon and to a lesser extent the *alp* operon.

All relevant strains were previously electroporated with a pBBR plasmid carrying the genetic sequence from -532 to -1 upstream of the *ampDh3* coding region which was directly linked to the *nanoluc luciferase* gene. This plasmid was called pBBR-ampDh3-532-luc (Figure 25 (A)). In similar, the strains were electroporated with pBBR-luc, a pBBR plasmid carrying the *nanoluc luciferase* gene without a

preceding promoter (Figure 25 (B)). It was used as a negative control to determine the basal luciferase transcriptional activity.

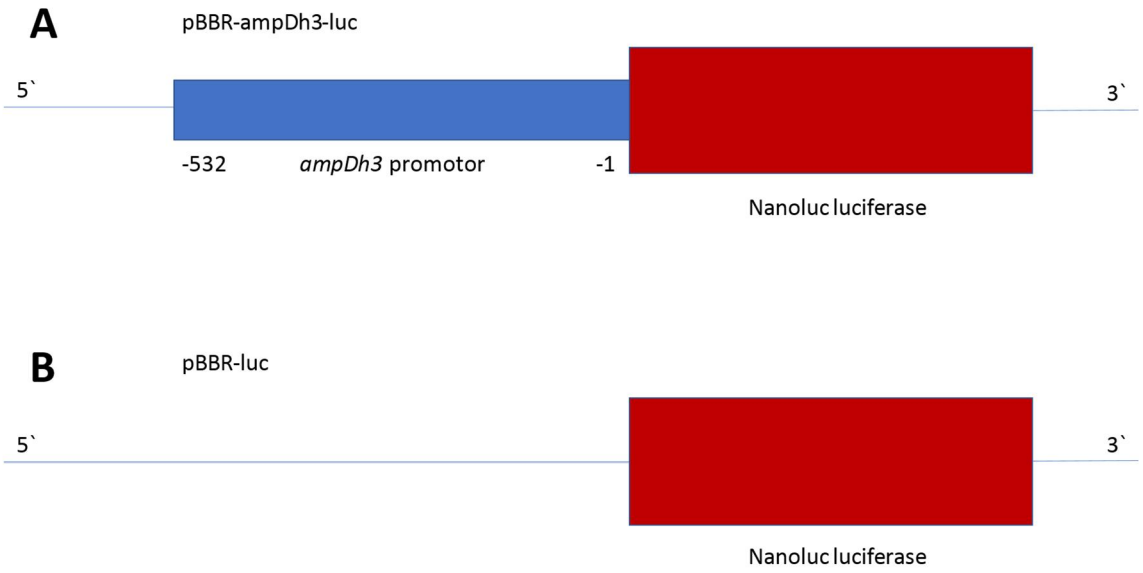

Figure 25: Model of pBBR plasmids encoding for Nanoluc luciferase

(A) pBBR-ampDh3-luc carries a -532 to -1 *ampDh3* promoter sequence before the gene area which encodes for Nanoluc luciferase.

(B) pBBR-luc encodes for Nanoluc luciferase without a preceding promoter and thus reflects background transcriptional activity.

The luciferase assay was carried out as described before (2.3.9). Essentially, bacterial cultures of the strains that carried a pBBR-ampDh3-532-luc or pBBR-luc plasmid were grown overnight and the next day subcultured for 2 hours. Subcultures were adjusted to a bacterial concentration of $2 \cdot 10^8$ / ml and well triplets were each filled with 50 µl of bacterial suspension. To each well, 50 µl reaction mix was added which contains furimazine, the substrate for the luciferase encoded in the pBBR plasmids. In strains carrying pBBR-ampDh3-luc, the promoter activation leads to luciferase transcription and subsequently luminescence production. The luminescence as a readout for the luciferase enzyme activity was measured with a Tecan plate reader and is depicted in arbitrary units. Background activity was measured in strains carrying the plasmid with the promoterless *nanoluc* gene.

3.2.1 Basal ampDh3 transcriptional activity is much higher in the strain Pa PA14 compared to Pa ID40

In contrast to ID40, the clinical isolate PA14 carries a functional *dacB* gene and is highly sensitive to treatment with β-lactam antibiotics. The *dacB* gene encodes for PBP4. To assess whether the functionality of the *dacB* gene might influence *ampDh3* promoter activity, transcriptional activation of the *ampDh3* promoter was compared in these strains. A three times higher *ampDh3* promoter activity could be observed for the PA14 strain compared to ID40 (Figure 26).

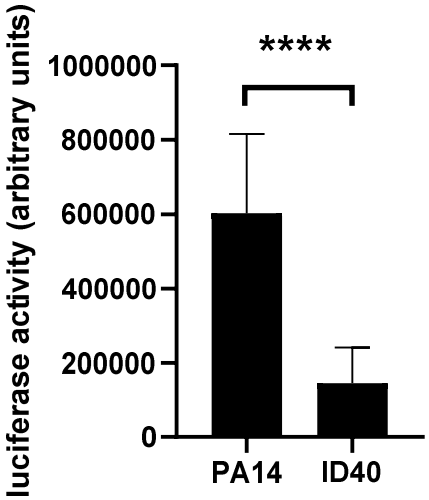

Figure 26: *ampDh3* promoter activity in ID40 and PA14 wildtype strains

Graph depicts the mean and standard deviation of the luciferase activity of 12 independent experiments. Asterisks indicate a significant difference (**** p<0.0001; t-test).

3.2.2 dacB inactivation modulates ampDh3 promoter activity to some extent

The significant difference in *ampDh3* promoter activity between the PA14 sensitive strain carrying a functional *dacB* gene and ID40 carrying an inactive *dacB* gene raised the question whether *dacB* inactivation contributes to transcriptional regulation of *ampDh3* promoter activity. To study this, the luciferase activity of complementation mutants, ID40::*dacB*(PA14) and ID40 Δ*creBC*::*dacB*(PA14) was analysed in the absence or presence of increasing

concentrations of rhamnose (Figure 27). As the complemented *dacB* gene of PA14 is rhamnose inducible, the effects of an increasing functional PBP4 production could be observed. While without rhamnose, the luciferase activity of ID40::*dacB*(PA14) shows nearly WT level, an increasing concentration of rhamnose raises luciferase activity levels. For ID40 Δ*creBC*::*dacB*(PA14), the observed increase in luciferase activity is similar, but starts at a lower basal level. ID40 Δ*ampR* luciferase activity resembles the WT level. From these data it can be concluded that the *dacB* inactivation in ID40 suppresses to some extent transcriptional activity of the *ampDh3* promoter.

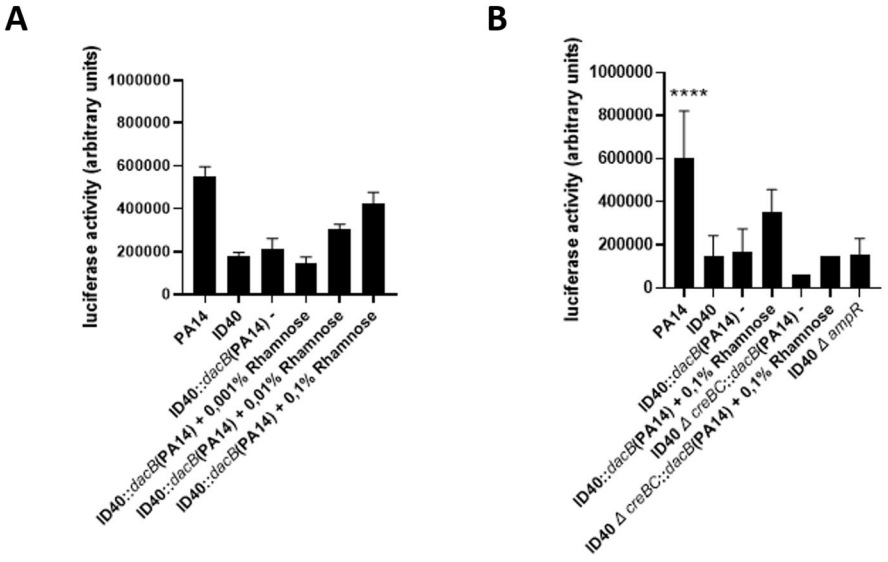

Figure 27: Luciferase activity of ID40 complementation mutants and ID40 Δ*ampR*

(A) Data depict the mean and standard deviation of 12 independent experiments for PA14 and ID40 carrying pBBR-ampDh3-532-luc. In addition, the mean and standard deviation of the triplicates for one experiment is shown in which ID40::*dacB*(PA14) carrying pBBR-ampDh3-532-luc was treated with indicated concentrations of rhamnose.

(B) The graph depicts the mean and standard deviation for indicated strains of independent experiments. The data represent for 12 independent experiments for PA14 and ID40 WT. ID40::*dacB*(PA14) was measured with and without 0,1% rhamnose treatment in four independent experiments. The luciferase activity of ID40 Δ*creBC*::*dacB*(PA14) strain was measured only in one experiment. Additionally, ID40 Δ*ampR* strain was analysed in four independent experiments. One-way ANOVA analysis was performed comparing ID40 with mutants. Asterisks indicate significant differences compared to ID40 (**** $p<0.0001$).

3.2.3 Impact of ygfB, creBC and ampR on ampDh3 promoter activity

Luciferase activity of ID40 Δ*creBC,* ID40 Δ*ampR* and ID40 Δ*ampR* Δ*creBC* resembled the ID40 WT level (Figure 28). Only the deletion of the *ygfB* gene in ID40 Δ*ygfB* and ID40 Δ*ygfB* Δ*creBC* led to increased luciferase activity for these strains in a highly significant manner which far surpasses PA14 WT levels. From this data it can be concluded that only *ygfB,* but not *creBC* and *ampR* is involved in the suppression of *ampDh3* transcriptional activity.

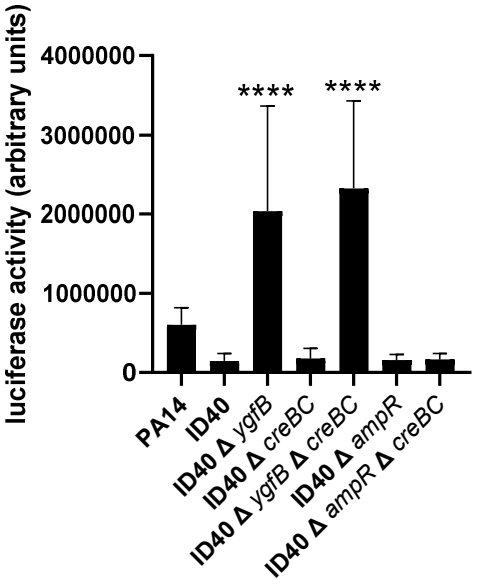

Figure 28: Luciferase reporter activity of ID40 deletion mutants

The graphs depict the mean and SD of independent experiments. Number of independent experiments: PA14 and ID40 n=12; ID40 Δ*ampR*, ID40 Δ*ampR* Δ*creBC*, ID40 Δ*ygfB* and ID40 Δ*creBC* n=4 and ID40 Δ*ygfB* Δ*creBC* n=3. One-way ANOVA analysis was performed comparing ID40 with mutants. Asterisks indicate significant differences compared to ID40 (**** p<0.0001).

Figure 29 (A) illustrates the luciferase activity of different PA14 deletion mutants. In comparison to the corresponding ID40 deletion mutants, PA14 Δ*creBC* and PA14 Δ*ampR* showed a very similar luciferase activity as their corresponding PA14 WT. Only the deletion in *ygfB* gene caused a notable increase in luciferase activity in PA14 Δ*ygfB,* PA14 Δ*ygfB* Δ*creBC* and PA14 Δ*creBC* Δ*ygfB* Δ*ampR.* From these data it can be concluded that similarly to its effects in *Pa* ID40, only *ygfB* is involved in the suppression of *ampDh3* transcriptional activity.

Luciferase activity of the mutants whose deletions include the *dacB* gene are visualized in Figure 29 (B).

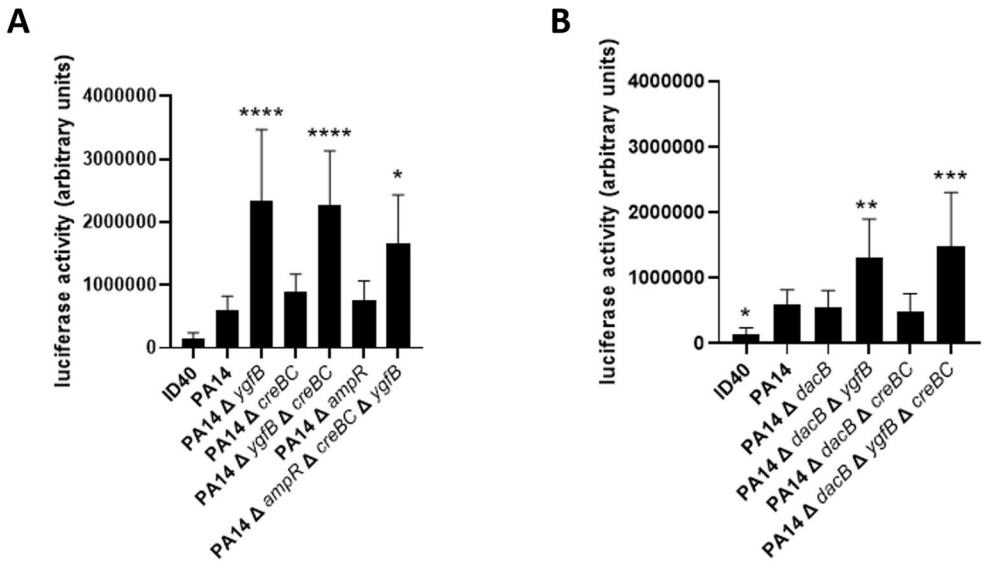

Figure 29: Luciferase activity of PA14 deletion mutants

(A) The graph depicts the mean and SD of the luciferase activity of various *Pa* strains measured in independent experiments. Number of independent experiments: PA14 and ID40 n=12; PA14 Δ*ygfB* and PA14 Δ*ygfB* Δ*creBC* n=7; PA14 Δ*ampR* and PA14 Δ*creBC* Δ*ygfB* Δ*ampR* n=4 and PA14 Δ*creBC* n=3. One-way ANOVA analysis was performed comparing ID40 with mutants. Asterisks indicate significant differences compared to ID40(* p<0,05, **** p<0.0001).

(B) The graph depicts the mean and SD of all performed experiments. PA14 and ID40 wildtypes were measured in 12 independent experiments. PA14 Δ*dacB*, PA14 Δ*dacB* Δ*ygfB* and PA14 Δ*dacB* Δ*ygfB* Δ*creBC* were analysed in five experiments and PA14 Δ*dacB* Δ*creBC* in three experiments. One-way ANOVA analysis was performed comparing ID40 with mutants. Asterisks indicate significant differences compared to ID40 (* p<0,05, ** p<0,01, *** p<0.001) The *dacB* deletion itself does not notably alter the luciferase activity in comparison to the PA14 WT strain. Only the combination with the *ygfB* deletion for PA14 Δ*dacB* Δ*ygfB* and PA14 Δ*dacB* Δ*ygfB* Δ*creBC* raises the luciferase activity of these strains significantly.

In summary it can be stated, that two genes caused alterations in *ampDh3* promoter and therefore luciferase activity in the analysed strains. Firstly, the induction of the complemented functional *dacB* gene in an otherwise *dacB* inactive ID40 strain raised promoter activity. *dacB* deletion in PA14 did not affect promoter activity in a considerable manner. Secondly, *ygfB* deletions caused a remarkable and mostly highly significant increase in promoter activity in all *ygfB* deficient strains in ID40 and PA14.

3.3 Impact of the deletions on antibiotic resistance

3.3.1 Measurement of β-lactamase activity

Genomic deletions had been created with the particular interest to investigate the influence of the respective genes on antibiotic resistance of the bacterial strains. β-lactamases are the intracellular enzymes capable of hydrolysing β-lactam rings that are present in molecules such as antibiotics and are therefore highly relevant concerning the β-lactam antibiotic resistance of *Pa* strains. AmpC is a serine cephalosporinase, an Ambler class C β-lactamase. Especially its derepression in Gram-negative bacteria is relevant for resistance enhancement (Drawz and Bonomo, 2010). AmpC is one of the fundamental reasons of β-lactam resistance in *Pa* (Tam et al., 2007). The nitrocefin assay allows the determination of β-lactamase activity.

Nitrocefin is a chromogenic cephalosporin which in case of hydrolysis due to β-lactamase activity changes the wavelength of its emitted light to 490 nm. This red-light emission is proportional to β-lactamase activity. To quantify β-lactamase activity, subcultures of different *Pa* strains were centrifuged, and the exact weight of the pellet was determined. After resuspension, bacterial cell lysis by means of sonification and centrifugation, the supernatant was diluted in two dilution steps and together with a specific reaction mix treansferred into well duplicates. A standard curve was recorded with different amounts of hydrolysed nitrocefin in order to determine the respective emission rate for each assay. Finally, a superordinate standard equation for nitrocefin turnover could be calculated on the basis of the single standard curves and could be applied for the calculation of the respective nitrocefin turnover in the different assays. The change in absorption constitutes a linear curve in relation to nitrocefin turnover. This superordinate standard curve is depicted in Figure 30.

$$\Delta\, OD_{600\,nm} = 0{,}02140 \cdot Nitrocefin\ turnover\ (nmol)$$

$$Nitrocefin\ turnover\ (nmol) = \frac{\Delta\, OD_{600\,nm}}{0{,}02140}$$

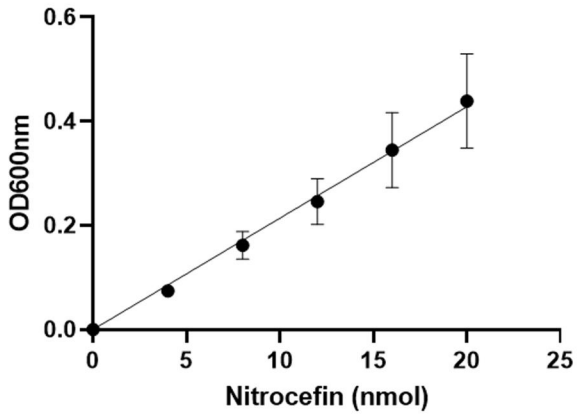

Figure 30: Superordinate standard curve

The absorption of different amounts of hydrolyzed nitrocefin (0-20nmol) was measured with a Tecan plate reader in order to assign a particular change in absorption to a certain amount of hydrolysed nitrocefin and calculate the specific nitrocefin turnover.

For each bacterial strain, 3 assays were performed. The enzyme rates were calculated considering nitrocefin turnover, previous dilution steps and time difference, and are stated in [nitrocefin turnover / (min·mg pellet per well)].

Figure 31 demonstrates the β-lactamase activity of ID40 and PA14 WT as well as different ID40 deletion mutants.

PA14 WT (0,4 nmol/ min·mg) showed a considerably lower β-lactamase activity compared to ID40 WT (77,4 nmol/ min·mg). Amongst ID40 deletion mutants, β-lactamase activity of ID40 Δ*creBC* (63,2 nmol/ min·mg) resembles the WT. *ygfB* deletion causes a significant decrease in β-lactamase activity in ID40 Δ*ygfB* (18,8 nmol/ min·mg) and ID40 Δ*ygfB* Δ*creBC* (14,1 nmol/ min·mg). In ID40 Δ*ygfB* Δ*ampDh3* (102,8 nmol/ min·mg) β-lactamase activity is restored and elevated above wildtype levels. ID40 Δ*ampR* (2,1 nmol/ min·mg) showed infinitesimally low β-lactamase activity.

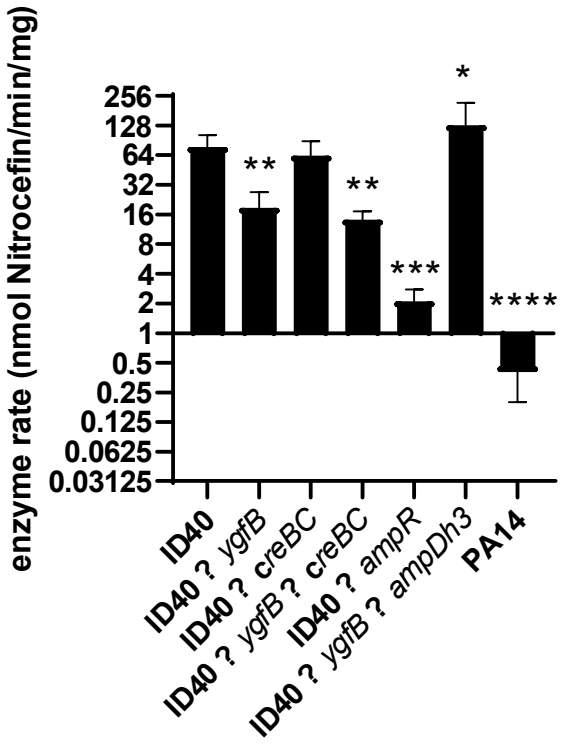

Figure 31: Measurement of β-lactamase activity for ID40 WT and different deletion mutants

For each strain, the nitrocefin assay was repeated three times. Only PA14 WT was measured six times. A multiple comparison one-way ANOVA analysis was performed. Significant differences between ID40 and other strains are indicated with Asteriks (* p<0,05, ** p<0,01, *** p<0,001, **** p<0,0001). Furthermore, it has to be mentioned that different attempts to measure the β-lactamase activity of the strains ID40 Δ*ampDh3* and ID40::*dacB*(PA14) (with and without addition of rhamnose) could not be performed successfully due to technical reasons.

As presented in Figure 32, PA14 WT β-lactamase activity (0,4 nmol/ min·mg) was further compared to two deletion mutants. *dacB* deletion in PA14 Δ*dacB* (1,7 nmol/ min·mg) increased β-lactamase activity by a factor of 4. An additional *ygfB* deletion in PA14 Δ*dacB* Δ*ygfB* (0,6 nmol/ min·mg) lowered β-lactamase activity to almost wildtype levels.

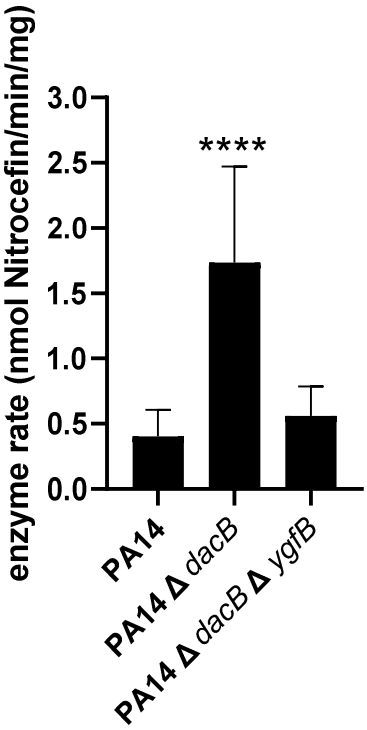

Figure 32: Measurement of β-lactamase activity for PA14, PA14 Δ*ygfB* and PA14 Δ*ygfB* Δ*dacB*

For each strain, the nitrocefin assay was repeated for three times. Only PA14 WT was measured for six times. A multiple comparison one-way ANOVA analysis found that the difference between PA14 WT and PA14 Δ*dacB* was significant (**** p<0,0001).

Accordingly, the findings indicate a considerably lower level of β-lactamase activity in PA14 strains. Similarly, a *dacB* deletion increased β-lactamase activity in PA14 strains. In PA14 Δ*dacB* Δ*ygfB*, *ygfB* deletion decreased β-lactamase activity.

3.3.2 Determination of minimal inhibitory concentrations (MIC)

In addition to β-lactamase activity of the bacterial strains, their basic sensitivity to antibiotics was highly important for this study. MIC values were determined for different ID40 and PA14 deletion mutants in order to determine their respective sensitivity to antibiotics. Therefore, an adjusted concentration of a bacterial suspension was incubated in growth media containing different antibiotics in increasing concentrations. The MIC is defined as the lowest concentration of an antibiotic present in the growth medium that impedes visible bacterial growth. In this study, bacterial growth was detected not only by visible turbidity of the bacterial culture but also by OD_{600nm} measurement using a Tecan plate reader.

After substraction of the blank OD_{600nm} value measured for the growth medium only, an OD_{600nm} value of 0,05 was defined as the cut-off value to distinguish between actual and inhibited growth of the bacterial culture.

MIC values were determined for meropenem (MEM), imipenem (IMI), cefepime (FEP), ceftazidime (CAZ), piperacillin (PIP), piperazillin/tazobactam (TZP) and aztreonam (AZT) utilizing Sensititre™ EUX2NF MIC plates (Thermo Fisher Scientific) and Sensititre™ GN2F MIC plates (Thermo Fisher Scientific). The applied MIC breakpoints originate from the European Committee on Antimicrobial Susceptibility Testing (EUCAST) and were published in January 2020.

When considering *Pa* ID40, the WT strain was found resistant to the exposure to all tested β-lactam antibiotics and the monobactam aztreonam (Table 31). With regard to its deletion mutants, a general decrease in all MIC values was observed for ID40 Δ*ygfB*, which restored sensitivity for cefepime and aztreonam according to EUCAST breakpoints. ID40 Δ*creBC* and ID40 Δ*ygfB* Δ*creBC* were similarly susceptible to all investigated antibiotics except for imipenem and cefepime, and sensitive to aztreonam. For ID40 Δ*ampDh3*, MIC values for ceftazidime, piperacillin and aztreonam were slightly reduced in comparison to the wildtype whereas for ID40 Δ*ygfB* Δ*ampDh3*, a minor increase in MIC values for cefepime and piperacillin/tazobactam could be noted. ID40 Δ*ampR* and ID40 Δ*creBC* Δ*ampR* showed a strikingly higher susceptibility and were sensitive to all investigated antibiotics according to EUCAST breakpoints.

The importance of the *dacB* inactivation for hyperresistance was demonstrated by using the strain ID40::*rha-dacB*(PA14), in which a functional *dacB*, derived from PA14, was chromosomally introduced under control of a rhamnose inducible promoter. While this strain without addition of rhamnose showed a similar β-lactam resistance as the ID40 WT strain, addition of 0.1% rhamnose led to reduced MIC levels for all tested antibiotics with exception of imipenem. Taken together, these findings clearly demonstrate that the point mutation in the *dacB* gene of ID40 contributes strongly to antibiotic resistance. In addition, the importance of AmpR, YgfB and to a lesser extent of CreBC for β-lactam resistance could be demonstrated.

Table 31: Minimal inhibitory concentrations for *Pa* ID40 deletion mutants for β-lactam antibiotics

		MEM	IMP	FEP	CAZ	PIP	TZP	ATM
µg/ml		0.125-128	1-64	1-128	0.25-128	4-128	1-128	0.5-32
MIC Breakpoint (mg/L)	S ≤	2	4	8	8	16	16	16
	R >	8	4	8	8	16	16	16
ID40 WT		8	32	16	>32	>128	128	32
ID40 *ΔygfB*		4	16	**8**	32	64	32	**16**
ID40 *ΔcreBC*		4	32	16	32	64	32	**16**
ID40 *ΔygfB ΔcreBC*		4	32	16	32	64	32	**16**
ID40 *ΔampDh3*		8	32	16	32	128	128	**16**
ID40 *ΔampDh3 ΔygfB*		8	32	32	>32	>128	>128	32
ID40 *ΔampR*		**2**	**<1**	**4**	**<1**	**<16**	**<16**	**2**
ID40 *ΔampR ΔcreBC*		**2**	**<1**	**8**	**2**	**<16**	**<16**	**4**
ID40::*dacB*(PA14)		8	64	16	32	128	32	**16**
ID40::*dacB*(PA14) + 0,1% Rhamnose		4	32	**8**	**8**	**<16**	**<16**	**4**

(MEM: meropenem, IMP: imipenem, FEP: cefepime, CAZ: ceftazidime, PIP: piperacillin, TZP: piperacillin/tazobactam, AZT: aztreonam) For each strain, MIC values were determined twice for meropenem, cefepime and piperacillin/tazobactam and once for imipenem, ceftazidime, piperacillin and aztreonam. MIC values indicate the susceptibility of bacterial strains to antibiotics. EUCAST MIC breakpoints were applied. A red coloured background shows MIC values which exceed WT level, in boxes with a green coloured background MIC values fell below WT levels. Bold values designate sensitivity according to EUCAST breakpoints.

Table 32 visualizes the MIC values for PA14 WT and deletion mutants.

In general, *Pa* PA14 WT is more susceptible to β-lactam antibiotics than ID40 WT to a considerable extent. Our findings indicate that deletions of the genes *ygfB*, *creBC*, both *ygfB* and *creBC* or *ampR* do not influence β-lactam resistance in a significant manner. However, *dacB* deletion causes an increase in MIC values at least for ceftazidime and piperacillin/tazobactam. Additional deletion of either *ygfB*, *creBC* or both, abrogates the increased resistance mediated by the *dacB* deletion for these antibiotics. Taken together, these data demonstrate that PA14 is fundamentally less resistant to treatment with β-lactam antibiotics. The importance of the CreBC two-component system and YgfB for β-lactam resistance in PA14 can only be shown in the *dacB* deletion mutant.

Table 32: Minimal inhibitory concentrations for *Pa* PA14 deletion mutants for β-lactam antibiotics

		MEM	IMP	FEP	CAZ	TZP	ATM
µg/ml		0.5-128	1-64	1-128	1-32	4-128	0.5-32
MIC Breakpoint (mg/L)	**S ≤**	2	4	8	8	16	16
	R >	8	4	8	8	16	16
PA14 WT		**<0,5**	**<1**	**<1**	**2**	**<4**	**4-8**
PA14 *ΔygfB*		**<0,5**	**<1**	**<1**	**2**	**<4**	**4**
PA14 *ΔygfB ΔcreBC*		**<0,5**	**<1**	**<1**	**2**	**<4**	**4**
PA14 *ΔampR*		**<0,5**	**<1**	**<1**	**2**	**<4**	**8**
PA14 *ΔdacB*		**<0,5**	**<1**	**<1**	**4**	**8**	**4**
PA14 *ΔdacB ΔygfB*		**<0,5**	**<1**	**<1**	**<1**	**<4**	**4**
PA14 *ΔdacB ΔcreBC*		**<0,5**	**<1**	**<1**	**2**	**<4**	**4**
PA14 *ΔdacB ΔygfB ΔcreBC*		**<0,5**	**<1**	**<1**	**2**	**<4**	**4**

(MEM: meropenem, IMP: imipenem, FEP: cefepime, CAZ: ceftazidime, PIP: piperacillin, TZP: piperacillin/tazobactam, AZT: aztreonam) For each strain, MIC values were determined twice for meropenem, cefepime and piperacillin/tazobactam and once for imipenem, ceftazidime, piperacillin and aztreonam. MIC values indicate the susceptibility of bacterial strains against antibiotics. EUCAST MIC breakpoints were applied. A red coloured background shows MIC values which exceed WT level, in boxes with a green coloured background MIC values fall below WT level. Bold values designate sensitivity according to EUCAST breakpoints.

3.4 Impact of Δ*ygfB* deletion on the amounts of YgfB, CreBC and AmpDh3

As described in the introduction, the aim of this work is to further elucidate the interplay between several genes involved in β-lactam resistance, namely *ygfB*, *creBC,* and *ampDh3*.

A Western Blot analysis was performed in order to investigate if YgfB, HA-CreB and AmpDh3-HiBiT protein levels differ between ID40 and PA14 WT and *ygfB* deletion mutants. RpoB was also analysed as it is a housekeeping protein and is considered to be expressed at comparable levels in each of the strains.

By performing SDS-PAGE and Western Blot analyses using whole cell extracts as described in materials and methods, the amounts of HA-CreB and AmpDh3-HiBiT were determined in both ID40 and PA14 WT and *ygfB* deletion mutants (Figure 33).

The HA-CreB levels were in tendency lower in the ∆*ygfB* strains compared to the WT strains. Striking differences were found for AmpDh3-HiBiT. PA14 strains showed a notably augmented AmpDh3-HiBiT level compared to ID40. The AmpDh3-HiBiT protein levels in the *ygfB* deletion mutants by far surpassed that of the WT strains. These results go along with our findings that *ygfB* deletion causes an increase in transcriptional activity of the *ampDh3* promoter. YgfB was not detectable in ID40 Δ*ygfB* and PA14 Δ*ygfB.* The small detected bands are unspecific bands. Interestingly, no difference in the amounts of YgfB could be seen between ID40 and PA14 WT strains, indicating that the difference in AmpDh3 protein levels between ID40 and PA14 are not associated with differences in YgfB protein levels.

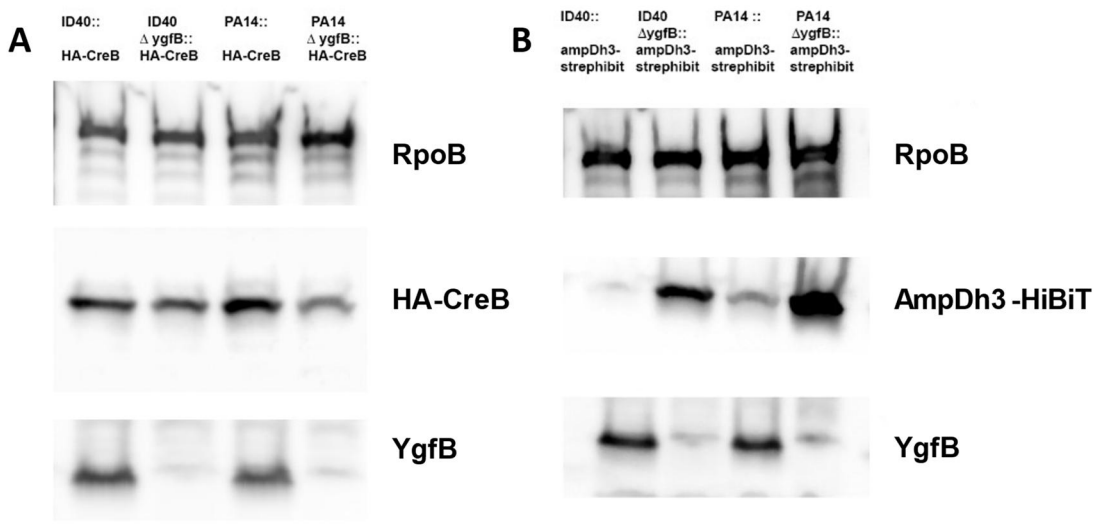

Figure 33: Western Blot analysis for proteins RpoB, HA-CreB, YgfB and AmpDh3-HiBiT

While RpoB and YgfB protein levels were determined in each Western Blot analysis, HA-CreB and AmpDh3-HiBiT were analysed in two different assays. Each assay was repeated for three times. Representative results are shown.

3.5 Impact of Δ*TUEID40_01954* deletion on bacterial growth

TUEID40_01954 or PA0808 is a protein involved in the protection of bacterial cells from the toxic amidase activity of AmpDh3 in the periplasm (Wang et al., 2020). We wanted to further explore the effect of TUEID40_01954 on bacterial growth and survival. Therefore, bacterial cultures were previously adjusted to a concentration of 10^7/ml. Then, the growth of ID40 and PA14 WT strains and *TUEID40_01954* deletion mutants was monitored for 15 hours (Figure 34).

In general, bacteria pass four consecutive growth phases. Firstly, bacteria acclimatise to the new environment in the lag phase. Cell divisions start in the logarithmic phase and can be seen as an exponential growth in growth curves. A stationary phase follows where bacterial growth becomes limited, e.g. due to the reduced presence of a nutrient in the growth medium. Eventually, bacterial growth ceases and the cells in the culture begin to die as oxygen supply is reduced, pH changes and toxic metabolic products accumulate.

In the 15 hours of the recorded growth curves in this study, bacterial cultures pass through lag and logarithmic phase until entering the stationary growth phase. PA14 cultures demonstrated slightly elevated growth rates than ID40 strains. With reference to the *TUEID40_01954* deletion, no difference in bacterial growth could be found compared to the WT strains.

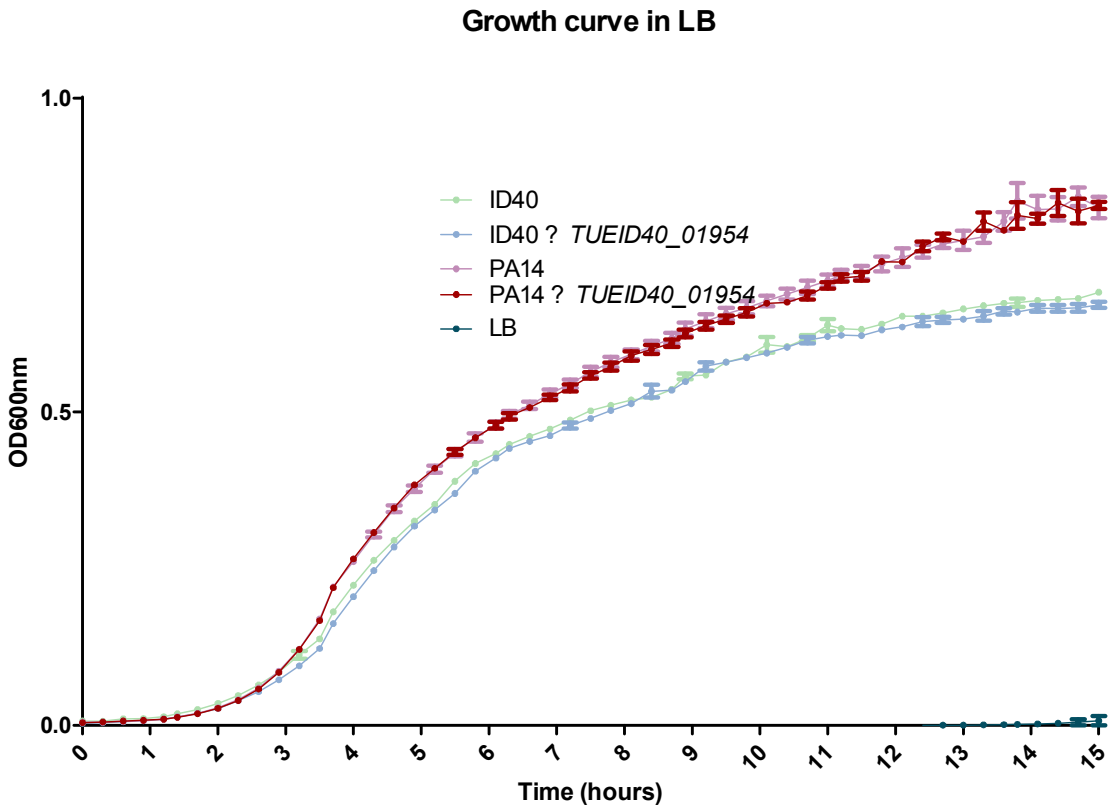

Figure 34: Growth curves of ID40 and PA14 WT and Δ*TUEID40_01954* strains

In order to observe growth differences between ID40 and PA14 WT and Δ*TUEID40_01954* strains, 1 ml (containing 10^7 cells) was transferred into a well. Each strain was measured in well triplicates. The growth was monitored for 15 hours with a Tecan plate reader.

4 Discussion

4.1 Wildtype strains

Many of the studies investigating *Pa* resistance genes have been performed with *Pa* PAO1 or *Pa* PA14 wildtype strains and respective deletion mutants. It could be considered a limitation of these studies to have investigated genes linked to antibiotic resistance of *Pa* in strains which are mostly sensitive to at least β-lactam antibiotics. Utilizing *Pa* ID40 in comparison to *Pa* PA14 in this work seemed a new, more appropriate approach to explore *Pa* resistance genes, especially *ygfB*, and to avoid this limitation.

It has previously been shown by Sonnabend et al (2020) that ID40 is more resistant to treatment with β-lactam antibiotics than the PA14 strain. This could be confirmed in the presented study by determination of the minimal inhibitory concentration of various β-lactam antibiotics (Sonnabend et al., 2020), showing that ID40 is much more resistant to β-lactam antibiotics than PA14. In similar, β-lactamase activity of PA14 was tremendously lower compared to ID40. Interestingly, the β-lactamase activity of PA14 was even lower than in an ID40 Δ*ampR* deletion mutant. Thus, in ID40 maybe even in the absence of AmpR there seems to be some mechanism acting which maintains some β-lactamase activity. Furthermore and apart from mechanisms involving the regulation of *ampC* expression, we assume that there do exist further mechanisms which contribute to MDR resistance of ID40.

Nevertheless, the deletion of *ampR* in ID40 clearly demonstrate that AmpR-mediated *ampC* overexpression is a decisive element of ID40 β-lactam resistance. Regarding AmpDh3, *ampDh3* promoter assays as well as the determination of AmpDh3 protein levels clearly demonstrated that transcriptional activation is associated with AmpDh3 production in both PA14 and ID40 and that YgfB suppresses transcriptional activation and production of AmpDh3. The difference in production of AmpDh3 may contribute to the differences in β-lactamase activity or β-lactam resistance but obviously there seem to exist much more mechanisms which are responsible for the striking differences in resistance in these two strains. For instance, expression levels of efflux pumps such as

MexAB/OprM and other factors as described in the introduction might also contribute to the striking differences between PA14 and ID40 in terms of β-lactam resistance.

4.2 YgfB

In preceding, so far unpublished investigations of the working group, it was demonstrated that in an ID40 strain, YgfB contributes to β-lactam resistance by suppression of transcriptional activity of the *ampDh3* promoter leading to increased *ampC* expression and finally to increased β-lactam resistance (Eggers et al., 2023). *ygfB* is potentially a very important resistance gene in *Pa*. It was found to contribute to high level β-lactam resistance, as its deletion in ID40 entailed a considerable decrease in MIC values, actually below resistance breakpoints (Sonnabend et al., 2020). In this study, the deletion mutant ID40 Δ*ygfB* presented highly reduced β-lactamase activity and MIC values (reaching susceptibility breakpoints for cefepime and aztreonam). Interestingly, in PA14 Δ*ygfB,* although strongly enhanced *ampDh3* transcriptional activity was observed, the β-lactam MIC values were not further diminished. This can be explained at least partially because of the detection limit of the microbroth dilution assays – as already in the PA14 WT strain very low minimal inhibitory concentrations were observed. However, we observed that although the MIC values for ceftazidime and aztreonam were above the detection limit, they were comparable in PA14 and PA14 Δ*ygfB*. An additional explanation for our findings might be that the PA14 β-lactamase activity converges to 0 and the *ygfB* deletion may therefore not further decrease *ampC* expression. This hypothesis is corrobated by the fact that PA14 Δ*dacB* actually shows elevated MIC values which could be reduced upon additionally knocking out *ygfB*. Taken together, it is very likely that the deletion of *ygfB* has similar effects on the susceptibility to β-lactam antibiotics in PA14, however, we could convincingly show this only if we created conditions that lead to an increase of AmpC activity and therefore allowed us to overcome the technical limitations of MIC determination.

ygfB deletion in ID40 is also responsible for increased *ampDh3* and *TUEID40_01954* transcription, and decreased AmpC production. A time

difference between the onset of *ampDh3* suppression and *ampC* induction that we have previously observed (Eggers et al., 2023) led us to the hypothesis that *ygfB* exerts its regulatory role on the β-lactamase AmpC by modulating AmpDh3 levels, which finally could be confirmed. Indeed, the deletion of *ygfB* strongly raised *ampDh3* transcriptional activity. To illustrate this point, for ID40 Δ*ygfB*, it even surpassed PA14 WT levels. Similarly, in WB analysis, ID40 Δ*ygfB* and PA14 Δ*ygfB* demonstrated highly elevated AmpDh3-HiBiT protein levels. These findings are in line with mRNA expression data previously performed in the working group (unpublished). Interestingly, the comparison of YgfB protein levels in the presented study clearly demonstrate that the difference in AmpDh3 production in PA14 and ID40 cannot be explained solely by different levels of YgfB in PA14 and ID40.

Recently, AlpA has been identified as a transcription factor important for the regulation of the *ampDh3-TUEID40_01954* operon, as well as the *alpBCDE* operon (Pena et al., 2021). The *alpBCDE* operon represents a genetically encoded cell lysis program (McFarland et al., 2015).

Figure 35 illustrates the structure of the *ampDh3* promoter. AlpA acts as a positive regulator of *ampDh3* transcription (Pena et al., 2021) and binds to the relatively small region -466 to -410 of the *ampDh3* promoter (Eggers et al., 2023). In comparison, YgfB acts as a negative regulator of *ampDh3* transcription somewhere between -479 and -418 of the *ampDh3* promoter, according to previous results of the working group (Eggers et al., 2023).

A lack of transcriptional activity when only -418 to -1 are present is due to a palindromic terminator region at position -178 to -137. A short promoter fragment (-77 to -1) is sufficient for YgfB-independent transcriptional activation (Eggers et al., 2023).

From these data it has been speculated that YgfB might suppress AlpA-mediated activation of the *ampDh3* promoter. Follow-up studies by the working group meanwhile demonstrated that YgfB interacts with AlpA and prevents AlpA-mediated transactivation (Eggers et al., 2023).

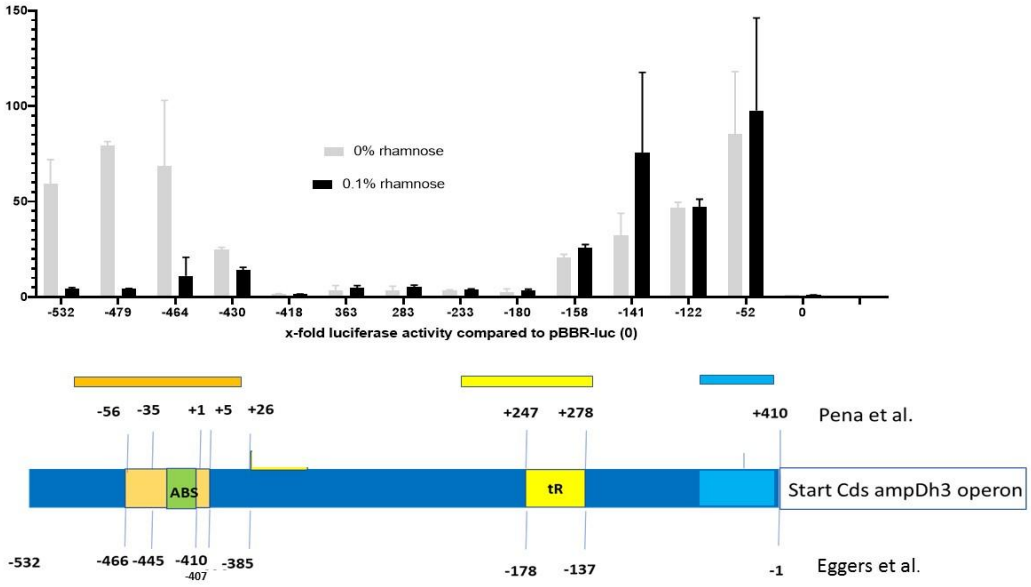

Figure 35: Characterization of the *ampDh3* promoter

(ABS: AlpA binding site; tR: terminator region)

ampDh3 promoter fragments were introduced upstream of the *ampDh3* coding sequence, fused to luciferase and inserted in the vector pBBR into the ID40 strain ID40 Δ*ygfB*::rha-*ygfB* (a strain producing YgfB after addition of rhamnose). The longest fragment comprised position -532 to -1 (luc -532) upstream of the start of the coding sequence fused to the luciferase and the shortest only the luciferase. These assays led to the suggestion that *ygfB*-mediated suppression of *ampDh3* promoter activity occurs somewhere between position -418 and -479. This figure was kindly provided by the working group, according to Eggers et al. (2023). The data included is also based on the findings of Pena et al. (2021).

Since the YgfB levels are similar in PA14 and ID40, this raises also the question whether the difference in AmpDh3 production of PA14 and ID40 is associated with differences in AlpA which requires also further investigations.

4.3 AmpDh3

AmpDh3 is an amidase enzyme and homologue of AmpD which is known to be involved in processing the PGN fragments released from the bacterial cell wall (Zhang et al., 2013) and thereby might also be involved in the regulation of *ampC* expression. Thus, it is important to know, whether the increase in AmpDh3 levels that we have observed upon deletion of *ygfB* is reflected in a corresponding decrease in β-lactamase activity and β-lactam resistance.

As already discovered in experiments of the working group (Eggers et al., 2023), it was confirmed herein that an additional *ampDh3* deletion in an ID40 Δ*ygfB* deletion mutant restores the reduced β-lactam resistance level of ID40 Δ*ygfB*

single mutants. In the same way, the β-lactamase activity of ID40 Δ*ygfB* Δ*ampDh3* was raised and restored to WT levels. In the ID40 Δ*ampDh3* single mutant, the β-lactam MIC values were only slightly affected. This observation again leads to the conclusion that the mechanism contributing to β-lactam resistance beyond the role of *ygfB* is presumably the modulation of AmpDh3 protein levels.

Regarding the localization of AmpDh3, the results of this study indicate that AmpDh3 is present in the cytoplasm. As the periplasmatic amidase activity of AmpDh3 seriously harms bacterial cells in the absence of the corresponding immunity protein, and causes considerable growth impairment, ID40 *ΔTUEID40_01954* and PA14 *ΔTUEID40_01954* mutants should face a serious growth and survival challenge if AmpDh3 is still present in their periplasm without being neutralized by TUEID40_01954 /PA0808. However, no significant growth differences to the respective WT strains could be observed. This suggests that the AmpDh3 enzyme is located in the bacterial cytoplasm. Our assumption goes along with the fact that AmpDh3 can be secreted via a T6SS from the cytoplasm and that it lacks a transport signal sequence for the periplasm (Wang et al., 2020, Zhang et al., 2013). Meanwhile, the cytoplasmic localization of AmpDh3 was also confirmed by the working group (Eggers et al., 2023).

Wang et al. (2020) have discovered that AmpDh3 can be secreted via a T6SS into bacteria like *Yersinia enterocolitica* or *E. coli* where it leads to growth impairment and cell death. This knowledge entails the question whether a deletion of *ygfB* might also be involved in the regulation of AmpDh3 translocation into competing bacterial species. In order to initiate such studies, a small part of this work was dedicated to the preparation of tools for future investigations, namely, the generation of ID40 Δ*icmF2* and PA14 Δ*icmF2* mutants. IcmF2 represents a protein complex which is located at the inner membrane of *Pa* with an essential role for the assembly of the T6SS (Cheng et al., 2019, Ma et al., 2009, Lin et al., 2015). In bacterial cells without a functional *icmF2* gene, no T6SS translocation can take place. AmpDh3 secretion assays will be included in future investigations and do necessarily require *icmF2* deletion mutants as negative control strains lacking any T6SS.

4.4 dacB

The current state of knowledge is that *dacB* inactivation leads to an enrichment of anhydro-MurNAc-pentapeptides (Torrens et al., 2019), because PBP4 no longer cleaves anhydro-MurNAc-pentapeptides into anhydro-MurNAc-tetrapeptides. Torrens et al. (2019) claim that anhydro-MurNAc-pentapeptides act in a much more activating way on AmpR-mediated derepression of *ampC* transcription than anhydro-MurNac-tripeptides. In addition, Moya et al. (2009) suggested that the two-component system consisting of CreB and CreC is activated upon *dacB* inactivation which also contributes to increased β-lactam resistance. However, the exact genetic and metabolic mechanisms which follow *dacB* inactivation and lead to β-lactam resistance are still a subject of investigation and discussion.

While PA14 is sensitive to treatment with β-lactam antibiotics and carries a functional *dacB* gene, ID40 is resistant and carries an inactive *dacB* due to a point mutation (Moya et al., 2009, Sonnabend et al., 2020). One could speculate that this is the decisive difference between these strains to explain sensitivity versus resistance. In line with that hypothesis, we found that the deletion of *dacB* in PA14 in fact increases resistance to some β-lactam antibiotics but despite the now lacking *dacB* gene, PA14 was still much more susceptible to β-lactam antibiotics than ID40. We observed that the complementation of ID40 with a rhamnose-inducible *dacB* gene derived from the PA14 strain (ID40::*dacB*(PA14)), actually can break the resistance to all tested β-lactam antibiotics in the presence of rhamnose in a similar manner as in an ID40 Δ*ampR* deletion mutant. This finding underlines the essential role of *dacB* inactivation for AmpC-mediated hyperresistance.

In this context, we hypothesized that *dacB* inactivation could lead to *creBC* activation which might entail *ygfB* activation, subsequent repression of AmpDh3 levels, and finally AmpR-mediated induction of *ampC* expression.

The difference between ID40 and PA14 might partially be explained by the different levels of AmpDh3, and it is possible that the absence of a functional *dacB* gene dampens by a yet unknown mechanism the transactivation of the

ampDh3 promoter. The 2-fold *ampDh3* promoter activity in the ID40::*dacB*(PA14) strain we have observed after induction with rhamnose actually suggests that *dacB* inactivation might modulate at least to some extent *ampDh3* promoter activation. However, the observed influence is only subtle compared to the impact of a *ygfB* deletion.

Accordingly, PA14 Δ*dacB* presented with slightly enhanced β-lactamase activity (4-fold) and only slightly increased resistance compared to PA14. In addition, the transcriptional activity of the *ampDh3* promoter remains unaltered compared to PA14 WT levels. Only an additional *ygfB* deletion in PA14 Δ*dacB* mutants can raise the transcriptional activity of the *ampDh3* promoter. We therefore hypothesized that AmpC hyperproduction following the *dacB* inactivation was due to reduced levels of AmpDh3. Actually, lowered AmpDh3 levels are the crucial regulatory step in our hypothesis. As PA14 Δ*dacB* shows β-lactam resistance to a high degree without an alteration of *ampDh3* transcriptional activity, we might however need to question our hypothesis and to presume a pathway of AmpC production upon *dacB* inactivation which does not imply *ampDh3* reduction.

However, there is evidence that *dacB* has an impact on *ampDh3* transactivation, as demonstrated in ID40::*dacB*(PA14) upon addition of rhamnose. It is though unclear and improbable that this effect is exerted via altered YgfB levels as ID40 and PA14 WT strains exhibit a similar signal intensity for YgfB protein levels in WB analysis. If *dacB* inactivation led to *ygfB* induction, ID40 would present significantly higher YgfB protein levels than PA14. Thus, *dacB* inactivation initiates a pathway which is independent of *ygfB*. Besides, the comparison between the levels of ID40 β-lactam resistance after *ygfB* deletion on the one hand and under conditions of *dacB* complementation on the other hand suggest that *dacB* cannot be responsible for the strong YgfB-mediated suppression of the *ampDh3* promoter. Taken together, this led us to the assumption that there are two mechanisms of *ampDh3* promoter transactivation: firstly, YgfB entails a strong suppression of AmpDh3 production, and secondly, in an independent and still unknown manner, *dacB* might exert a certain decreasing influence on *ampDh3* promoter activity as well. In the view of this assumption, the small effect

of *dacB* deletion in PA14 on *ampDh3* promoter activity may seem more comprehendible.

In future investigations, it would be helpful to consider not only *ampDh3* promoter activity, but also AmpDh3 and YgfB protein levels in ID40::*dacB*(PA14) and PA14 Δ*dacB* in order to elucidate this question. Because of time constraints an ID40::*dacB*(PA14) strain in which also *ampDh3* is tagged with ampDh3-strepHibit was not created within this work.

4.5 creBC

The two-component system CreBC is involved in the transcriptional regulation of various genes, referred to as the *cre* regulon, and globally influences the bacterial metabolism (Zamorano et al., 2014, Juan et al., 2017).

In the study presented herein we wanted to find out whether there is a link between the CreBC two-component system, YgfB-mediated suppression of AmpDh3 levels and β-lactam resistance.

PA14 shows a slightly enhanced signal intensity for CreB protein levels in the WB analysis compared to ID40. This contradicts our initial hypothesis and previous findings according to which *dacB* inactivation entails CreBC activation (Moya et al., 2009). Accordingly, the signal intensity should be elevated in ID40. However, the observed difference in CreBC production is small. Therefore, we think that it is not possible to take into account this subtle difference because the accuracy of determining WB signal intensities is rather low. Thus, probably no conclusions should be drawn out of the results of these WB.

Moya et al. (2009) proposed that if *dacB* is inactivated, CreBC is activated. At least in a PAO1 Δ*dacB* strain which is more resistant to β-lactam antibiotics compared to PAO1, the additional deletion of the two-component system reduces β-lactam MIC values. This indicates that CreBC indeed contributes to antibiotic resistance. In line with that, previous studies indicated that *creBC* deletions do not, but *dacB* and *creBC* double deletions do reduce β-lactam MIC values and resistance (Moya et al., 2009, Zamorano et al., 2014).

It could be shown in this work that in ID40 Δ*creBC, ampDh3* transcriptional activity is not altered compared to the wildtype strain. Furthermore, in ID40 Δ*creBC*, β-lactamase activity remained unchanged. This is in line with previous studies where *creBC* did not affect *ampC* expression and β-lactamase activity (Moya et al., 2009, Juan et al., 2017). However, as expected, *creBC* deletion led to a decrease in MIC values of all tested β-lactams with the exception of imipenem and cefepime. Nevertheless, the impact of CreBC on β-lactam resistance can be judged as rather low. In ID40 *ΔcreBC ΔygfB, ampDh3* transcriptional activity increased and β-lactamase activity decreased, even to a slightly stronger degree than in ID40 *ΔygfB* single mutants. This could represent a cumulative effect of the concomitant deletion of *ygfB* and *creBC*. Though, the MIC values of the ID40 *ΔcreBC ΔygfB* double mutant are comparable to those of the ID40 *ΔcreBC* single mutant. An additional *creBC* deletion in PA14 Δ*dacB* did not modify the transcriptional activity of the *ampDh3* promoter, however, it similarly reduced the elevated MIC values that could be observed in the PA14 Δ*dacB* single mutant to WT levels.

The small effect of *creBC* on β-lactam resistance is thus not related to changes in *ampDh3* transciption or β-lactamase activity. Considering the confirmed association between *ygfB* and *ampDh3* and the absence of a change in *ampDh3* transcriptional activity in Δ*creBC* mutants, it can be concluded that there is no association between *ygfB* induction by CreBC. Although we are not aware of the exact underlying mechanism, we could confirm that *creBC* though has a certain impact on β-lactam resistance in *Pa*. But now we have indictations that this mechanism presumably acts differently and independently of YgfB and AmpDh3. Regarding the possible connection between *dacB* inactivation and *creBC* activation leading to β-lactam resistance, we could confirm the increase of resistance upon *dacB* deletion and the return to a WT resistance level upon double deletion of *dacB* and *creBC* in *Pa* PA14 which had previously been described by Moya et al. (2009). Although neither *dacB* nor *creBC* interfere with *ampDh3* transcription to a high degree, only *dacB* inactivation (e.g. in PA14 Δ*dacB*) seems to entail an elevated β-lactamase activity. The question of a

common pathway thus remains doubtful and needs to be addressed in further investigations.

To summarize, it can be concluded that ID40 and PA14 exhibit different levels of *ampDh3* transcription and AmpDh3 production which do not originate in different YgfB levels. The strains differ in the sequences of their *dacB* gene, however, this is not likely to be the only mechanism distinguishing the two employed WT strains.

dacB inactivation is indeed relevant for AmpC-mediated β-lactam resistance and is able to modulate the *ampDh3* promoter to some extent, but in a still uncharacterized, and YgfB-independent manner.

AmpR-mediated AmpC overproduction presents a crucial resistance mechanism mediating high-level β-lactam resistance of ID40. CreBC has a small impact on β-lactam resistance but does neither influence the *ampDh3* promoter nor induce YgfB. YgfB in contrast is highly responsible for β-lactam resistance, causing a highly significant decrease in *ampDh3* transcriptional activity and AmpDh3 protein levels. AmpDh3 levels, in turn, are inversely correlated to AmpC activity, MIC values and resistance.

5 Summary

Pseudomonas aeruginosa is a Gram-negative rod that is widely distributed in the environment. As for human infections, it primarily causes nosocomial infections such as pneumonia, burn infections, wound infections, and blood stream infections in immunocompromised patients. These infections are often characterized by particular antibiotic resistance as *Pseudomonas aeruginosa* has diverse intrinsic, acquired and adapted resistance mechanisms to antibiotic drugs. These include low membrane permeability, porins, efflux pumps, and various antibiotic inactivating enzymes. A central enzyme in this regard is the β-lactamase AmpC, which inactivates penicillins and cephalosporins. AmpC is encoded chromosomally, and its production can be induced by the administration of various antibiotics such as imipenem, cefepime, ampicillin and others. Interestingly, its activation is closely related to a metabolic pathway involving many enzymes and genes by which cell wall peptidoglycan is progressively exchanged, metabolized and recycled.

Since *ampC* overexpression is a key resistance mechanism of *Pseudomonas aeruginosa* and is also increasingly causing resistance in the clinical context, it is crucial to understand the exact mechanisms leading to *ampC* overexpression. Previous studies demonstrated that multidrug resistance can be found in *P. aeruginosa* strains such as ID40, which carry a loss of function mutant of the *dacB* gene encoding the Penicillin binding protein 4 (PBP4) involved in peptidoglycan synthesis/recycling. It was assumed that the reason for hyperresistance of such *dacB* mutants is the high activation of the transcriptional activator AmpR which induces *ampC* hyperexpression and in addition activation of a two-component system consisting of CreB and CreC. As shown here deletion of *ampR* abrogates β-lactam resistance. Moreover, preceding studies demonstrated that the uncharacterized protein YgfB contributes in ID40 to high *ampC* expression by suppression of the production of the amidase AmpDh3 (Eggers et al., 2023). The main question of this study was to investigate whether the gene products of the genes *dacB* and *creBC* influence YgfB-mediated suppression of AmpDh3. To address this question, different deletion mutants for these genes were produced in the antibiotic-resistant wildtype strain ID40 and the

more sensitive wildtype strain PA14. Likewise, the ID40 strain carrying a loss of function mutant of the *dacB* gene encoding for PBP4 was complemented with a functional *dacB* gene. In addition, ID40 strains were generated encoding chromosomally for fusion proteins consisting of a Tag (used for protein detection) and CreB or AmpDh3, respectively. Subsequently, the produced set of mutants was analyzed for antibiotic resistance, minimal inhibitory concentrations for β-lactam antibiotics, for β-lactamase activity, for the transcriptional activity of the *ampDh3* promoter, and for the protein levels of AmpDh3, YgfB, and CreB.

It could be observed that YgfB causes increased activity of the β-lactamase AmpC and thereby increased minimal inhibitory concentrations for β-lactam antibiotics. Thus, YgfB has a significant effect on β-lactam resistance in ID40 and PA14. YgfB represses *ampDh3* expression at the transcriptional level, which is also reflected at the protein level. The amount of amidase AmpDh3 in turn inversely correlates with β-lactamase AmpC activity and antibiotic resistance. First evidence that AmpDh3 is localized in the cytoplasm was collected. Furthermore, in this study it could be confirmed that the loss of function of PBP4 encoded by *dacB* affects as well as the presence of the transcriptional regulator AmpR strongly contribute to β-lactam resistance in ID40. The presence of a functional PBP4 clearly increases slightly transcriptional *ampDh3* activity but this is not linked to changes in YgfB levels and occurs in a so far unknown manner. In addition, it could be demonstrated that the two-component system CreBC contributes to some extent to the β-lactam resistance of ID40 but not via induction of YgfB-mediated supression of AmpDh3 production. How CreBC influences β-lactam resistance remains unclear.

It can be considered highly relevant to understand the activation pathways of the β-lactamase AmpC in a more detailed way as the future development of specific inhibitors tailored to the genes and proteins involved in the activation mechanism will be based on this comprehension. In this way, understanding the β-lactam resistance of *Pseudomonas aeruginosa* may provide the opportunity to combat it in the future.

6 Deutsche Zusammenfassung

Pseudomonas aeruginosa ist ein weit in der Umwelt verbreitetes, Gram-negatives Stäbchen. Was Infektionen beim Menschen anbelangt, so verursacht es vor allem nosokomiale Infektionen wie Pneumonien, Verbrennungs- und Wundinfektionen sowie Bakteriämien bei immungeschwächten Patienten. Diese Infektionen sind häufig durch eine besondere Antibiotikaresistenz gekennzeichnet, da *Pseudomonas aeruginosa* über verschiedene intrinsische, erworbene und angepasste Resistenzmechanismen gegen Antibiotika verfügt. Dazu gehören beispielsweise die niedrige Membranpermeabilität, Porine, Effluxpumpen und verschiedene Antibiotika-spaltende Enzyme. Ein in diesem Zusammenhang zentrales Enzym ist die β-Laktamase AmpC, die Penicilline und Cefalosporine inaktiviert. AmpC wird chromosomal kodiert und seine Produktion kann durch die Gabe verschiedener Antibiotika wie beispielsweise Imipenem, Cefepime oder Ampicillin induziert werden. Interessanterweise steht die Aktivierung von AmpC in einem engen Zusammenhang mit einem zahlreiche Enzyme und Gene umfassenden Stoffwechselweg, über den die Peptidoglykane der Zellwand schrittweise ausgetauscht, metabolisiert und recycelt werden.

Da die *ampC*-Überexpression ein zentraler Resistenzmechanismus von *Pseudomonas aeruginosa* ist und auch im klinischen Kontext zunehmend Resistenzen verursacht, ist es sehr bedeutsam, ihren genauen Mechanismus zu verstehen. Vorstudien haben gezeigt, dass Multiresistenz in *P. aeruginosa*-Stämmen wie ID40 vorkommt, die ein funktionsloses *dacB* Gen tragen. Das *dacB* Gen kodiert für das Penicillin-bindende Protein 4 (PBP4), welches an der Peptidoglykan-Synthese und dem Peptidoglykan-Recycling beteiligt ist. Es wurde angenommen, dass der Grund für die Hyperresistenz solcher *dacB*-Mutanten in der starken Aktivierung des Transkriptionsaktivators AmpR liegt, der eine *ampC*-Hyperexpression und zusätzlich die Aktivierung eines aus CreB und CreC bestehenden Zweikomponentensystems bewirkt. Tatsächlich führt wie hier gezeigt die Deletion von *ampR* zum Verlust der β-laktamresistenz von ID40. Darüber hinaus haben frühere Studien gezeigt, dass das nicht charakterisierte Protein YgfB in ID40 zu einer hohen *ampC*-Expression beiträgt, indem es die Produktion der Amidase AmpDh3 unterdrückt (Eggers et al., 2023). Die

grundsätzliche Frage dieser Studie war es, zu untersuchen, ob es einen Zusammenhang zwischen der Aktivität der durch die Gene *dacB* und *creBC* kodierten Proteine und der Stärke der durch YgfB vermittelten Hemmung der Produktion von AmpDh3 gibt.

Um diese Frage beantworten zu können, wurden im Zuge dieser Arbeit verschiedene Deletionsmutanten in diesen Genen für den Antibiotika-resistenten Wildtypstamm ID40 und den sensibleren Wildtypstamm PA14 hergestellt. ID40, dessen *dacB* Gen für ein funktionsloses PBP4 Protein kodiert, wurde mit einem funktionellen *dacB* Gen komplementiert. Ebenso wurde die Gene von *creB* und *ampDh3* so mutiert, dass sie für mit einem Tag versehene Fusionsproteine zum Nachweis der Proteinlevel kodieren. Anschließend wurden die hergestellten Mutanten auf Antibiotikaresistenz, minimale Hemmkonzentrationen für β-Laktam-Antibiotika, β-Laktamaseaktivität, transkriptionelle Aktivität des *ampDh3* Promotors und auf die Proteinmengen von AmpDh3, YgfB und CreB hin untersucht.

Es konnte gezeigt werden, dass YgfB eine erhöhte Aktivität der β-Laktamase AmpC sowie erhöhte minimale Hemmkonzentrationen für β-Laktam-Antibiotika bewirkt. Somit hat es einen signifikanten Einfluss auf die β-Laktamresistenz in ID40 und PA14. YgfB unterdrückt *ampDh3* auf einer transkriptionellen Ebene, was sich auch auf Proteinebene widerspiegelt. Die Amidase AmpDh3 wiederum korreliert invers mit der Aktivität der β-Laktamase AmpC und der Antibiotikaresistenz. Es konnten zudem Hinweise für die zytoplasmatische Lokalisation von AmpDh3 gesammelt werden. Darüber hinaus konnte bestätigt werden, dass eine Mutation im *dacB* Gen von ID40 die β-Laktamresistenz erhöht. Allerdings hat diese Mutation keinen Einfluss auf die YgfB Produktion, erhöht jedoch um einen Faktor von etwa 2 die transkriptionelle Aktivität des *ampDh3* Promotors auf unbekannte Art und Weise (in geringerem Ausmaß als durch YgfB). Das Zweikomponentensystem CreBC. trägt in einem gewissen Maße zur β-Laktamresistenz von ID40 bei, dieser Beitrag ist jedoch unabhängig von der Modulation der *ampDh3*-Expression. Die zentrale Rolle von *ampR* für die *ampC*-vermittelte β-Laktamresistenz von ID40 und generell wurde bestätigt.

Die Relevanz eines genaueren Verständnisses der Aktivierungswege der β-Laktamase AmpC liegt auch darin begründet, dass die zukünftige Entwicklung spezifischer, auf die im Aktivierungsmechanismus involvierten Gene und Proteine zugeschnittener Inhibitoren auf diesem Verständnis basieren wird. So könnte das Verständnis der β-Laktamresistenz von *Pseudomonas aeruginosa* die Möglichkeit bieten, diese Resistenz in Zukunft zu bekämpfen.

7 Literaturverzeichnis:

ADAIR, C. G., GORMAN, S. P., FERON, B. M., BYERS, L. M., JONES, D. S., GOLDSMITH, C. E., MOORE, J. E., KERR, J. R., CURRAN, M. D., HOGG, G., WEBB, C. H., MCCARTHY, G. J. & MILLIGAN, K. R. 1999. Implications of endotracheal tube biofilm for ventilator-associated pneumonia. *Intensive Care Med,* 25**,** 1072-6.

AFESSA, B. & GREEN, B. 2000. Bacterial pneumonia in hospitalized patients with HIV infection: the Pulmonary Complications, ICU Support, and Prognostic Factors of Hospitalized Patients with HIV (PIP) Study. *Chest,* 117**,** 1017-22.

AGUILERA ROSSI, C. G., GOMEZ-PUERTAS, P. & AYALA SERRANO, J. A. 2016. In vivo functional and molecular characterization of the Penicillin-Binding Protein 4 (DacB) of Pseudomonas aeruginosa. *BMC Microbiol,* 16**,** 234.

AKASAKA, T., TANAKA, M., YAMAGUCHI, A. & SATO, K. 2001. Type II topoisomerase mutations in fluoroquinolone-resistant clinical strains of Pseudomonas aeruginosa isolated in 1998 and 1999: role of target enzyme in mechanism of fluoroquinolone resistance. *Antimicrob Agents Chemother,* 45**,** 2263-8.

ARMOUR, A. D., SHANKOWSKY, H. A., SWANSON, T., LEE, J. & TREDGET, E. E. 2007. The impact of nosocomially-acquired resistant Pseudomonas aeruginosa infection in a burn unit. *J Trauma,* 63**,** 164-71.

AUSSEL, L., PIERREL, F., LOISEAU, L., LOMBARD, M., FONTECAVE, M. & BARRAS, F. 2014. Biosynthesis and physiology of coenzyme Q in bacteria. *Biochim Biophys Acta,* 1837**,** 1004-11.

AVISON, M. B., HORTON, R. E., WALSH, T. R. & BENNETT, P. M. 2001. Escherichia coli CreBC is a global regulator of gene expression that responds to growth in minimal media. *J Biol Chem,* 276**,** 26955-61.

AVISON, M. B., NIUMSUP, P., NURMAHOMED, K., WALSH, T. R. & BENNETT, P. M. 2004. Role of the 'cre/blr-tag' DNA sequence in regulation of gene expression by the Aeromonas hydrophila beta-lactamase regulator, BlrA. *J Antimicrob Chemother,* 53**,** 197-202.

AZGHANI, A. O. 1996. Pseudomonas aeruginosa and epithelial permeability: role of virulence factors elastase and exotoxin A. *Am J Respir Cell Mol Biol,* 15**,** 132-40.

BALASUBRAMANIAN, D., KUMARI, H. & MATHEE, K. 2015. Pseudomonas aeruginosa AmpR: an acute-chronic switch regulator. *Pathog Dis,* 73**,** 1-14.

BALASUBRAMANIAN, D., SCHNEPER, L., MERIGHI, M., SMITH, R., NARASIMHAN, G., LORY, S. & MATHEE, K. 2012. The regulatory repertoire of Pseudomonas aeruginosa AmpC ss-lactamase regulator AmpR includes virulence genes. *PLoS One,* 7**,** e34067.

BALCEWICH, M. D., REEVE, T. M., ORLIKOW, E. A., DONALD, L. J., VOCADLO, D. J. & MARK, B. L. 2010. Crystal structure of the AmpR

effector binding domain provides insight into the molecular regulation of inducible ampc beta-lactamase. *J Mol Biol,* 400**,** 998-1010.
BARRETEAU, H., KOVAC, A., BONIFACE, A., SOVA, M., GOBEC, S. & BLANOT, D. 2008. Cytoplasmic steps of peptidoglycan biosynthesis. *FEMS Microbiol Rev,* 32**,** 168-207.
BARTOWSKY, E. & NORMARK, S. 1993. Interactions of wild-type and mutant AmpR of Citrobacter freundii with target DNA. *Mol Microbiol,* 10**,** 555-65.
BERUBE, B. J., RANGEL, S. M. & HAUSER, A. R. 2016. Pseudomonas aeruginosa: breaking down barriers. *Curr Genet,* 62**,** 109-13.
BLANC, D. S., PETIGNAT, C., JANIN, B., BILLE, J. & FRANCIOLI, P. 1998. Frequency and molecular diversity of Pseudomonas aeruginosa upon admission and during hospitalization: a prospective epidemiologic study. *Clin Microbiol Infect,* 4**,** 242-247.
BORISOVA, M., GISIN, J. & MAYER, C. 2014. Blocking peptidoglycan recycling in Pseudomonas aeruginosa attenuates intrinsic resistance to fosfomycin. *Microb Drug Resist,* 20**,** 231-7.
BORISOVA, M., GISIN, J. & MAYER, C. 2017. The N-Acetylmuramic Acid 6-Phosphate Phosphatase MupP Completes the Pseudomonas Peptidoglycan Recycling Pathway Leading to Intrinsic Fosfomycin Resistance. *mBio,* 8.
BOTELHO, J., GROSSO, F. & PEIXE, L. 2019. Antibiotic resistance in Pseudomonas aeruginosa - Mechanisms, epidemiology and evolution. *Drug Resist Updat,* 44**,** 100640.
BOUHSS, A., CROUVOISIER, M., BLANOT, D. & MENGIN-LECREULX, D. 2004. Purification and characterization of the bacterial MraY translocase catalyzing the first membrane step of peptidoglycan biosynthesis. *J Biol Chem,* 279**,** 29974-80.
BREIDENSTEIN, E. B., DE LA FUENTE-NUNEZ, C. & HANCOCK, R. E. 2011. Pseudomonas aeruginosa: all roads lead to resistance. *Trends Microbiol,* 19**,** 419-26.
BRINKMAN, F. S., BAINS, M. & HANCOCK, R. E. 2000. The amino terminus of Pseudomonas aeruginosa outer membrane protein OprF forms channels in lipid bilayer membranes: correlation with a three-dimensional model. *J Bacteriol,* 182**,** 5251-5.
BROWN, K., VIAL, S. C., DEDI, N., WESTCOTT, J., SCALLY, S., BUGG, T. D., CHARLTON, P. A. & CHEETHAM, G. M. 2013. Crystal structure of the Pseudomonas aeruginosa MurG: UDP-GlcNAc substrate complex. *Protein Pept Lett,* 20**,** 1002-8.
BRUCHMANN, S., DOTSCH, A., NOURI, B., CHABERNY, I. F. & HAUSSLER, S. 2013. Quantitative contributions of target alteration and decreased drug accumulation to Pseudomonas aeruginosa fluoroquinolone resistance. *Antimicrob Agents Chemother,* 57**,** 1361-8.
BURNS, J. L., GIBSON, R. L., MCNAMARA, S., YIM, D., EMERSON, J., ROSENFELD, M., HIATT, P., MCCOY, K., CASTILE, R., SMITH, A. L. & RAMSEY, B. W. 2001. Longitudinal assessment of Pseudomonas aeruginosa in young children with cystic fibrosis. *J Infect Dis,* 183**,** 444-52.
BUSH, K. 2010. Bench-to-bedside review: The role of beta-lactamases in antibiotic-resistant Gram-negative infections. *Crit Care,* 14**,** 224.

CABOT, G., BRUCHMANN, S., MULET, X., ZAMORANO, L., MOYA, B., JUAN, C., HAUSSLER, S. & OLIVER, A. 2014. Pseudomonas aeruginosa ceftolozane-tazobactam resistance development requires multiple mutations leading to overexpression and structural modification of AmpC. *Antimicrob Agents Chemother,* 58**,** 3091-9.

CABOT, G., FLORIT-MENDOZA, L., SANCHEZ-DIENER, I., ZAMORANO, L. & OLIVER, A. 2018. Deciphering beta-lactamase-independent beta-lactam resistance evolution trajectories in Pseudomonas aeruginosa. *J Antimicrob Chemother,* 73**,** 3322-3331.

CABOT, G., OCAMPO-SOSA, A. A., TUBAU, F., MACIA, M. D., RODRIGUEZ, C., MOYA, B., ZAMORANO, L., SUAREZ, C., PENA, C., MARTINEZ-MARTINEZ, L., OLIVER, A. & SPANISH NETWORK FOR RESEARCH IN INFECTIOUS, D. 2011. Overexpression of AmpC and efflux pumps in Pseudomonas aeruginosa isolates from bloodstream infections: prevalence and impact on resistance in a Spanish multicenter study. *Antimicrob Agents Chemother,* 55**,** 1906-11.

CARISS, S. J., TAYLER, A. E. & AVISON, M. B. 2008. Defining the growth conditions and promoter-proximal DNA sequences required for activation of gene expression by CreBC in Escherichia coli. *J Bacteriol,* 190**,** 3930-9.

CAVALLARI, J. F., LAMERS, R. P., SCHEURWATER, E. M., MATOS, A. L. & BURROWS, L. L. 2013. Changes to its peptidoglycan-remodeling enzyme repertoire modulate beta-lactam resistance in Pseudomonas aeruginosa. *Antimicrob Agents Chemother,* 57**,** 3078-84.

CHEN, L., ZOU, Y., SHE, P. & WU, Y. 2015. Composition, function, and regulation of T6SS in Pseudomonas aeruginosa. *Microbiol Res,* 172**,** 19-25.

CHENG, Y., YAM, J. K. H., CAI, Z., DING, Y., ZHANG, L. H., DENG, Y. & YANG, L. 2019. Population dynamics and transcriptomic responses of Pseudomonas aeruginosa in a complex laboratory microbial community. *NPJ Biofilms Microbiomes,* 5**,** 1.

CHEVALIER, S., BOUFFARTIGUES, E., BODILIS, J., MAILLOT, O., LESOUHAITIER, O., FEUILLOLEY, M. G. J., ORANGE, N., DUFOUR, A. & CORNELIS, P. 2017. Structure, function and regulation of Pseudomonas aeruginosa porins. *FEMS Microbiol Rev,* 41**,** 698-722.

CHOI, K. H., MIMA, T., CASART, Y., RHOLL, D., KUMAR, A., BEACHAM, I. R. & SCHWEIZER, H. P. 2008. Genetic tools for select-agent-compliant manipulation of Burkholderia pseudomallei. *Appl Environ Microbiol,* 74**,** 1064-75.

CHOI, K. H. & SCHWEIZER, H. P. 2006. mini-Tn7 insertion in bacteria with single attTn7 sites: example Pseudomonas aeruginosa. *Nat Protoc,* 1**,** 153-61.

DAVIES, J. C. & BILTON, D. 2009. Bugs, biofilms, and resistance in cystic fibrosis. *Respir Care,* 54**,** 628-40.

DIEKEMA, D. J., PFALLER, M. A., JONES, R. N., DOERN, G. V., WINOKUR, P. L., GALES, A. C., SADER, H. S., KUGLER, K. & BEACH, M. 1999. Survey of bloodstream infections due to gram-negative bacilli: frequency of occurrence and antimicrobial susceptibility of isolates collected in the

United States, Canada, and Latin America for the SENTRY Antimicrobial Surveillance Program, 1997. *Clin Infect Dis,* 29**,** 595-607.
DIETZ, H., PFEIFLE, D. & WIEDEMANN, B. 1997. The signal molecule for beta-lactamase induction in Enterobacter cloacae is the anhydromuramyl-pentapeptide. *Antimicrob Agents Chemother,* 41**,** 2113-20.
DONLAN, R. M. 2002. Biofilms: microbial life on surfaces. *Emerg Infect Dis,* 8**,** 881-90.
DRAWZ, S. M. & BONOMO, R. A. 2010. Three decades of beta-lactamase inhibitors. *Clin Microbiol Rev,* 23**,** 160-201.
DRIFFIELD, K., MILLER, K., BOSTOCK, J. M., O'NEILL, A. J. & CHOPRA, I. 2008. Increased mutability of Pseudomonas aeruginosa in biofilms. *J Antimicrob Chemother,* 61**,** 1053-6.
DUNHAM, S. A., MCPHERSON, C. J. & MILLER, A. A. 2010. The relative contribution of efflux and target gene mutations to fluoroquinolone resistance in recent clinical isolates of Pseudomonas aeruginosa. *Eur J Clin Microbiol Infect Dis,* 29**,** 279-88.
EGGERS, O., RENSCHLER, F. A., MICHALEK, L. A., WACKLER, N., WALTER, E., SMOLLICH, F., KLEIN, K., SONNABEND, M. S., EGLE, V., ANGELOV, A., ENGESSER, C., BORISOVA, M., MAYER, C., SCHUTZ, M. & BOHN, E. 2023. YgfB increases beta-lactam resistance in Pseudomonas aeruginosa by counteracting AlpA-mediated ampDh3 expression. *Commun Biol,* 6**,** 254.
EMORI, T. G. & GAYNES, R. P. 1993. An overview of nosocomial infections, including the role of the microbiology laboratory. *Clin Microbiol Rev,* 6**,** 428-42.
EUROPEAN CENTRE FOR DISEASE PREVENTION AND CONTROL (ECDC). 2019. *Antimicrobial resistance in the EU/EEA (EARS-Net)*

Annual Epidemiological Report for 2019 [Online]. Available: https://www.ecdc.europa.eu/sites/default/files/documents/surveillance-antimicrobial-resistance-Europe-2019.pdf [Accessed 2021].
FASANI, R. A. & SAVAGEAU, M. A. 2015. Unrelated toxin-antitoxin systems cooperate to induce persistence. *J R Soc Interface,* 12**,** 20150130.
FEINBAUM, R. L., URBACH, J. M., LIBERATI, N. T., DJONOVIC, S., ADONIZIO, A., CARVUNIS, A. R. & AUSUBEL, F. M. 2012. Genome-wide identification of Pseudomonas aeruginosa virulence-related genes using a Caenorhabditis elegans infection model. *PLoS Pathog,* 8**,** e1002813.
FISHER, J. F. & MOBASHERY, S. 2014. The sentinel role of peptidoglycan recycling in the beta-lactam resistance of the Gram-negative Enterobacteriaceae and Pseudomonas aeruginosa. *Bioorg Chem,* 56**,** 41-8.
FUMEAUX, C. & BERNHARDT, T. G. 2017. Identification of MupP as a New Peptidoglycan Recycling Factor and Antibiotic Resistance Determinant in Pseudomonas aeruginosa. *mBio,* 8.
GAYNES, R., EDWARDS, J. R. & NATIONAL NOSOCOMIAL INFECTIONS SURVEILLANCE, S. 2005. Overview of nosocomial infections caused by gram-negative bacilli. *Clin Infect Dis,* 41**,** 848-54.
GELLATLY, S. L. & HANCOCK, R. E. 2013. Pseudomonas aeruginosa: new insights into pathogenesis and host defenses. *Pathog Dis,* 67**,** 159-73.

GIBSON, D. G., YOUNG, L., CHUANG, R. Y., VENTER, J. C., HUTCHISON, C. A., 3RD & SMITH, H. O. 2009. Enzymatic assembly of DNA molecules up to several hundred kilobases. *Nat Methods,* 6**,** 343-5.

GIL-PEROTIN, S., RAMIREZ, P., MARTI, V., SAHUQUILLO, J. M., GONZALEZ, E., CALLEJA, I., MENENDEZ, R. & BONASTRE, J. 2012. Implications of endotracheal tube biofilm in ventilator-associated pneumonia response: a state of concept. *Crit Care,* 16**,** R93.

GISIN, J., SCHNEIDER, A., NAGELE, B., BORISOVA, M. & MAYER, C. 2013. A cell wall recycling shortcut that bypasses peptidoglycan de novo biosynthesis. *Nat Chem Biol,* 9**,** 491-3.

GOMIS-FONT, M. A., CABOT, G., SANCHEZ-DIENER, I., FRAILE-RIBOT, P. A., JUAN, C., MOYA, B., ZAMORANO, L. & OLIVER, A. 2020. In vitro dynamics and mechanisms of resistance development to imipenem and imipenem/relebactam in Pseudomonas aeruginosa. *J Antimicrob Chemother,* 75**,** 2508-2515.

HAN, Y., WANG, T., CHEN, G., PU, Q., LIU, Q., ZHANG, Y., XU, L., WU, M. & LIANG, H. 2019. A *Pseudomonas aeruginosa* type VI secretion system regulated by CueR facilitates copper acquisition. *PLoS Pathog,* 15**,** e1008198.

HANSON, N. D. & SANDERS, C. C. 1999. Regulation of inducible AmpC beta-lactamase expression among Enterobacteriaceae. *Curr Pharm Des,* 5**,** 881-94.

HAUSER, A. R., COBB, E., BODI, M., MARISCAL, D., VALLES, J., ENGEL, J. N. & RELLO, J. 2002. Type III protein secretion is associated with poor clinical outcomes in patients with ventilator-associated pneumonia caused by Pseudomonas aeruginosa. *Crit Care Med,* 30**,** 521-8.

HENIKOFF, S., HAUGHN, G. W., CALVO, J. M. & WALLACE, J. C. 1988. A large family of bacterial activator proteins. *Proc Natl Acad Sci U S A,* 85**,** 6602-6.

HENRICHFREISE, B., WIEGAND, I., PFISTER, W. & WIEDEMANN, B. 2007. Resistance mechanisms of multiresistant Pseudomonas aeruginosa strains from Germany and correlation with hypermutation. *Antimicrob Agents Chemother,* 51**,** 4062-70.

HEYLAND, D. K., COOK, D. J., GRIFFITH, L., KEENAN, S. P. & BRUN-BUISSON, C. 1999. The attributable morbidity and mortality of ventilator-associated pneumonia in the critically ill patient. The Canadian Critical Trials Group. *Am J Respir Crit Care Med,* 159**,** 1249-56.

HMELO, L. R., BORLEE, B. R., ALMBLAD, H., LOVE, M. E., RANDALL, T. E., TSENG, B. S., LIN, C., IRIE, Y., STOREK, K. M., YANG, J. J., SIEHNEL, R. J., HOWELL, P. L., SINGH, P. K., TOLKER-NIELSEN, T., PARSEK, M. R., SCHWEIZER, H. P. & HARRISON, J. J. 2015. Precision-engineering the Pseudomonas aeruginosa genome with two-step allelic exchange. *Nat Protoc,* 10**,** 1820-41.

HOANG, T. T., KARKHOFF-SCHWEIZER, R. R., KUTCHMA, A. J. & SCHWEIZER, H. P. 1998. A broad-host-range Flp-FRT recombination system for site-specific excision of chromosomally-located DNA sequences: application for isolation of unmarked Pseudomonas aeruginosa mutants. *Gene,* 212**,** 77-86.

HOF, H. & SCHLÜTER, D. 2019. *Medizinische Mikrobiologie, 7th edition*, Thieme.
HOGARDT, M. & HEESEMANN, J. 2010. Adaptation of Pseudomonas aeruginosa during persistence in the cystic fibrosis lung. *Int J Med Microbiol,* 300**,** 557-62.
HOLTJE, J. V., KOPP, U., URSINUS, A. & WIEDEMANN, B. 1994. The negative regulator of beta-lactamase induction AmpD is a N-acetyl-anhydromuramyl-L-alanine amidase. *FEMS Microbiol Lett,* 122**,** 159-64.
HORCAJADA, J. P., MONTERO, M., OLIVER, A., SORLI, L., LUQUE, S., GOMEZ-ZORRILLA, S., BENITO, N. & GRAU, S. 2019. Epidemiology and Treatment of Multidrug-Resistant and Extensively Drug-Resistant Pseudomonas aeruginosa Infections. *Clin Microbiol Rev,* 32.
HUANG, H. & HANCOCK, R. E. 1993. Genetic definition of the substrate selectivity of outer membrane porin protein OprD of Pseudomonas aeruginosa. *J Bacteriol,* 175**,** 7793-800.
HUANG, H. H., LIN, Y. T., CHEN, W. C., HUANG, Y. W., CHEN, S. J. & YANG, T. C. 2015. Expression and Functions of CreD, an Inner Membrane Protein in Stenotrophomonas maltophilia. *PLoS One,* 10**,** e0145009.
IKEDA, M., WACHI, M., JUNG, H. K., ISHINO, F. & MATSUHASHI, M. 1991. The Escherichia coli mraY gene encoding UDP-N-acetylmuramoyl-pentapeptide: undecaprenyl-phosphate phospho-N-acetylmuramoyl-pentapeptide transferase. *J Bacteriol,* 173**,** 1021-6.
IRAZOKI, O., HERNANDEZ, S. B. & CAVA, F. 2019. Peptidoglycan Muropeptides: Release, Perception, and Functions as Signaling Molecules. *Front Microbiol,* 10**,** 500.
JACOBS, C., FRERE, J. M. & NORMARK, S. 1997. Cytosolic intermediates for cell wall biosynthesis and degradation control inducible beta-lactam resistance in gram-negative bacteria. *Cell,* 88**,** 823-32.
JACOBS, C., HUANG, L. J., BARTOWSKY, E., NORMARK, S. & PARK, J. T. 1994. Bacterial cell wall recycling provides cytosolic muropeptides as effectors for beta-lactamase induction. *EMBO J,* 13**,** 4684-94.
JACOBS, C., JORIS, B., JAMIN, M., KLARSOV, K., VAN BEEUMEN, J., MENGIN-LECREULX, D., VAN HEIJENOORT, J., PARK, J. T., NORMARK, S. & FRERE, J. M. 1995. AmpD, essential for both beta-lactamase regulation and cell wall recycling, is a novel cytosolic N-acetylmuramyl-L-alanine amidase. *Mol Microbiol,* 15**,** 553-9.
JACOBY, G. A. 2009. AmpC beta-lactamases. *Clin Microbiol Rev,* 22**,** 161-82, Table of Contents.
JACQUES, I., DERELLE, J., WEBER, M. & VIDAILHET, M. 1998. Pulmonary evolution of cystic fibrosis patients colonized by Pseudomonas aeruginosa and/or Burkholderia cepacia. *Eur J Pediatr,* 157**,** 427-31.
JAFFAR-BANDJEE, M. C., LAZDUNSKI, A., BALLY, M., CARRERE, J., CHAZALETTE, J. P. & GALABERT, C. 1995. Production of elastase, exotoxin A, and alkaline protease in sputa during pulmonary exacerbation of cystic fibrosis in patients chronically infected by Pseudomonas aeruginosa. *J Clin Microbiol,* 33**,** 924-9.
JUAN, C., MOYA, B., PEREZ, J. L. & OLIVER, A. 2006. Stepwise upregulation of the Pseudomonas aeruginosa chromosomal cephalosporinase

conferring high-level beta-lactam resistance involves three AmpD homologues. *Antimicrob Agents Chemother,* 50**,** 1780-7.
JUAN, C., TORRENS, G., GONZALEZ-NICOLAU, M. & OLIVER, A. 2017. Diversity and regulation of intrinsic beta-lactamases from non-fermenting and other Gram-negative opportunistic pathogens. *FEMS Microbiol Rev,* 41**,** 781-815.
KAYSER, F. H., BÖTTGER, E. C., ZINKERNAGEL, R. M., HALLER, O., ECKERT, J. & DEPLAZES, P. 2010. *Taschenlehrbuch Medizinische Mikrobiologie, 12th edition*, Thieme.
KENNA, D. T., DOHERTY, C. J., FOWERAKER, J., MACASKILL, L., BARCUS, V. A. & GOVAN, J. R. W. 2007. Hypermutability in environmental Pseudomonas aeruginosa and in populations causing pulmonary infection in individuals with cystic fibrosis. *Microbiology (Reading),* 153**,** 1852-1859.
KLOCKGETHER, J., CRAMER, N., WIEHLMANN, L., DAVENPORT, C. F. & TUMMLER, B. 2011. Pseudomonas aeruginosa Genomic Structure and Diversity. *Front Microbiol,* 2**,** 150.
KOLLEF, M. H., SHORR, A., TABAK, Y. P., GUPTA, V., LIU, L. Z. & JOHANNES, R. S. 2005. Epidemiology and outcomes of health-care-associated pneumonia: results from a large US database of culture-positive pneumonia. *Chest,* 128**,** 3854-62.
KONG, K. F., AGUILA, A., SCHNEPER, L. & MATHEE, K. 2010. *Pseudomonas aeruginosa* beta-lactamase induction requires two permeases, AmpG and AmpP. *BMC Microbiol,* 10**,** 328.
KONG, K. F., JAYAWARDENA, S. R., INDULKAR, S. D., DEL PUERTO, A., KOH, C. L., HOIBY, N. & MATHEE, K. 2005. Pseudomonas aeruginosa AmpR is a global transcriptional factor that regulates expression of AmpC and PoxB beta-lactamases, proteases, quorum sensing, and other virulence factors. *Antimicrob Agents Chemother,* 49**,** 4567-75.
KOUIDMI, I., LEVESQUE, R. C. & PARADIS-BLEAU, C. 2014. The biology of Mur ligases as an antibacterial target. *Mol Microbiol,* 94**,** 242-53.
KOVACH, M. E., ELZER, P. H., HILL, D. S., ROBERTSON, G. T., FARRIS, M. A., ROOP, R. M., 2ND & PETERSON, K. M. 1995. Four new derivatives of the broad-host-range cloning vector pBBR1MCS, carrying different antibiotic-resistance cassettes. *Gene,* 166**,** 175-6.
LAMBERT, P. A. 2002. Mechanisms of antibiotic resistance in Pseudomonas aeruginosa. *J R Soc Med,* 95 Suppl 41**,** 22-6.
LEE, M., HESEK, D., BLAZQUEZ, B., LASTOCHKIN, E., BOGGESS, B., FISHER, J. F. & MOBASHERY, S. 2015. Catalytic spectrum of the penicillin-binding protein 4 of Pseudomonas aeruginosa, a nexus for the induction of beta-lactam antibiotic resistance. *J Am Chem Soc,* 137**,** 190-200.
LI, H., LUO, Y. F., WILLIAMS, B. J., BLACKWELL, T. S. & XIE, C. M. 2012. Structure and function of OprD protein in Pseudomonas aeruginosa: from antibiotic resistance to novel therapies. *Int J Med Microbiol,* 302**,** 63-8.
LIAM, C. K., LIM, K. H. & WONG, C. M. 2001. Community-acquired pneumonia in patients requiring hospitalization. *Respirology,* 6**,** 259-64.
LIN, J., CHENG, J., CHEN, K., GUO, C., ZHANG, W., YANG, X., DING, W., MA, L., WANG, Y. & SHEN, X. 2015. The icmF3 locus is involved in multiple

adaptation- and virulence-related characteristics in Pseudomonas aeruginosa PAO1. *Front Cell Infect Microbiol,* 5**,** 70.
LINDBERG, F., LINDQUIST, S. & NORMARK, S. 1988. Genetic basis of induction and overproduction of chromosomal class I beta-lactamase in nonfastidious gram-negative bacilli. *Rev Infect Dis,* 10**,** 782-5.
LINDBERG, F., WESTMAN, L. & NORMARK, S. 1985. Regulatory components in Citrobacter freundii ampC beta-lactamase induction. *Proc Natl Acad Sci U S A,* 82**,** 4620-4.
LINDQUIST, S., LINDBERG, F. & NORMARK, S. 1989. Binding of the Citrobacter freundii AmpR regulator to a single DNA site provides both autoregulation and activation of the inducible ampC beta-lactamase gene. *J Bacteriol,* 171**,** 3746-53.
LISTER, P. D., WOLTER, D. J. & HANSON, N. D. 2009. Antibacterial-resistant *Pseudomonas aeruginosa*: clinical impact and complex regulation of chromosomally encoded resistance mechanisms. *Clin Microbiol Rev,* 22**,** 582-610.
LIVERMORE, D. M. 1992. Interplay of impermeability and chromosomal beta-lactamase activity in imipenem-resistant Pseudomonas aeruginosa. *Antimicrob Agents Chemother,* 36**,** 2046-8.
LODGE, J., BUSBY, S. & PIDDOCK, L. 1993. Investigation of the Pseudomonas aeruginosa ampR gene and its role at the chromosomal ampC beta-lactamase promoter. *FEMS Microbiol Lett,* 111**,** 315-20.
LODGE, J. M., MINCHIN, S. D., PIDDOCK, L. J. & BUSBY, S. J. 1990. Cloning, sequencing and analysis of the structural gene and regulatory region of the Pseudomonas aeruginosa chromosomal ampC beta-lactamase. *Biochem J,* 272**,** 627-31.
MA, L. S., LIN, J. S. & LAI, E. M. 2009. An IcmF family protein, ImpLM, is an integral inner membrane protein interacting with ImpKL, and its walker a motif is required for type VI secretion system-mediated Hcp secretion in Agrobacterium tumefaciens. *J Bacteriol,* 191**,** 4316-29.
MAISONNEUVE, E. & GERDES, K. 2014. Molecular mechanisms underlying bacterial persisters. *Cell,* 157**,** 539-48.
MAITI, S. N., PHILLIPS, O. A., MICETICH, R. G. & LIVERMORE, D. M. 1998. Beta-lactamase inhibitors: agents to overcome bacterial resistance. *Curr Med Chem,* 5**,** 441-56.
MASUDA, N., SAKAGAWA, E., OHYA, S., GOTOH, N., TSUJIMOTO, H. & NISHINO, T. 2000. Substrate specificities of MexAB-OprM, MexCD-OprJ, and MexXY-oprM efflux pumps in Pseudomonas aeruginosa. *Antimicrob Agents Chemother,* 44**,** 3322-7.
MATHEE, K. 2018. Forensic investigation into the origin of Pseudomonas aeruginosa PA14 - old but not lost. *J Med Microbiol,* 67**,** 1019-1021.
MCFARLAND, K. A., DOLBEN, E. L., LEROUX, M., KAMBARA, T. K., RAMSEY, K. M., KIRKPATRICK, R. L., MOUGOUS, J. D., HOGAN, D. A. & DOVE, S. L. 2015. A self-lysis pathway that enhances the virulence of a pathogenic bacterium. *Proc Natl Acad Sci U S A,* 112**,** 8433-8.
MENA, A., SMITH, E. E., BURNS, J. L., SPEERT, D. P., MOSKOWITZ, S. M., PEREZ, J. L. & OLIVER, A. 2008. Genetic adaptation of Pseudomonas

aeruginosa to the airways of cystic fibrosis patients is catalyzed by hypermutation. *J Bacteriol,* 190**,** 7910-7.

MONSO, E., GARCIA-AYMERICH, J., SOLER, N., FARRERO, E., FELEZ, M. A., ANTO, J. M., TORRES, A. & INVESTIGATORS, E. 2003. Bacterial infection in exacerbated COPD with changes in sputum characteristics. *Epidemiol Infect,* 131**,** 799-804.

MORADALI, M. F., GHODS, S. & REHM, B. H. 2017. Pseudomonas aeruginosa Lifestyle: A Paradigm for Adaptation, Survival, and Persistence. *Front Cell Infect Microbiol,* 7**,** 39.

MOYA, B., BECEIRO, A., CABOT, G., JUAN, C., ZAMORANO, L., ALBERTI, S. & OLIVER, A. 2012. Pan-beta-lactam resistance development in Pseudomonas aeruginosa clinical strains: molecular mechanisms, penicillin-binding protein profiles, and binding affinities. *Antimicrob Agents Chemother,* 56**,** 4771-8.

MOYA, B., DOTSCH, A., JUAN, C., BLAZQUEZ, J., ZAMORANO, L., HAUSSLER, S. & OLIVER, A. 2009. Beta-lactam resistance response triggered by inactivation of a nonessential penicillin-binding protein. *PLoS Pathog,* 5**,** e1000353.

MOYA, B., JUAN, C., ALBERTI, S., PEREZ, J. L. & OLIVER, A. 2008. Benefit of having multiple ampD genes for acquiring beta-lactam resistance without losing fitness and virulence in Pseudomonas aeruginosa. *Antimicrob Agents Chemother,* 52**,** 3694-700.

MULCAHY, L. R., BURNS, J. L., LORY, S. & LEWIS, K. 2010. Emergence of Pseudomonas aeruginosa strains producing high levels of persister cells in patients with cystic fibrosis. *J Bacteriol,* 192**,** 6191-9.

NATIONAL NOSOCOMIAL INFECTIONS SURVEILLANCE (NNIS) SYSTEM. 2004. *National Nosocomial Infections Surveillance (NNIS) System Report, data summary from January 1992 through June 2004, issued October 2004* [Online]. Atlanta, Georgia: Am J Infect Control Available: https://www.ajicjournal.org/action/showPdf?pii=S0196-6553%2804%2900542-5 [Accessed 2021].

NICAS, T. I. & HANCOCK, R. E. 1983. Pseudomonas aeruginosa outer membrane permeability: isolation of a porin protein F-deficient mutant. *J Bacteriol,* 153**,** 281-5.

NORMARK, S. 1995. beta-Lactamase induction in gram-negative bacteria is intimately linked to peptidoglycan recycling. *Microb Drug Resist,* 1**,** 111-4.

OLIVER, A., CANTON, R., CAMPO, P., BAQUERO, F. & BLAZQUEZ, J. 2000. High frequency of hypermutable Pseudomonas aeruginosa in cystic fibrosis lung infection. *Science,* 288**,** 1251-4.

PARK, J. T. & UEHARA, T. 2008. How bacteria consume their own exoskeletons (turnover and recycling of cell wall peptidoglycan). *Microbiol Mol Biol Rev,* 72**,** 211-27, table of contents.

PATEL, I. S., SEEMUNGAL, T. A., WILKS, M., LLOYD-OWEN, S. J., DONALDSON, G. C. & WEDZICHA, J. A. 2002. Relationship between bacterial colonisation and the frequency, character, and severity of COPD exacerbations. *Thorax,* 57**,** 759-64.

PATERSON, D. L. & BONOMO, R. A. 2005. Extended-spectrum beta-lactamases: a clinical update. *Clin Microbiol Rev,* 18**,** 657-86.

PELOSI, L., DUCLUZEAU, A. L., LOISEAU, L., BARRAS, F., SCHNEIDER, D., JUNIER, I. & PIERREL, F. 2016. Evolution of Ubiquinone Biosynthesis: Multiple Proteobacterial Enzymes with Various Regioselectivities To Catalyze Three Contiguous Aromatic Hydroxylation Reactions. *mSystems,* 1.

PENA, J. M., PREZIOSO, S. M., MCFARLAND, K. A., KAMBARA, T. K., RAMSEY, K. M., DEIGHAN, P. & DOVE, S. L. 2021. Control of a programmed cell death pathway in Pseudomonas aeruginosa by an antiterminator. *Nat Commun,* 12**,** 1702.

PERLEY-ROBERTSON, G. E., YADAV, A. K., WINOGRODZKI, J. L., STUBBS, K. A., MARK, B. L. & VOCADLO, D. J. 2016. A Fluorescent Transport Assay Enables Studying AmpG Permeases Involved in Peptidoglycan Recycling and Antibiotic Resistance. *ACS Chem Biol,* 11**,** 2626-35.

PUGIN, J., DUNN-SIEGRIST, I., DUFOUR, J., TISSIERES, P., CHARLES, P. E. & COMTE, R. 2008. Cyclic stretch of human lung cells induces an acidification and promotes bacterial growth. *Am J Respir Cell Mol Biol,* 38**,** 362-70.

PUTMAN, M., VAN VEEN, H. W. & KONINGS, W. N. 2000. Molecular properties of bacterial multidrug transporters. *Microbiol Mol Biol Rev,* 64**,** 672-93.

RAHME, L. G., STEVENS, E. J., WOLFORT, S. F., SHAO, J., TOMPKINS, R. G. & AUSUBEL, F. M. 1995. Common virulence factors for bacterial pathogenicity in plants and animals. *Science,* 268**,** 1899-902.

REITH, J. & MAYER, C. 2011. Peptidoglycan turnover and recycling in Gram-positive bacteria. *Appl Microbiol Biotechnol,* 92**,** 1-11.

RELLO, J., RUE, M., JUBERT, P., MUSES, G., SONORA, R., VALLES, J. & NIEDERMAN, M. S. 1997. Survival in patients with nosocomial pneumonia: impact of the severity of illness and the etiologic agent. *Crit Care Med,* 25**,** 1862-7.

RESTREPO, M. I., BABU, B. L., REYES, L. F., CHALMERS, J. D., SONI, N. J., SIBILA, O., FAVERIO, P., CILLONIZ, C., RODRIGUEZ-CINTRON, W., ALIBERTI, S. & GLIMP 2018. Burden and risk factors for Pseudomonas aeruginosa community-acquired pneumonia: a multinational point prevalence study of hospitalised patients. *Eur Respir J,* 52.

SACHA, P., WIECZOREK, P., HAUSCHILD, T., ZORAWSKI, M., OLSZANSKA, D. & TRYNISZEWSKA, E. 2008. Metallo-beta-lactamases of Pseudomonas aeruginosa--a novel mechanism resistance to beta-lactam antibiotics. *Folia Histochem Cytobiol,* 46**,** 137-42.

SADIKOT, R. T., BLACKWELL, T. S., CHRISTMAN, J. W. & PRINCE, A. S. 2005. Pathogen-host interactions in Pseudomonas aeruginosa pneumonia. *Am J Respir Crit Care Med,* 171**,** 1209-23.

SAFDAR, N., CRNICH, C. J. & MAKI, D. G. 2005. The pathogenesis of ventilator-associated pneumonia: its relevance to developing effective strategies for prevention. *Respir Care,* 50**,** 725-39; discussion 739-41.

SCHAEFER, P. & BAUGH, R. F. 2012. Acute otitis externa: an update. *Am Fam Physician,* 86**,** 1055-61.

SCHEETZ, M. H., HOFFMAN, M., BOLON, M. K., SCHULERT, G., ESTRELLADO, W., BARABOUTIS, I. G., SRIRAM, P., DINH, M., OWENS, L. K. & HAUSER, A. R. 2009. Morbidity associated with

Pseudomonas aeruginosa bloodstream infections. *Diagn Microbiol Infect Dis,* 64**,** 311-9.
SCHMIDT, T. G. & SKERRA, A. 2007. The Strep-tag system for one-step purification and high-affinity detection or capturing of proteins. *Nat Protoc,* 2**,** 1528-35.
SCHMIDTKE, A. J. & HANSON, N. D. 2008. Role of ampD homologs in overproduction of AmpC in clinical isolates of Pseudomonas aeruginosa. *Antimicrob Agents Chemother,* 52**,** 3922-7.
SCHROTH, M. N., CHO, J. J., GREEN, S. K., KOMINOS, S. D. & MICROBIOLOGY SOCIETY, P. 2018. Epidemiology of Pseudomonas aeruginosa in agricultural areas(). *J Med Microbiol,* 67**,** 1191-1201.
SCHULTZ, M. J., SPEELMAN, P., ZAAT, S. A., HACK, C. E., VAN DEVENTER, S. J. & VAN DER POLL, T. 2000. The effect of pseudomonas exotoxin A on cytokine production in whole blood exposed to Pseudomonas aeruginosa. *FEMS Immunol Med Microbiol,* 29**,** 227-32.
SHAM, L. T., BUTLER, E. K., LEBAR, M. D., KAHNE, D., BERNHARDT, T. G. & RUIZ, N. 2014. Bacterial cell wall. MurJ is the flippase of lipid-linked precursors for peptidoglycan biogenesis. *Science,* 345**,** 220-2.
SHU, J. C., KUO, A. J., SU, L. H., LIU, T. P., LEE, M. H., SU, I. N. & WU, T. L. 2017. Development of carbapenem resistance in Pseudomonas aeruginosa is associated with OprD polymorphisms, particularly the amino acid substitution at codon 170. *J Antimicrob Chemother,* 72**,** 2489-2495.
SILBY, M. W., WINSTANLEY, C., GODFREY, S. A., LEVY, S. B. & JACKSON, R. W. 2011. Pseudomonas genomes: diverse and adaptable. *FEMS Microbiol Rev,* 35**,** 652-80.
SKURNIK, D., ROUX, D., CATTOIR, V., DANILCHANKA, O., LU, X., YODER-HIMES, D. R., HAN, K., GUILLARD, T., JIANG, D., GAULTIER, C., GUERIN, F., ASCHARD, H., LECLERCQ, R., MEKALANOS, J. J., LORY, S. & PIER, G. B. 2013. Enhanced in vivo fitness of carbapenem-resistant oprD mutants of Pseudomonas aeruginosa revealed through high-throughput sequencing. *Proc Natl Acad Sci U S A,* 110**,** 20747-52.
SMITH, E. E., BUCKLEY, D. G., WU, Z., SAENPHIMMACHAK, C., HOFFMAN, L. R., D'ARGENIO, D. A., MILLER, S. I., RAMSEY, B. W., SPEERT, D. P., MOSKOWITZ, S. M., BURNS, J. L., KAUL, R. & OLSON, M. V. 2006. Genetic adaptation by Pseudomonas aeruginosa to the airways of cystic fibrosis patients. *Proc Natl Acad Sci U S A,* 103**,** 8487-92.
SONNABEND, M. S., KLEIN, K., BEIER, S., ANGELOV, A., KLUJ, R., MAYER, C., GROSS, C., HOFMEISTER, K., BEUTTNER, A., WILLMANN, M., PETER, S., OBERHETTINGER, P., SCHMIDT, A., AUTENRIETH, I. B., SCHUTZ, M. & BOHN, E. 2020. Identification of Drug Resistance Determinants in a Clinical Isolate of Pseudomonas aeruginosa by High-Density Transposon Mutagenesis. *Antimicrob Agents Chemother,* 64.
SOPENA, N., SABRIA, M., PEDRO-BOTET, M. L., MANTEROLA, J. M., MATAS, L., DOMINGUEZ, J., MODOL, J. M., TUDELA, P., AUSINA, V. & FOZ, M. 1999. Prospective study of community-acquired pneumonia of bacterial etiology in adults. *Eur J Clin Microbiol Infect Dis,* 18**,** 852-8.
STEWART, P. S. & COSTERTON, J. W. 2001. Antibiotic resistance of bacteria in biofilms. *Lancet,* 358**,** 135-8.

STOVER, C. K., PHAM, X. Q., ERWIN, A. L., MIZOGUCHI, S. D., WARRENER, P., HICKEY, M. J., BRINKMAN, F. S., HUFNAGLE, W. O., KOWALIK, D. J., LAGROU, M., GARBER, R. L., GOLTRY, L., TOLENTINO, E., WESTBROCK-WADMAN, S., YUAN, Y., BRODY, L. L., COULTER, S. N., FOLGER, K. R., KAS, A., LARBIG, K., LIM, R., SMITH, K., SPENCER, D., WONG, G. K., WU, Z., PAULSEN, I. T., REIZER, J., SAIER, M. H., HANCOCK, R. E., LORY, S. & OLSON, M. V. 2000. Complete genome sequence of Pseudomonas aeruginosa PAO1, an opportunistic pathogen. *Nature,* 406**,** 959-64.

STUBBS, K. A., SCAFFIDI, A., DEBOWSKI, A. W., MARK, B. L., STICK, R. V. & VOCADLO, D. J. 2008. Synthesis and use of mechanism-based protein-profiling probes for retaining beta-D-glucosaminidases facilitate identification of Pseudomonas aeruginosa NagZ. *J Am Chem Soc,* 130**,** 327-35.

TAM, V. H., CHANG, K. T., SCHILLING, A. N., LAROCCO, M. T., GENTY, L. O. & GAREY, K. W. 2009. Impact of AmpC overexpression on outcomes of patients with Pseudomonas aeruginosa bacteremia. *Diagn Microbiol Infect Dis,* 63**,** 279-85.

TAM, V. H., SCHILLING, A. N., LAROCCO, M. T., GENTRY, L. O., LOLANS, K., QUINN, J. P. & GAREY, K. W. 2007. Prevalence of AmpC over-expression in bloodstream isolates of Pseudomonas aeruginosa. *Clin Microbiol Infect,* 13**,** 413-8.

TAYLER, A. E., AYALA, J. A., NIUMSUP, P., WESTPHAL, K., BAKER, J. A., ZHANG, L., WALSH, T. R., WIEDEMANN, B., BENNETT, P. M. & AVISON, M. B. 2010. Induction of beta-lactamase production in Aeromonas hydrophila is responsive to beta-lactam-mediated changes in peptidoglycan composition. *Microbiology (Reading),* 156**,** 2327-2335.

TEMPLIN, M. F., URSINUS, A. & HOLTJE, J. V. 1999. A defect in cell wall recycling triggers autolysis during the stationary growth phase of Escherichia coli. *EMBO J,* 18**,** 4108-17.

TORRENS, G., HERNANDEZ, S. B., AYALA, J. A., MOYA, B., JUAN, C., CAVA, F. & OLIVER, A. 2019. Regulation of AmpC-Driven beta-Lactam Resistance in *Pseudomonas aeruginosa*: Different Pathways, Different Signaling. *mSystems,* 4.

VAKULENKO, S. B. & MOBASHERY, S. 2003. Versatility of aminoglycosides and prospects for their future. *Clin Microbiol Rev,* 16**,** 430-50.

VENKATAKRISHNAN, A., STECENKO, A. A., KING, G., BLACKWELL, T. R., BRIGHAM, K. L., CHRISTMAN, J. W. & BLACKWELL, T. S. 2000. Exaggerated activation of nuclear factor-kappaB and altered IkappaB-beta processing in cystic fibrosis bronchial epithelial cells. *Am J Respir Cell Mol Biol,* 23**,** 396-403.

VIDAL, F., MENSA, J., MARTINEZ, J. A., ALMELA, M., MARCO, F., GATELL, J. M., RICHART, C., SORIANO, E. & JIMENEZ DE ANTA, M. T. 1999. Pseudomonas aeruginosa bacteremia in patients infected with human immunodeficiency virus type 1. *Eur J Clin Microbiol Infect Dis,* 18**,** 473-7.

VOLLMER, W., BLANOT, D. & DE PEDRO, M. A. 2008. Peptidoglycan structure and architecture. *FEMS Microbiol Rev,* 32**,** 149-67.

WANG, T., HU, Z., DU, X., SHI, Y., DANG, J., LEE, M., HESEK, D., MOBASHERY, S., WU, M. & LIANG, H. 2020. A type VI secretion system delivers a cell wall amidase to target bacterial competitors. *Mol Microbiol,* 114**,** 308-321.

WIEGAND, I., MARR, A. K., BREIDENSTEIN, E. B., SCHUREK, K. N., TAYLOR, P. & HANCOCK, R. E. 2008. Mutator genes giving rise to decreased antibiotic susceptibility in *Pseudomonas aeruginosa*. *Antimicrob Agents Chemother,* 52**,** 3810-3.

WILLIAMS, B. J., DEHNBOSTEL, J. & BLACKWELL, T. S. 2010. Pseudomonas aeruginosa: host defence in lung diseases. *Respirology,* 15**,** 1037-56.

WILLMANN, M., GÖTTING, S., BEZDAN, D., MAČEK, B., VELIC, A., MARSCHAL, M., VOGEL, W., FLESCH, I., MARKERT, U., SCHMIDT, A., KÜBLER, P., HAUG, M., JAVED, M., JENTZSCH, B., OBERHETTINGER, P., SCHÜTZ, M., BOHN, E., SONNABEND, M., KLEIN, K., AUTENRIETH, I., OSSOWSKI, S., SCHWARZ, S. & PETER, S. 2018. *Multi-omics approach identifies novel pathogen-derived prognostic biomarkers in patients with Pseudomonas aeruginosa bloodstream infection* [Online]. bioRxiv. Available: https://www.biorxiv.org/content/10.1101/309898v1 [Accessed 2021].

WOLFGANG, M. C., JYOT, J., GOODMAN, A. L., RAMPHAL, R. & LORY, S. 2004. Pseudomonas aeruginosa regulates flagellin expression as part of a global response to airway fluid from cystic fibrosis patients. *Proc Natl Acad Sci U S A,* 101**,** 6664-8.

WOOD, T. E., HOWARD, S. A., FORSTER, A., NOLAN, L. M., MANOLI, E., BULLEN, N. P., YAU, H. C. L., HACHANI, A., HAYWARD, R. D., WHITNEY, J. C., VOLLMER, W., FREEMONT, P. S. & FILLOUX, A. 2019. The Pseudomonas aeruginosa T6SS Delivers a Periplasmic Toxin that Disrupts Bacterial Cell Morphology. *Cell Rep,* 29**,** 187-201 e7.

YOSHIMURA, F. & NIKAIDO, H. 1982. Permeability of Pseudomonas aeruginosa outer membrane to hydrophilic solutes. *J Bacteriol,* 152**,** 636-42.

ZAMORANO, L., MOYA, B., JUAN, C., MULET, X., BLAZQUEZ, J. & OLIVER, A. 2014. The *Pseudomonas aeruginosa* CreBC two-component system plays a major role in the response to beta-lactams, fitness, biofilm growth, and global regulation. *Antimicrob Agents Chemother,* 58**,** 5084-95.

ZAMORANO, L., MOYA, B., JUAN, C. & OLIVER, A. 2010a. Differential beta-lactam resistance response driven by ampD or dacB (PBP4) inactivation in genetically diverse Pseudomonas aeruginosa strains. *J Antimicrob Chemother,* 65**,** 1540-2.

ZAMORANO, L., REEVE, T. M., DENG, L., JUAN, C., MOYA, B., CABOT, G., VOCADLO, D. J., MARK, B. L. & OLIVER, A. 2010b. NagZ inactivation prevents and reverts beta-lactam resistance, driven by AmpD and PBP 4 mutations, in Pseudomonas aeruginosa. *Antimicrob Agents Chemother,* 54**,** 3557-63.

ZAMORANO, L., REEVE, T. M., JUAN, C., MOYA, B., CABOT, G., VOCADLO, D. J., MARK, B. L. & OLIVER, A. 2011. AmpG inactivation restores susceptibility of pan-beta-lactam-resistant Pseudomonas aeruginosa clinical strains. *Antimicrob Agents Chemother,* 55**,** 1990-6.

ZANNONI, D. 1989. The respiratory chains of pathogenic pseudomonads. *Biochim Biophys Acta,* 975**,** 299-316.
ZHANG, W., LEE, M., HESEK, D., LASTOCHKIN, E., BOGGESS, B. & MOBASHERY, S. 2013. Reactions of the three AmpD enzymes of *Pseudomonas aeruginosa*. *J Am Chem Soc,* 135**,** 4950-3.
ZIHA-ZARIFI, I., LLANES, C., KOHLER, T., PECHERE, J. C. & PLESIAT, P. 1999. In vivo emergence of multidrug-resistant mutants of Pseudomonas aeruginosa overexpressing the active efflux system MexA-MexB-OprM. *Antimicrob Agents Chemother,* 43**,** 287-91.

8 Erklärung zum Eigenanteil

Die Arbeit wurde im Institut für Medizinische Mikrobiologie und Hygiene unter Betreuung von PD Dr. rer. nat. Erwin Bohn durchgeführt.

Die Konzeption der Studie erfolgte durch PD Dr. rer. nat. Erwin Bohn und PD Dr. Monika Schütz.

Sämtliche Versuche wurden nach Einarbeitung durch die Labormitglieder PD Dr. Erwin Bohn, PD Dr. Monika Schütz, Dr. Karolin Birkle, Dr. Michael Sonnabend, Dr. Fabian Renschler und Kathrin Vöhringer von mir eigenständig durchgeführt. Um die Mutagenese zu beschleunigen, übernahm PD Dr. Erwin Bohn die Generierung der Komplementationsmutanten im *dacB* Gen sowie einzelne Schritte in der Herstellung der Deletionsmutanten an Wochenenden.

Die statistische Auswertung erfolgte nach Anleitung durch PD Dr. Erwin Bohn durch mich.

Ich versichere, das Manuskript selbständig verfasst zu haben und keine weiteren als die von mir angegebenen Quellen verwendet zu haben.

Einige Ergebnisse der hier vorgelegten Dissertation fließen in den Artikel „The uncharacterized protein YgfB contributes to β-lactam resistance in *Pseudomonas aeruginosa* by counteracting AlpA-mediated ampDh3 expression“ (Eggers et al., 2023) ein. Dieser wurde bei Communications Biology veröffentlicht. Ich war beteiligt an der Erhebung der hier beschriebenen Ergebnisse, jedoch habe ich den Artikel nicht mitverfasst.

Tübingen, den 05.07.2023

9 Publikationen

Folgende Publikation wurde bei Communications Biology veröffentlicht:

Eggers O, Renschler F, Michalek LM, Wackler N, Walter E, Smollich F, Klein K, Sonnabend M, V Egle V, Angelov A, Engesser C, Borisova M, Mayer C, Monika Schütz M and Bohn E. 2023. The uncharacterized protein YgfB contributes to β-lactam resistance in *Pseudomonas aeruginosa* by counteracting AlpA-mediated ampDh3 expression. Commun Biol.

10 Danksagung

Ich möchte mich sehr herzlich für die vielfältige Unterstützung bedanken, die mir während meiner Promotion zuteilgeworden ist.

Allen voran möchte ich mich bei PD Dr. Erwin Bohn für die Ermöglichung und Konzeption des Projekts, für meine Einarbeitung in den Laboralltag sowie für seine ausgesprochen fachkundige, umfassende, aufmerksame, humorvolle und geduldige Betreuung bedanken. PD Dr. Monika Schütz möchte ich danken ebenso für die Konzeption des Projekts, das gründliche und überaus hilfreiche Korrekturlesen sowie für ihre so offene, positive und hilfsbereite Unterstützung.

Für die offene, warmherzige, humorvolle und unheimlich unterstützende Stimmung bin ich allen Mitgliedern der AG Schütz/Bohn sowie der Nachbar-Arbeitsgruppen sehr dankbar. Ich bedanke mich bei PD Dr. Erwin Bohn, PD Dr. Monika Schütz, Dr. Karolin Birkle, Dr. Fabian Renschler, Dr. Michael Sonnabend, Tanja Späth, Anette Maier, Dr. med. Johanna Kemper, Elias Walter, Sara Pereira, Kathrin Vöhringer, Lydia Anita Michalek, Laura Luib, Ole Eggers, Valentin Egle, Elena Weber und Janes Krusche, Kristina Engesser und Manuela Löffler, Nadine Hofmann, Andrea Schäfer und Thomas Hagemann. Ich habe mich in meiner Umgebung sehr wohlgefühlt und meine Laborarbeit als sehr intensive und auch persönlich sehr wertvolle Zeit erleben dürfen.

Unzählige Gespräche und Anregungen haben mir viel bedeutet.

Magdalena Bucher möchte ich für das gemeinsame Schreiben in der Bibliothek und ihre besondere Unterstützung danken, sowie Pascal Wackler, Dr. med. Yoko Tamamushi und Rainer Grimm für die Beantwortung meiner Rückfragen.

Danke auch an Luise, Johannes, Sophie und meine Familie für die beständige und einzigartige Begleitung.